DYNAMICS AND CONTROL OF A PREDATOR-PREY SYSTEM WITH THE SUPPLY OF ADDITIONAL FOOD TO PREDATORS

by

Dinesh Kumar

DEPARTMENT OF MATHEMATICS

INDIAN INSTITUTE OF TECHNOLOGY GUWAHATI

GUWAHATI-781039, INDIA

December, 2014

DYNAMICS AND CONTROL OF A PREDATOR-PREY SYSTEM WITH THE SUPPLY OF ADDITIONAL FOOD TO PREDATORS

A Thesis submitted

in partial fulfillment of the requirements

for the degree of

DOCTOR OF PHILOSOPHY

by

Dinesh Kumar

(Roll Number: 09612314)

to the

DEPARTMENT OF MATHEMATICS

INDIAN INSTITUTE OF TECHNOLOGY GUWAHATI

December, 2014

Declaration

It is certified that the work contained in this thesis entitled **"Dynamics and control of a predator-prey system with the supply of additional food to predators"** was done by me, under the supervision of **Dr. Siddhartha Pratim Chakrabarty**, Assistant Professor, Department of Mathematics, Indian Institute of Technology Guwahati for the award of the degree of Doctor of Philosophy and this work has not been submitted elsewhere for a degree.

December, 2014

Dinesh Kumar
Roll No. 09612314
Department of Mathematics
Indian Institute of Technology Guwahati

Certificate

It is certified that the work contained in this thesis entitled **"Dynamics and control of a predator-prey system with the supply of additional food to predators"** by **Dinesh Kumar,** a student in Department of Mathematics, Indian Institute of Technology Guwahati, for the award of the degree of Doctor of Philosophy has been carried out under my supervision and this work has not been submitted elsewhere for a degree.

December, 2014

Dr. Siddhartha Pratim Chakrabarty
Assistant Professor
Department of Mathematics
Indian Institute of Technology Guwahati

To

My Parents

Acknowledgements

Every great experience requires the help and support of many people, I would like to take the opportunity of thanking all those who have extended a helping hand whenever I needed. In the first place I would like to express my deepest gratitude to my Ph.D Supervisor, Dr. Siddhartha P. Chakrabarty, for introducing me the wonderful subject of Mathematical Biology. My completion of thesis could not have been accomplished without his extraordinary support, patient guidance, enthusiastic encouragement and useful critiques of this research work.

I would like to express my deepest appreciation to my doctoral committee chair, Professor Rajen Kumar Sinha, who has polite conversation and the substance of a genius. I want to convey my sincere thanks to my other committee members Dr. K.V. Srikanth and Professor Jiten C. Kalita for reviewing my research work and giving valuable suggestions for improvements in my research work. I sincerely acknowledge Indian Institute of Technology Guwahati for providing me with the various facilities necessary to carry out my research. I am most grateful to Ministry of Human and Resource Development, Government of India, for providing me with financial assistance for the completion of my thesis work.

I offer my heartiest gratitude to a great mathematician, an excellent teacher, a nice human being Dr. K.V. Srikanth, for giving me moral support. Your constant encouragement are much appreciated. In addition, a special and sincere thanks to Dr. Anjan K. Chakrabarty (having excellent mathematics presentation skill), Dr. Sukanta Pati (an experienced and skilled mathematician), Professor Swaroop Nandan Bora, Professor Srinivasan Natesan and Dr. P.A.S. Sree Krishna (who introduced me to pst plots). I thank all the staff members of the Department of Mathematics, IIT Guwahati for their assistance in official and technical matters.

I am also thankful to all my research scholar friends of the Department of Mathematics, IIT Guwahati for their love and company during my stay in the IIT campus. Especially, I want to thank those friends of mine with whom I used to discuss mathematics: Pratibhamoy, Murali, Raj Bhawan, Gowri (who also helped in MatLab programming for pattern formation) and Jitender.

I do not have enough words to adequately thank my parents and my brother for everything they have done to enable me to be as ambitious as I wanted. Thanks for being proud of me even without knowing very well about what I have been working on during these years. At the same time, I have to thank all my relatives for their support. Many thanks to my wonderful wife Usha-wouldn't have made it without her selfless love, support and tolerating the long periods of being neglected because of my thesis..

Finally, I want to use this opportunity to thank the almighty God for his strange favour in my life.

IIT Guwahati — Dinesh Kumar

Abstract

This thesis examines the efficient and important role of additional food in a predator-prey system. In this work, we derive and study a model for two species. The prey population is assumed to be growing logistically in absence of predators, with the predators having an additional food (non-prey) source apart from natural prey and the functional response is assumed to be ratio-dependent. This leads to the development of a modified ratio-dependent model. We study the modified ratio-dependent model via stability (local and global) analysis and analyze the consequences of providing additional food to the predators. By taking the spatial component into account we consider a diffusive modified ratio-dependent model and obtain the necessary conditions for Turing instability to occur. We determine the role of additional food supply in the formation of Turing patterns. We also look into the effect of prey harvesting in the system with and without additional food supply to predators. This is accomplished by examining the stability analysis results and obtaining the optimal harvesting policy for both the ratio-dependent and modified ratio-dependent model with prey harvesting. Finally, we study a minimum time optimal control problem for controlling pest (prey) population, where the quality of additional food is taken as the control variable.

Contents

List of Figures

List of Tables

Chapter 1

Introduction and Thesis Outline

1.1 Introduction

In the ecological world there are complex interactions between and amongst the species that constitute the ecological environment. These competition come in various forms, the most common being competition for food (intra species) and predator-prey relation (inter species). The pioneering model of predator-prey interaction due to Lotka and Volterra [1] has motivated extensive study in the area of ecological modeling. The predator-prey models typically incorporates, through a functional response, how a predator responds to changes in the prey density per unit time per predator [2]. Different choices of the functional response has given rise to a wide variety of models. Holling developed three types of functional response (known as Holling type I, II and III) [1, 3, 4, 5] based on empirical field data. These functional forms (linear, hyperbolic and sigmoidal) were motivated by the nature of consumption of the prey by the predator.

The traditional approach to predator-prey models, which involves the assumption that the functional response depends only on the density of the prey population, has come under a lot of scrutiny. An alternative model proposed by Arditi and Ginzburg [6], is based on the assumption that the functional response should be dependent on the densities of both the predator and prey population. They argued that the traditional functional response describes the consumption rate of predators on fast (behavioral) time scale (minutes or hours) as compared to the growth of population which is on slow time scale (days or months). They further suggested that functional response should be considered on the slow time scale of population dynamics for consistency, and presented the ratio-dependent model. The ratio-dependent model has been extensively studied and analyzed by various authors [2, 7, 8, 9]. Kuang and Baretta [7] and Xiao and Ruan [8] studied the global dynamics of the ratio dependent system. Jost et al. [9] studied the deterministic extinction of such models, while Bandyopadhyay and Chattopadhyay [2] analyzed the model by including stochasticity in the form of white noise.

Another important aspect of ecological modeling is the study of the consequence of providing

additional food to the predators and the impact on the dynamics of the predator-prey system. There could be several motivation behind this, such as conservation of species or control of a pest population. One such example is of plants protecting themselves by controlling the size of herbivorous arthropods. They accomplish this by providing alternative food to the predators of herbivorous arthropods [10]. Several articles dealing with the concept of alternative food and the effect on the targeted prey population have appeared in literature [11, 12, 13, 14, 15, 16, 17, 18, 19]. Holt [12] explains the notion of *apparent competition* (competition that arises between focal and alternative prey where presence of alternative prey intensifies the predation of the focal prey [15]) leading to decrease in the equilibrium density due to alternative food available to the predator. Holt [14] suggests that segregation of alternative prey species could play a key role in the coexistence of such species. Sabelis and Van Rijn [16] study the role of alternative food in biological control, especially conditions which could lead to extermination, decline or no effect on the densities of the species.

We follow the work of Srinivasu et. al. [11], in which they study biological control through provision of additional food to predators in a modified Holling type II model. The modified Holling type II model predicts unbounded growth of predator density with limited quantity of additional food. This unrealistic result is attributed to the lack of intraspecific competition among the predator species. Taking this into account, we present a modified version of the classical ratio-dependent predator-prey model, by incorporating the supply of additional food to the predator population. The assumption is that the additional food supply is not time varying, but rather is maintained at a constant level [11, 17]. As pointed out in [11, 17], this assumption extends the advantage of dimensional reduction of the problem as well as simplifying the analysis of the consequences of additional food supply. Also, in the modified Holling type-II model, the quality of additional food is characterized by the handling time of the predators, which means that the predators have an important role in the decision on the quality of additional food. In order to make the quality independent of the predator's role, in our modified ratio-dependent model, the nutritional values of prey and additional food are taken into account.

The heterogeneity in an ecological environment influences the population dynamics of the biological species inhabiting the environment [20]. For instance, the mite experiment of Huffaker [21] concluded that two species of mites could rapidly go towards extinction in a small homogeneous environment but exhibit long term persistence if they were a part of an appropriate heterogenous environment. The study of spatiotemporal patterns in the population distribution of species in an ecological environment was greatly influences by the pioneering work of Alan Turing. In his 1952 seminal work [22], Turing, showed that reaction and diffusion in a system of chemical substances could give rise to inhomogeneous patterns and structures. This theory was applied to population dynamics by Segel and Jackson [23] who observed analogies between ecological interactions

and chemical interactions and analyzed a dissipative structure for a predator-prey model. They introduced diffusion (which usually acts as a stabilizing influence) to explain the spatiotemporal inhomogeneity that is observed as a result of interactions in an ecological system. Reaction-diffusion equations have been used to explain several spatiotemporal ecological dynamics, such as waves of invasion, pattern formation and impact of shape, size and heterogeneity of the spatial domain (see [24, 25] and the references therein).

Malchow [26] showed how differential fluxes can disturb the stability of interactive chemical or biological systems which can lead to the formation of stationary or travelling spatial structures. He illustrated this through a two-species predator-prey system. Medvinsky et al. [27] in their review article investigate in detail the complexities and chaos that arise in aquatic ecosystems from spatiotemporal dynamics. Correlation between Rosenzweig's paradox of enrichment and the evolution of chaotic spatiotemporal chaos, is demonstrated in [28], by making use of two different spatiotemporal models, which are reaction-diffusion in nature with one of them having a cutoff at low population densities. The simulation based demonstration showed that the emerging patterns are self-organized and does not arise as a result of initial spatial heterogeneity that existed. Reaction-diffusion models for predator-prey interaction have been extensively studied resulting in a wide range of patterns arising because of Turing instability as well non-Turing ones like spatiotemporal chaos (see [24, 25] and the references therein).

In [29] a modified Leslie-Gower model which incorporates prey refuge is investigated for spatiotemporal dynamics. Five different types of complex Turing patterns are observed in this model, which is a consequence of prey refuge. The impact of cannibalism by the predator could result in self-organized Turing patterns for a predator-prey system with a Holling-type II functional response [30]. A spatiotemporal study on a predator-prey system with Ivlev-type functional response leads to spiral and chaotic spiral patterns [31]. A study of Beddington-DeAngelis predator-prey model reveals several bifurcations (codimension-2 Turing-Hopf, Turing-Saddle-node, Turing-Transcritical bifurcation and the codimension-3 Turing-Takens-Bogdanov bifurcation) leading to various complex patterns [32]. Baurman et al. [33] study a generalized predator-prey model by incorporation diffusion and identify codimension-2 Turing-Hopf bifurcation and codimension-3 Turing-Takens-Bogdanov bifurcation. Simulations showed various long-term consequences such as homogeneous distributions, stationary spatial patterns and complex spatiotemporal patterns. A predator-prey system with logistic growth but nonlinear diffusion for the predator population is studied in [34]. Wang et al. [35] studied a reaction-diffusion predator model induced by Allee effect and observed rich and complex patterns as a result of the diffusion as well as the Allee effect.

The impact of diffusion on the stability of a ratio-dependent predator-prey model is discussed in [36] and the conditions under which Turing instability occurs are derived. A diffusion driven predator-prey model resulting in self replication patterns is discussed by Banerjee [37]. Turing

instability in a ratio-dependent predator-prey model with the predator mortality being an increasing function of predator density leads to Turing bifurcation, resulting in non-homogeneous patterns [38]. We study the nature of spatiotemporal dynamics and patterns for a diffusive modified ratio-dependent model under supply of additional food to the predators and examine the role of additional food in the formation of spatiotemporal patterns.

In addition to ecological motivations for studying predator-prey systems, there are practical considerations also such as harvesting for food and commercial purposes. The balance between harvesting and conservation is a key problem in bioeconomic management of species in an ecological environment. There has been significant amount of work in bioeconomic modeling and management of renewable resources. The book by Clark [39] is a classical and excellent introduction in this area and is devoted to the theoretical study on management of renewable resources under bioeconomic conservation. The application and usefulness of optimal control theory in bioeconomic management of population of species in an ecological environment is discussed in detail by Goh [40]. Bioeconomics of a renewable resource, namely the prey population, in presence of a predator is discussed in [41]. A part of the effort during the harvesting process is dedicated towards prey harvesting while the remaining effort is directed at decreasing the levels of predator population. The determination of optimal strategy for prey harvesting while ensuring conservation of the predator population is discussed in [42] under several considerations. The dynamical properties under a non-zero constant rate of harvesting of prey population for classical ratio-dependent model is studied in [43]. The implications of incorporating two different non-constant harvesting functions for predator harvesting and the resulting dynamics for a ratio-dependent model are presented in [44]. More recently, Kar and Ghosh [45] studied the consequences of additional food being supplied to the predators and the effect of harvesting of both the prey as well as predator population modeled through a Holling type-II functional response. Taking the adverse impact of over exploitation of populations, a harvesting model with a two-patch environment was proposed in [46]. The predator-prey model with a Holling type-II functional response was considered in an area with two patches, one in which free fishing was allowed and the other patch which was a reserve area with a prohibition on fishing effort.

We consider a predator-prey system in which the prey population is subject to harvesting while the predator population is excluded from the harvesting process. The latter exclusion can be alluded to various reasons such as lack of economic viability of such harvesting, predator conservation etc. In effect, both the predator and the harvester are competing for the same resource, namely, the prey population. While the harvesting effort does not have an explicit effect on the predator population levels, the indirect effect (as a consequence of harvesting induced reduced availability of prey) does exist. On the other hand, the predator population also has an implicit effect on the harvesting, resulting in reduced economic gains for the harvesters. As noted in our study, the

provision of additional food (non-prey) for the predators reduces the pressure of natural predation of prey population by the predators. Also, this could lead to the growth of the predator population independent of the preys. One would expect that in both the cases, the harvesters will achieve greater economic benefit as compared to the system where no additional food is available to the predators. The idea of introducing the predators to this additional food (as a part of total harvest effort) can be helpful in conservation of both the species as well as better economic returns. To examine the role of additional food in prey harvesting, we consider a predator-prey system with the ratio-dependent and modified ratio-dependent functional response. We study these two models with the incorporation of the harvesting term.

Another practical considerations for studying predator-prey system is pest (prey) control. It is reasonable to expect the pest population can be controlled and driven to a desired level in the minimum possible time. This leads to what is known as time optimal control problem. Goh [40] discusses several possible scenarios of optimal control theory being applied in predator-prey systems. Srinivasu and Prasad [18] considered a Holling type-II predator-prey system with additional food being made available to predators. The system was analyzed from the perspective of pest management and biological conservation. A prey-predator system with a general functional response was studied in an optimal control problem setting in [47, 48] where the control function is taken as the rate of mixture of the populations. We consider the optimal control problem with minimum time subject to the ratio-dependent system with additional food supply to predators (or modified ratio-dependent model). We examine the role of additional food supply in controlling pest population by making use of an optimal control strategy.

1.2 Thesis Outline

The organization of the thesis is as follows.

In Chapter 2, we introduce a modified ratio-dependent model by incorporating the supply of additional food to the predators. The supply of this additional food to predator species is uniformly distributed and constant with respect to time, while the chosen functional response is ratio-dependent.

For better understanding of the role of provision of additional food to predators, each of the problem in this thesis have been studied under two natural conditions on the ratio-dependent predator-prey system (before the supply of additional food is taken into account). Firstly, either predator or both predator and prey populations go towards extinction with the passage of time. Secondly, both the predator and prey populations coexist forever. We describe these natural conditions by three mathematically equivalent cases: (i) when interior equilibrium point of the ratio-dependent model does not exist, (ii) when interior equilibrium point of the ratio-dependent

model does exist but unstable in nature and (iii) interior equilibrium point of the ratio-dependent model does exist and stable in nature.

In Chapter 3, we deal with the local and global stability analysis of the modified ratio-dependent model. Our study shows that the supply of additional food supply plays a crucial role in management of the populations and the conclusions justify the practicality of the problem. Numerical examples support the theoretical results obtained.

In Chapter 4, we consider the spatiotemporal modified ratio-dependent model with both the predator and prey species exhibiting diffusivity. We determine the necessary conditions for Turing instability to occur, by making use of the separation of variable technique locally. The additional food parameters hold the key to obtaining spatiotemporal patterns. By using a finite difference numerical scheme, we perform a series of numerical simulations which shows the occurrence of spatiotemporal patterns for both the prey and predator species with the additional food supply.

In Chapter 5, we examine the effect of prey harvesting on both the ratio-dependent and the modified ratio-dependent predator-prey system. We analyze both the models from two perspectives. Firstly, we do the stability analysis, which determines the interval (range) for ecologically sustainable harvesting effort. We observe that in case of the modified ratio-dependent model, this interval is dependent on the additional food parameters. For the second approach, we use control theory (Pontryagin's maximum principle) to determine the optimal harvesting policy for both the models. Results show that system can sustain much improved optimal prey harvesting rate with additional food supply. We present some illustrative numerical examples which are consistent with the theoretical results.

In Chapter 6, we study one more application of providing additional food to predator species. From stability analysis of the modified ratio-dependent model studied in Chapter 3, we observe that the quality of additional food plays a direct role in the control of pest (prey) population. It is desirable that pest population is driven to an ideal level in the minimum possible time. To serve this purpose, we formulate and study a minimum time optimal control problem where the target state is specified. Numerical examples under the three natural conditions are presented.

Finally, we conclude and outline the future directions of the thesis in Chapter 7. The numerical simulations for this thesis, were carried out using using MatLab™ .

Chapter 2

The Modified Ratio-Dependent Model

In this chapter, we present a modified ratio-dependent model by incorporating the supply of additional food to the predators. This is accomplished by considering a classical ratio-dependent predator-prey system where the prey is assumed to be growing logistically in absence of predation and the predator has a constant mortality rate. We assume that additional food is being supplied to the predators at a constant level. The construction of the functional response for the modified system is the same as the classical ratio-dependent system, with the only difference being the number of sources of food available to the predators.

2.0.1 Model without Additional Food

The considered classical ratio-dependent predator-prey model due to Arditi and Ginzburg [6] is given by,

$$\begin{aligned} \frac{dN}{dT} &= rN\left(1-\frac{N}{K}\right) - \frac{e_1(\frac{N}{P})}{1+e_1h_1(\frac{N}{P})}P, \\ \frac{dP}{dT} &= \frac{n_1e_1(\frac{N}{P})}{1+e_1h_1(\frac{N}{P})}P - m'P. \\ N(0) > 0, P(0) > 0,\ & r, K, e_1, h_1, n_1, m' > 0, \end{aligned} \tag{2.0.1}$$

which is defined for all $(N,P) \in [0,\infty)\times[0,\infty)/(0,0)$, and $\frac{dN}{dT} = 0 = \frac{dP}{dT}$, when $(N,P) = (0,0)$. Here $N(T)$ and $P(T)$ represent the prey and predator population density at time T respectively. The parameter r is the intrinsic growth rate of the prey in absence of predation, K is the carrying capacity of the prey and m' is the per capita mortality rate of the predators. The parameter e_1 is the rate of predator attack on prey, h_1 is the handling time (per predator per prey). Finally, the parameter n_1 is the nutritional value of the prey.

Derivation of the Functional Response (on the lines of [1]):

Let $\mathcal{T}$ be the total time spent by predators in encounter of prey and V be the number of prey

victims. Assuming that the number of prey victims is proportional to the ratio N/P (average share of prey per predator) and total searching time spent by each predator for each prey item, we get

$$V = e_1(\mathcal{T} - h_1 V)\left(\frac{N}{P}\right),$$

where e_1 is the proportionality constant. Now solving for V, we obtain

$$V = \frac{e_1\mathcal{T}(\frac{N}{P})}{1 + e_1 h_1\left(\frac{N}{P}\right)}.$$

Thus the total number of prey victims per predator per unit time is,

$$V = \frac{e_1(\frac{N}{P})}{1 + e_1 h_1\left(\frac{N}{P}\right)}.$$

2.0.2 Model with Additional Food

We now present a modified ratio-dependent model that incorporates the supply of additional food to the predators. The biomass A of this additional food supply is assumed to be available uniformly within the ecological domain at a constant level. The advantage of a constant rate of provision of additional food to predators is in the reduction of dimension of the system as well as simplification of the analysis. The governing coupled differential equations of the predator-prey system with additional food being provided to predators, is given by,

$$\begin{aligned} \frac{dN}{dT} &= rN\left(1 - \frac{N}{K}\right) - \frac{e_1(\frac{N}{P})}{1 + e_1 h_1(\frac{N}{P}) + e_2 h_2(\frac{A}{P})}P, \\ \frac{dP}{dT} &= \frac{n_1 e_1(\frac{N}{P}) + n_2 e_2(\frac{A}{P})}{1 + e_1 h_1(\frac{N}{P}) + e_2 h_2(\frac{A}{P})}P - m'P. \end{aligned} \tag{2.0.2}$$

$$N(0) > 0, P(0) > 0,\ r, K, e_1, h_1, e_2, h_2, n_1, n_2, m' > 0,$$

which is defined for all $(N, P) \in [0, \infty) \times [0, \infty)$. Here, parameter e_2 is the rate of predator attack on additional food, h_2 is the handling time (per predator per unit of the ratio A/P additional food biomass) and n_2 is the nutritional value of the additional food. The dimension of all the parameters that appear in system (2.0.1) and (2.0.2) are presented in Table 2.1.

Derivation of the Functional Response:

Assuming that the number of prey victims is proportional to ratio N/P (average share of prey per predator) and total searching time as well as inversely proportional to ratio A/P (average share of additional food per predator) and handling time h_2, we get

$$V = e_1 e_2^{-1} h_2^{-1}(\mathcal{T} - h_1 V)\left(\frac{N}{P}\right)\left(\frac{A}{P}\right)^{-1},$$

where $e_1e_2^{-1}$ is the proportionality constant. Now solving for V, we obtain

$$\begin{aligned} &= e_1e_2^{-1}h_2^{-1}\mathcal{T}\left(\frac{N}{P}\right)\left(\frac{A}{P}\right)^{-1}, \\ V &= \frac{e_1\mathcal{T}\left(\frac{N}{P}\right)}{e_1h_1\left(\frac{N}{P}\right)+e_2h_2\left(\frac{A}{P}\right)} \end{aligned}$$

Hence, the total number of prey victims per predator per unit time in presence of additional food supply to predators is

$$V = \frac{e_1(\frac{N}{P})}{e_1h_1\left(\frac{N}{P}\right)+e_2h_2\left(\frac{A}{P}\right)}.$$

For all discussion from now onwards, we shall refer to the model without additional food as "classical ratio-dependent model" and the model with additional food as "modified ratio-dependent model".

Parameters	r	K	m'	e_1	e_2	n_1	n_2	h_1	h_2	A
Dimension	time^{-1}	biomass	time^{-1}	time^{-1}	time^{-1}	percent	percent	time	time	biomass

Table 2.1: Dimension of the parameters present in system (2.0.1) and (2.0.2).

2.1 Non-Dimensionalized Form of the Model

We simplify both the models by making use of the following transformations,

$$x = N/K, y = P/Ke_1h_1, t = rT.$$

Using the chain rule, we get,

$$\begin{aligned} \frac{dx}{dt} &= \frac{dx}{dN}\times\frac{dN}{dT}\times\frac{dT}{dt} = \frac{1}{Kr}\times\frac{dN}{dT}, \\ \frac{dy}{dt} &= \frac{dy}{dP}\times\frac{dP}{dT}\times\frac{dT}{dt} = \frac{1}{Ke_1h_1r}\times\frac{dP}{dT}. \end{aligned} \tag{2.1.1}$$

2.1.1 Ratio-Dependent Model

From equation (2.0.1) and (2.1.1), we have

$$\begin{aligned} \frac{dx}{dt} &= \frac{N}{K}\left(1-\frac{N}{K}\right)-\frac{(\frac{e_1}{r})\frac{N}{K}(\frac{P}{Ke_1h_1})}{(\frac{P}{Ke_1h_1})+\frac{N}{K}}, \\ \frac{dy}{dt} &= \frac{\frac{n_1e_1}{re_1h_1}\frac{N}{K}(\frac{P}{Ke_1h_1})}{(\frac{P}{Ke_1h_1})+\frac{N}{K}}-\frac{m'}{r}\left(\frac{P}{Ke_1h_1}\right) \end{aligned}$$

Introduction of the parameters $c = e_1/r$, $m = m'/r$ and $b = n_1/m'h_1$ results in the following non-dimensionalized form of the ratio-dependent model

$$\begin{aligned} \frac{dx}{dt} &= x\,(1-x) - \frac{cxy}{x+y}, \\ \frac{dy}{dt} &= m\left(\frac{bx}{x+y} - 1\right) y. \end{aligned} \tag{2.1.2}$$

2.1.2 Modified Ratio-Dependent Model

From equation (2.0.2) and (2.1.1), we have

$$\begin{aligned} \frac{dx}{dt} &= \frac{N}{K}\left(1 - \frac{N}{K}\right) - \frac{(\frac{e_1}{r})\frac{N}{K}(\frac{P}{Ke_1h_1})}{(\frac{P}{Ke_1h_1}) + \frac{N}{K} + \frac{e_2h_2}{e_1h_1}\frac{A}{K}}, \\ \frac{dy}{dt} &= \frac{\frac{n_1e_1}{re_1h_1}\left[\frac{N}{K} + \frac{n_2e_2}{n_1e_1}\frac{A}{K}\right](\frac{P}{Ke_1h_1})}{(\frac{P}{Ke_1h_1}) + \frac{N}{K} + \frac{e_2h_2}{e_1h_1}\frac{A}{K}} - \frac{m'}{r}\left(\frac{P}{Ke_1h_1}\right). \end{aligned}$$

The introduction of the parameters $c = e_1/r$, $\alpha = n_1h_2/n_2h_1$, $\xi = \eta A/K$, $m = m'/r$, $b = n_1/m'h_1$ and $\eta = n_2e_2/n_1e_1$ reduces the modified ratio-dependent model to the following non-dimensionalized form

$$\begin{aligned} \frac{dx}{dt} &= x\,(1-x) - \frac{cxy}{x+y+\alpha\xi}, \\ \frac{dy}{dt} &= m\left(\frac{b\,[x+\xi]}{x+y+\alpha\xi} - 1\right) y. \end{aligned} \tag{2.1.3}$$

Here the parameters c, m and b (also in the original model) are ecological in nature, while α and ξ are the control parameters that can be manipulated by humans. The parameter α characterizes the quality of the additional food relative to the prey, with respect to their nutritional value, while ξ is representative of the quantity of additional food being made available to the predators.

Chapter 3

Dynamics of the Modified Ratio-Dependent Model

In this chapter, the dynamics of the modified ratio-dependent model is analyzed in terms of local and global stability analysis. The conditions for local stability and global stability of all equilibria of the model are established. In this study, transcritical, saddle-node and Hopf bifurcations are observed. The impact of additional food supply in predator-prey system is discussed and numerical simulations supporting the analysis is presented.

3.1 Ratio-Dependent Model

3.1.1 Existence of Equilibrium Points

The ratio-dependent system (2.1.2) admits a trivial equilibrium point $(0,0)$ (for detail see [9]), an axial equilibrium point $(1,0)$ and an interior equilibrium point $(\check{x},\check{y})$. Here, $(\check{x},\check{y})$ is obtained by solving the prey isocline, $(1-x)-\frac{cy}{x+y}=0$ and the predator isocline, $\frac{bx}{x+y}-1=0$. The point $(0,0)$ corresponds to both the species being extinct while $(1,0)$ corresponds to the prey being at its carrying capacity and predators being extinct. Finally, $(\check{x},\check{y})$ represents the coexistence of both the species, where

$$\check{x}=(1-c)+\frac{c}{b}$$

and $\check{y}=(b-1)\check{x}$. Thus the conditions $b>1$ and $c<\frac{b}{b-1}$ need to be satisfied for the existence of $(\check{x},\check{y})$.

The conditions on the model parameters, required for the existence of the three equilibrium points are given in Table 3.1,

3.1.2 Boundedness of the Solution

Theorem 3.1.1. *If $(x(t),y(t))$ represents the solution of system (2.1.2), $x(t)$ will be bounded for any initial condition $x(0)\geq 0$, $y(0)\geq 0$.*

Equilibrium point	Existential Conditions
$(0,0)$	-
$(1,0)$	-
$(\check{x},\check{y}) = (1-c+\frac{c}{b},(b-1)\check{x})$	$b>1$ and $c<\frac{b}{b-1}$

Table 3.1: Conditions on parameters for existence of equilibrium points of the ratio-dependent system (2.1.2).

Proof. To begin with, a simple vector field analysis can be used to show that the solutions of the modified system (2.1.2) are non-negative.
Also, from the first equation in (2.1.2),

$$\frac{dx}{dt} \leq x(1-x) \;\Rightarrow\; \lim_{t\to+\infty} \sup x(t) \leq 1.$$

Hence $x(t)$ is bounded for any non-negative initial condition. □

Theorem 3.1.2. *If $(x(t),y(t))$ represents the solution of system (2.1.2) and $x(t)$ is bounded above, then $y(t)$ is also bounded above for any initial condition $x(0)\geq 0$, $y(0)\geq 0$.*

Proof. Since $\lim_{t\to+\infty} \sup x(t) \leq 1$, that is for any $\epsilon>0$ there exist a $T>0$, s.t. $x(t)\leq 1+\epsilon/b$ $\forall\, t\geq T$, then it follows from the predator equation,

$$\frac{dy}{dt} = m\left(\frac{bx}{x+y}-1\right)y \leq m\left(b\left(1+\frac{\epsilon}{b}\right)-y\right),\; t\geq T \;\Rightarrow\; \lim_{t\to+\infty}\sup y(t) \leq b+\epsilon$$

Since $\epsilon>0$ is arbitrary, we have $\lim_{t\to+\infty}\sup y(t)\leq b$. Hence $y(t)$ is bounded for any non-negative initial condition. □

3.1.3 Local Stability Analysis

The Jacobian matrix for (2.1.2) is given by

$$J = \begin{bmatrix} (1-x)-\frac{cy}{x+y}+x\left[-1+\frac{cy}{(x+y)^2}\right] & -\frac{cx^2}{(x+y)^2} \\ \frac{bmy^2}{(x+y)^2} & m\left(\frac{bx}{x+y}-1\right)-\frac{bmxy}{(x+y)^2} \end{bmatrix}.$$

The Jacobian matrix at $(1,0)$ is of the form

$$J_{(1,0)} = \begin{bmatrix} -1 & -c \\ 0 & m(b-1) \end{bmatrix}.$$

Thus $(1,0)$ is stable when $b<1$. Note that whenever $(1,0)$ is stable, the interior equilibrium point $(\check{x},\check{y})$ does not exist. However, whenever the interior equilibrium point exists, $(1,0)$ is always a saddle point.

The Jacobian matrix evaluated at $(\check{x},\check{y})$ is given by

$$J_{(\check{x},\check{y})} = \begin{bmatrix} \check{x}\left[-1+\frac{c\check{y}}{(\check{x}+\check{y})^2}\right] & -\frac{c\check{x}^2}{(\check{x}+\check{y})^2} \\ \frac{bm\check{y}^2}{(\check{x}+\check{y})^2} & -\frac{bm\check{x}\check{y}}{(\check{x}+\check{y})^2} \end{bmatrix}$$

This was obtained by substituting the prey and the predator isocline in J. Using the Routh-Hurwitz criterion it can be shown that the interior equilibrium point (if it exists) is stable if

$$c < \frac{b\,(m(b-1)+b)}{b^2-1}.$$

At the trivial equilibrium point $(0,0)$, the Jacobian cannot be evaluated, since it involves terms which are undefined for $(0,0)$. To analyze the behaviour around $(0,0)$ we use a transformed system after Jost et al. [9]. The transformed system to be called the $u-y$ system and the $x-v$ system are given by $u=\frac{x}{y}, y=y$ and $x=x, v=\frac{y}{x}$ respectively. The system (2.1.2) in the transformed $u-y$ system is given by,

$$\begin{aligned} \frac{du}{dt} &= u\,(1+m-uy) - \frac{u(c+bmu)}{u+1}, \\ \frac{dy}{dt} &= m\left(\frac{bu}{u+1}-1\right)y. \end{aligned}$$

The corresponding Jacobian for the $u-y$ system is given by

$$J^{(u,y)} = \begin{bmatrix} (1+m-uy) - \frac{(c+bmu)}{u+1} + u\left[-y-\frac{bm-c}{(u+1)^2}\right] & -u^2 \\ \frac{mby}{(u+1)^2} & m\left(\frac{bu}{u+1}-1\right) \end{bmatrix},$$

which evaluated at $(0,0)$ gives,

$$J^{(u,y)}_{(0,0)} = \begin{bmatrix} 1+m-c & 0 \\ 0 & -m \end{bmatrix}.$$

The point $(0,0)$ in this system is a saddle for $c<m+1$ and an attractor for $c>m+1$.
Similarly equation (2.1.2) in the transformed $x-v$ system is given by,

$$\begin{aligned} \frac{dx}{dt} &= x\left[(1-x)-\frac{cv}{v+1}\right] \\ \frac{dv}{dt} &= v(x-1-m)+\frac{v(bm+cv)}{v+1} \end{aligned}$$

The corresponding Jacobian for the $x-v$ system is given by

$$J^{(x,v)} = \begin{bmatrix} \left[(1-x)-\frac{cv}{v+1}\right]-x & x\left[-\frac{(v+1)c-cv}{(v+1)^2}\right] \\ v & v\left[\frac{(v+1)c-(bm+cv)}{(v+1)^2}\right]+(x-1-m)+\frac{(bm+cv)}{v+1} \end{bmatrix},$$

whose value at $(0,0)$ is,

$$J^{(x,v)}_{(0,0)} = \begin{bmatrix} 1 & 0 \\ 0 & -1-m+bm \end{bmatrix}.$$

In this case $(0,0)$ is a saddle when $b < (m+1)/m$ and both eigenvalues are positive when $b > (m+1)/m$. Thus the point $(0,0)$ in this system is always unstable.

Following the analysis of Jost et al. [9] we conclude that $(0,0)$ in the $u-y$ system is a saddle for $c < m+1$. On the other hand for $c > m+1$, $(0,0)$ in the $u-y$ system is an attractor. The consequence of this in the $x-y$ system is that a trajectory can reach $(0,0)$ in the $x-y$ system only if x approaches 0 faster as compared to y.

3.1.4 Global Stability Analysis

Theorem 3.1.3. *Suppose that the interior equilibrium point $(\check{x},\check{y})$ is locally asymptotically stable and the condition $m(b-1) \geq 1$ holds, then $(\check{x},\check{y})$ is also globally stable.*

Proof. We consider the following function,

$$L_1(x,y) = \frac{\partial}{\partial x}\left(B_1(x,y)f_1(x,y)\right) + \frac{\partial}{\partial y}\left(B_1(x,y)g_1(x,y)\right),$$

where $f_1(x,y) = x\left(1-x\right) - \frac{cxy}{x+y}$, $g_1(x,y) = m\left(\frac{bx}{x+y} - 1\right)y$ and $B_1(x,y) = \frac{x+y}{xy^2}$.
After simplification, we obtain,

$$L_1(x,y) \quad = \quad \frac{1-(b-1)m-2x-y}{y^2}.$$

Now, $L_1(x,y) < 0$ whenever $x > 0$ and $y > 0$, since $m(b-1) \geq 1$. Thus, by using the Dulac's criterion [49], the system (2.1.2) will not have any non-trivial periodic orbit in $\mathbb{R}^2_+$. Note that both the trivial and the axial equilibrium points are saddle and have $y-$axis and $x-$axis as their respective stable manifolds. Using this in conjunction with the Poincare-Bendixson Theorem [49] gives us that the interior equilibrium point $(\check{x},\check{y})$ will be globally stable. □

Assuming that both the predator and prey populations coexist before the supply of additional food takes place, one of the following two things can happen with the passage of time,

- Either predator or both predator and prey populations go towards extinction.
- Both the predator and prey populations coexist forever.

In view of boundedness of the solution of system (2.1.2) and the Poincare-Bendixson theorem [49], the above two cases are converted into following three mathematically equivalent cases, which arise from the existence and stability conditions for the interior equilibrium point of ratio-dependent model (2.1.2):

1. When the interior equilibrium point does not exist.

2. When the interior equilibrium point exists with unstable nature.

3. When the interior equilibrium point exists with stable (globally) nature.

Cases	Conditions	Ensures
Case 1		
(i)	$b > 1,\ c \geq \frac{b}{b-1}$	$(\check{x}, \check{y})$ does not exist
(ii)	$b < 1$	$(\check{x}, \check{y})$ does not exist
(iii)	$b = 1$	$(\check{x}, \check{y})$ does not exist
Case 2	$c < \frac{b}{b-1}$	$(\check{x}, \check{y})$ is exist
	$c > \frac{b}{b^2-1}\,(b + m(b-1))$	$(\check{x}, \check{y})$ is unstable
Case 3	$c < m + 1$	$(0, 0)$ is saddle
	$b > 1$	$(1, 0)$ is saddle
	$c < \frac{b}{b-1},\ m(b-1) \geq 1$	$(\check{x}, \check{y})$ is globally stable

Table 3.2: Conditions on parameters for the classical ratio-dependent system (2.1.2) under all the three cases.

Note that $\frac{b}{b-1} \leq \frac{b}{b^2-1}(b + m(b-1)) \Longleftrightarrow m(b-1) \geq 1$.

3.2 Modified Ratio-Dependent Model

3.2.1 Existence of Equilibrium Points

The modified ratio-dependent system (2.1.3) admits a trivial equilibrium point, $(0, 0)$ and two axial equilibrium points, $(1, 0)$ and $(0, (b-\alpha)\xi)$ (when $b > \alpha$). The interior equilibrium points of the system (2.1.3) can be obtained by setting,

$$(b-1)x + (b-\alpha)\xi = \frac{(1-x)\,(x+\alpha\xi)}{x+c-1} \Longrightarrow x^2 + \left(c - 1 - \frac{c}{b} + \xi\right)x + \xi\left(c - 1 - \frac{\alpha c}{b}\right) = 0.$$

The roots of the above equation are given by,

$$x_{1,2} = \frac{1}{2}\left[-\left(c - 1 - \frac{c}{b} + \xi\right) \mp \sqrt{\left(c - 1 - \frac{c}{b} + \xi\right)^2 - 4\xi\left(c - 1 - \frac{\alpha c}{b}\right)}\right]$$

Thus the system can admit the following equilibrium points,

1. Trivial : $A(0,0)$
2. Axial :
   - $B(1,0)$
   - $C\,(0,(b-\alpha)\xi)$
3. Interior :
   - $D(x_1,y_1)$
   - $E(x_2,y_2)$

where $y_i=(b-1)x_i+(b-\alpha)\xi$ for $i=1,2$. Taking $\Delta=\left(c-1-\frac{c}{b}+\xi\right)^2-4\xi\left(c-1-\frac{\alpha c}{b}\right)$, we obtain the conditions (given in Table 3.3) on the model parameters, required for the existence of the above equilibrium points.

Equilibrium point	**Existential conditions**
$A(0,0)$	-
$B(1,0)$	-
$C(0,(b-\alpha)\xi)$	$b>\alpha$
$D(x_1,y_1)$	$c-1-\frac{c}{b}+\xi<0,\ c-1-\frac{\alpha c}{b}>0,\ \Delta>0,\ x_1<1$ or $c-1-\frac{c}{b}+\xi<0,\ \Delta=0,\ x_1<1$
$E(x_2,y_2)$	$c-1-\frac{c}{b}+\xi<0,\ c-1-\frac{\alpha c}{b}>0,\ \Delta>0,\ x_2<1$ or $c-1-\frac{c}{b}+\xi<0,\ c-1-\frac{\alpha c}{b}=0,\ x_2<1$ or $c-1-\frac{c}{b}+\xi<0,\ \Delta=0,\ x_2<1$ or $c-1-\frac{\alpha c}{b}<0,\ x_2<1$

Table 3.3: Conditions on parameters for existence of equilibrium points of the system (2.1.3).

Note that if $0<x_i<1$, then $y_i>0$. To prove this, consider $y_i=\frac{(1-x_i)(x_i+\alpha\xi)}{x_i+c-1}$. It is easy to see that $y_i>0$ for $c\geq 1$. So we need to only check for case when $c<1$. Recalling that $x=1-c$ is an asymptote to the prey isocline $y=\frac{(1-x)(x+\alpha\xi)}{x+c-1}$, we conclude that $x_i>1-c$. Thus $y_i>0$ for $c<1$ also.

The location of the existence/non-existence of the equilibria in (α, ξ)-parameter space is given in Figure 3.1 (for existential condition of the interior equilibria see Appendix A)

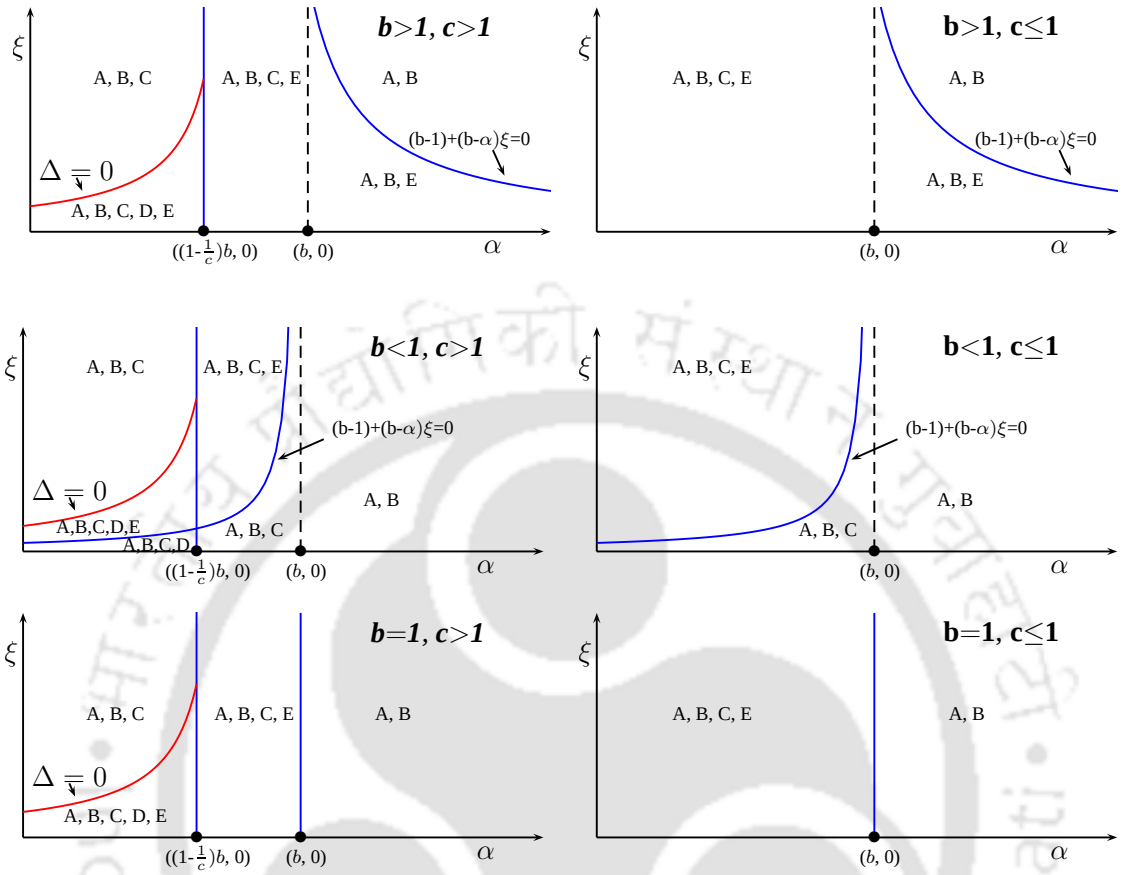

Figure 3.1: Figure illustrates the locations of existence of various equilibria of the system (2.1.3) in (α, ξ)-plane, under all possible behavior of ecological parameters c, b and m. The appearances of the equilibria in particular subdomain of the (α, ξ)-plane shows their existence in it.

3.2.2 Boundedness of the Solution

Theorem 3.2.1. *If $(x(t), y(t))$ represents the solution of system (2.1.3), $x(t)$ will be bounded for any initial condition $x(0) \geq 0$, $y(0) \geq 0$.*

Proof. To begin with, a simple vector field analysis can be used to show that the solutions of the modified system (2.1.3) are non-negative.
Also, from the first equation in (2.1.3),

$$\frac{dx}{dt} \leq x(1-x) \;\Rightarrow\; \lim_{t\to+\infty} \sup x(t) \leq 1.$$

Hence $x(t)$ is bounded for any non-negative initial condition. □

Theorem 3.2.2. *If $(x(t), y(t))$ represents the solution of system (2.1.3) and $x(t)$ is bounded above, then $y(t)$ is also bounded above for any initial condition $x(0) \geq 0$, $y(0) \geq 0$.*

Proof. Since $\lim_{t\to+\infty} \sup x(t) \leq 1$, that is for any $\epsilon > 0$ there exist a $T > 0$, s.t. $x(t) \leq 1 + \epsilon/b$ $\forall\ t \geq T$, then it follows from the predator equation,

$$\frac{dy}{dt} = m\left(\frac{b\,[x+\xi]}{x+y+\alpha\xi} - 1\right) y \leq m\left(b\left(1+\frac{\epsilon}{b}+\xi\right) - y\right)\ , t \geq T\ \Rightarrow\ \lim_{t\to+\infty} \sup y(t) \leq b(1+\xi) + \epsilon$$

Since $\epsilon > 0$ is arbitrary, we have $\lim_{t\to+\infty} \sup y(t) \leq b(1+\xi)$. Hence $y(t)$ is bounded for any non-negative initial condition. □

3.2.3 Local Stability Analysis

The Jacobian matrix for (2.1.3) is given by

$$J = \begin{bmatrix} (1-x) - \frac{cy}{x+y+\alpha\xi} + x\left[-1 + \frac{cy}{(x+y+\alpha\xi)^2}\right] & -\frac{cx(x+\alpha\xi)}{(x+y+\alpha\xi)^2} \\ \frac{bmy(y+\alpha\xi-\xi)}{(x+y+\alpha\xi)^2} & m\left(\frac{b[x+\xi]}{x+y+\alpha\xi} - 1\right) - \frac{bm(x+\xi)y}{(x+y+\alpha\xi)^2} \end{bmatrix}$$

Hence the Jacobian matrix for the equilibrium points A, B, C, D, and E are of the following form,

$$J_{(0,0)} = \begin{bmatrix} 1 & 0 \\ 0 & \frac{m}{\alpha}(b-\alpha) \end{bmatrix}$$

$$J_{(1,0)} = \begin{bmatrix} -1 & -\frac{c}{1+\alpha\xi} \\ 0 & \frac{m(b-1+(b-\alpha)\xi)}{1+\alpha\xi} \end{bmatrix}$$

$$J_{(0,(b-\alpha)\xi)} = \begin{bmatrix} 1-c+\frac{c\alpha}{b} & 0 \\ \frac{m(b-\alpha)(b-1)}{b} & -\frac{m(b-\alpha)}{b} \end{bmatrix}$$

$$J_{(x_i,y_i)} = \begin{bmatrix} x_i\left[-1 + \frac{cy_i}{(x_i+y_i+\alpha\xi)^2}\right] & -\frac{cx_i(x_i+\alpha\xi)}{(x_i+y_i+\alpha\xi)^2} \\ \frac{bmy_i(y_i+\alpha\xi-\xi)}{(x_i+y_i+\alpha\xi)^2} & -\frac{bm(x_i+\xi)y_i}{(x_i+y_i+\alpha\xi)^2} \end{bmatrix}$$

Note that $J_{(x_i,y_i)}$ is the Jacobian for both equilibrium points D and E. $J_{(x_i,y_i)}$ was obtained by substituting the two isoclines, $1 - x_i - \frac{cy_i}{x_i+y_i+\alpha\xi} = 0$ and $m\left(\frac{b[x_i+\xi]}{x_i+y_i+\alpha\xi} - 1\right) = 0$ in J. Now using the basic properties of determinants as well as the relation $x_i + y_i + \alpha\xi = b(x_i+\xi)$, we obtain (see Appendix A),

$$\det J_{(x_i,y_i)} \quad = \quad \frac{bcmx_iy_i}{(x_i+y_i+\alpha\xi)^3}\left[\xi(\alpha-1) + \frac{b}{c}(x_i+\xi)^2\right].$$

Also, using the two isoclines, we obtain,

$$tr\ J_{(x_i,y_i)} \quad = \quad \frac{-(b+1)x_i^2 - [(b\xi-1) + m(b-1)]\,x_i - m(b-\alpha)\xi}{b(x_i+\xi)}.$$

We will now discuss the dynamics of the modified ratio-dependent system (2.1.3), under each of the three cases (defined in Table 3.2). The casewise discussion is based on the various ranges of parameter α which are categorized into three parts: (a) $0 < \alpha < \left(1 - \frac{1}{c}\right) b$, (b) $\left(1 - \frac{1}{c}\right) b < \alpha < b$, and (c) $\alpha > b$.

3.2.4 Case 1

(i) : We first consider the range $0 < \alpha < \left(1 - \frac{1}{c}\right) b$, where the trivial equilibrium point A exists and is a repeller. Also, both the axial equilibrium points B and C exist, with the former being saddle in nature and the latter being stable for all values of ξ. Neither of the interior equilibrium points exist in this range.

As α moves into the range $\left(1 - \frac{1}{c}\right) b < \alpha < b$, the stability nature of A and B remains unchanged from the previous range. The axial equilibrium point C loses its stability and a single interior equilibrium point E comes into existence. The stability of E depends on the values of α and ξ. If $\Delta_1 < 0$ or $x_2 \notin I_1$, then E is stable for all values of ξ and a transcritical bifurcation takes place at $\alpha = \left(1 - \frac{1}{c}\right) b$. By fixing the value of ξ in the range $\left(0, \frac{1-m(b-1)}{b}\right)$ and varying α in the range$\left(\left(1 - \frac{1}{c}\right) b, b\right)$, a Hopf-bifurcation occurs for some value of α provided $tr\ \ J_{(x_2,y_2)} = 0$.

Finally, when $\alpha > b$, the trivial equilibrium point becomes a saddle, the axial equilibrium point C disappears and the interior equilibrium point E is stable if $x_2 \notin I_2$. Hopf-bifurcation will occur in this range of α also (provided $tr\ J_{(x_2,y_2)} = 0$). By fixing the value of $\alpha > b$ and increasing ξ, a transcritical bifurcation will take place at $\xi = \frac{b-1}{\alpha-b}$, since the single interior equilibrium point E disappears and the axial equilibrium point B becomes stable in nature. The summary of these results are presented in Figure 3.2. Note that here,

$$\begin{aligned}
\Delta_1 &= ((b\xi - 1) + m(b-1))^2 - 4m(b-\alpha)(b+1)\xi, \\
I_1 &= \left[-\frac{m(b-1) + (b\xi - 1) + \sqrt{\Delta_1}}{2(b+1)}, -\frac{m(b-1) + (b\xi - 1) - \sqrt{\Delta_1}}{2(b+1)}\right], \\
I_2 &= \left(0, -\frac{m(b-1) + (b\xi - 1) - \sqrt{\Delta_1}}{2(b+1)}\right].
\end{aligned}$$

(ii) : In the range $0 < \alpha < \left(1 - \frac{1}{c}\right) b$, if $\xi < \frac{1-b}{b-\alpha}$ then A exists as a repeller, both the axial equilibrium points B and C exist with stable nature and their corresponding domain of attraction separated by the separatrices of interior equilibrium D, which exists with saddle nature. The interior equilibrium E does not exist. As we increase the value of ξ further in such way that $\xi > \frac{1-b}{b-\alpha}$ and $\Delta > 0$, then the equilibrium B loses its stability while E gains stability (provided $tr\ \ J_{(x_2,y_2)} < 0$). The equilibria A, C and D have no change in their stability. With a further increment of ξ (in same range α), both the equilibrium cease to

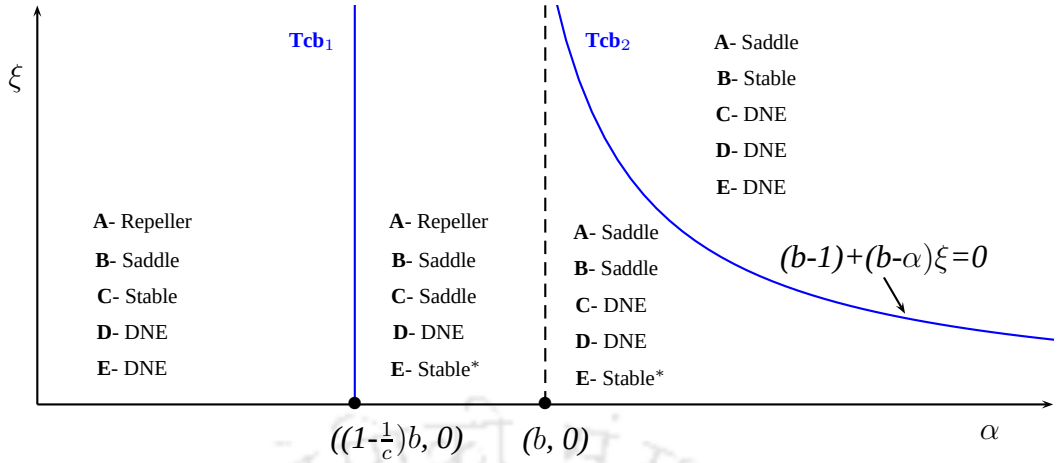

Figure 3.2: Stability region of the equilibria of system (2.1.3) in (α, ξ)-plane under Case 1(i). Here DNE stands for does not exist and $*$ indicates that the stability of equilibrium $E(x_2, y_2)$ depends on the sign of $tr\ J_{(x_2,y_2)}$. $E(x_2, y_2)$ is stable when $tr\ J_{(x_2,y_2)} < 0$ and unstable when $tr\ J_{(x_2,y_2)} > 0$ and a Hopf bifurcation occurs when $tr\ J_{(x_2,y_2)} = 0$. The curve Tcb_1 (Tcb_2) represents the transcritical bifurcation curve, through which equilibrium C (B) transfer its stability to interior equilibrium E and vice-versa provided $tr\ J_{(x_2,y_2)} < 0$.

exist through curve $\Delta = 0$, while rest of equilibria carry same nature of stability. The curve $\Delta = 0$ is the saddle-node curve for this range of α.

As we enter the range $\left(1 - \frac{1}{c}\right) b < \alpha < b$ and if $\xi < \frac{1-b}{b-\alpha}$ then C loses its stability while D ceases to exist and the stability of the rest of the equilibria are similar to the previous range of α with $\xi < \frac{1-b}{b-\alpha}$. As we increase the value of ξ in this α range, E come into existence with stable nature provided $\Delta_1 < 0$ or $x_2 \notin I_1$ holds true, and B loses its stability through curve $\xi = \frac{1-b}{b-\alpha}$. The remaining equilibria have same nature as for the previous value of ξ in this range of α.

Now, when $\alpha > b$, then only two equilibria exist, namely, A and B, the former with saddle nature while the latter with stable nature.

Results for Case 1(ii) are summarized in Figure 3.3.

(iii) : The stability of all the equilibria are similar to Case 1(i) in the ranges $0 < \alpha < \left(1 - \frac{1}{c}\right) b$ and $\left(1 - \frac{1}{c}\right) b < \alpha < b$, while in range $\alpha > b$ the stability of the equilibria are similar to Case 1(ii). The results for Case 1(iii) are illustrated in Figure 3.4.

3.2.5 Case 2

For this case, the stability results are same as for Case 1(i) except for the results in the range $0 < \alpha < \left(1 - \frac{1}{c}\right) b$. In this case, when $\Delta > 0$, then both the interior equilibria, D and E will

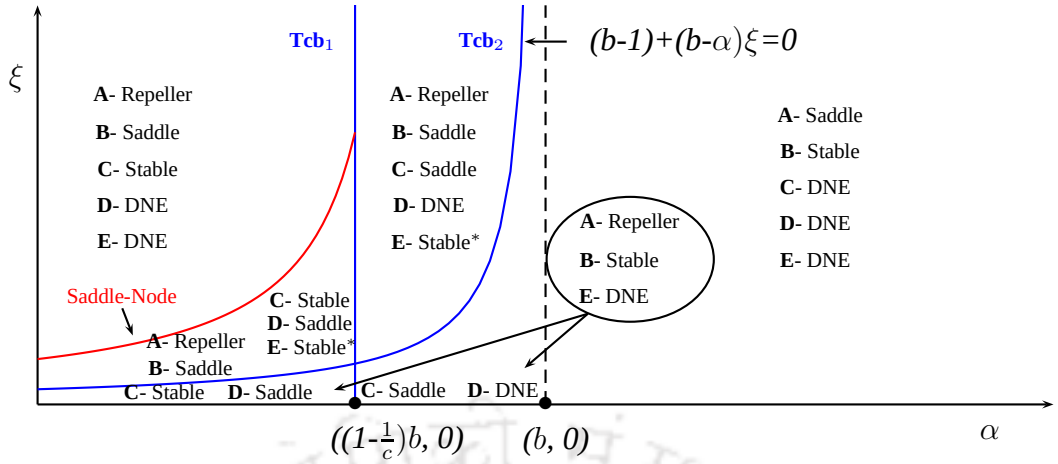

Figure 3.3: Stability region of the equilibria of system (2.1.3) in (α, ξ)-plane under Case 1(ii). Here DNE stands for does not exist and $*$ indicates that the stability of equilibrium $E(x_2, y_2)$ depends on the sign of $tr\ J_{(x_2,y_2)}$. In this case, a saddle-node bifurcation occurs (when $0 < \alpha < (1 - \frac{1}{c})b$) along with one Hopf bifurcation and two transcritical bifurcations (Tcb$_1$,Tcb$_2$).

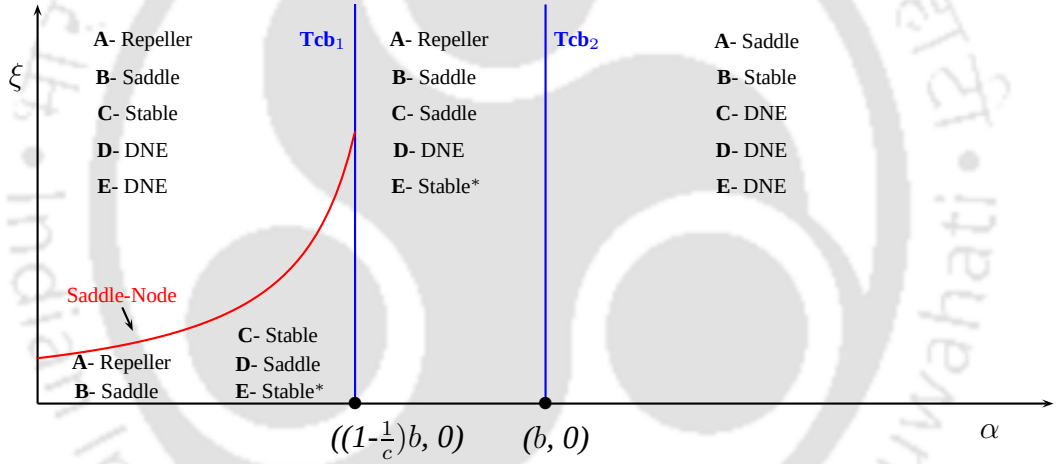

Figure 3.4: Stability region of the equilibria of system (2.1.3) in (α, ξ)-plane under Case 1(iii). Here DNE stands for does not exist and $*$ indicates that the stability of equilibrium $E(x_2, y_2)$ depends on the sign of $tr\ J_{(x_2,y_2)}$. In this case also, one saddle-node bifurcation, one Hopf bifurcation, and two transcritical bifurcations (Tcb$_1$,Tcb$_2$) occurs.

exist (along with the other three equilibria), with the former being a saddle and the latter being stable provided $tr\ J_{(x_2,y_2)} < 0$. There are two bifurcations observed in this range of α. The first one is saddle-node bifurcation through which the two interior equilibria appears/disappears simultaneously. The second one is Hopf bifurcation through which E loses/gains its stability. In this range of α, the stability nature of the trivial and two axial equilibria will remain the same as in Case 1 and when $\Delta > 0$ and $tr\ J_{(x_2,y_2)} < 0$, we have bistability where both the equilibria C and

E are stable. The corresponding basin of attraction is separated by the separatrices of the interior equilibrium D. For this case, the results are summarized in Figure 3.5.

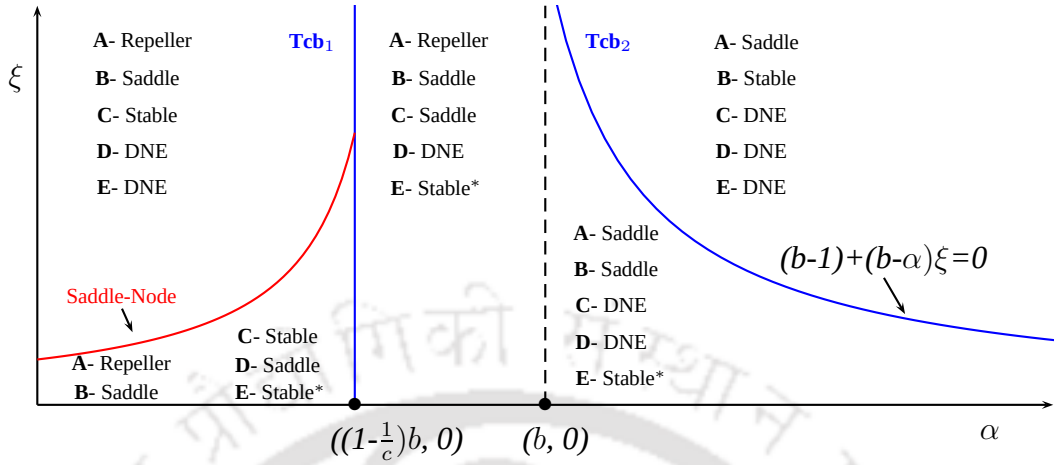

Figure 3.5: Stability region of the equilibria of system (2.1.3) in (α, ξ)-plane under Case 2. Here DNE stands for does not exist and $*$ indicates that the stability of equilibrium $E(x_2, y_2)$ depends on the sign of $tr\ J_{(x_2,y_2)}$. In this case also, saddle-node bifurcation occurs along with one Hopf bifurcation and two transcritical bifurcations (Tcb_1,Tcb_2).

3.2.6 Case 3

The stability of all the equilibria is similar to that of Case 2, except E, which is stable for all ranges of α. Consequently, there will be no Hopf-bifurcation in this case. The summary of the results for this case is given in Figure 3.6.

3.2.7 Limit Cycle

The condition $tr\ J_{(x_2,y_2)} \geq 0$ ($x_2 \in I_1$ or I_2) with $\alpha > (1 - \frac{1}{c})b$ ensures the existence of a limit cycle. $tr\ J_{(x_2,y_2)} \geq 0$ is the necessary condition for a limit cycle to exist and $\alpha > (1 - \frac{1}{c})b$ ensures that the boundary equilibrium C is not stable. The Hopf-bifurcation theorem and the boundedness of the solution of system (2.1.3) along with Poincare-Bendixson theorem guarantees the existence of a limit cycle when $tr\ J_{(x_2,y_2)} = 0$ and $tr\ J_{(x_2,y_2)} > 0$ respectively.

3.2.8 Global Stability Analysis

In this section we will prove the global stability for the interior equilibrium point $E(x_2, y_2)$ as well as the two axial equilibrium points $B(1, 0)$ and $C(0, (b - \alpha)\xi)$.

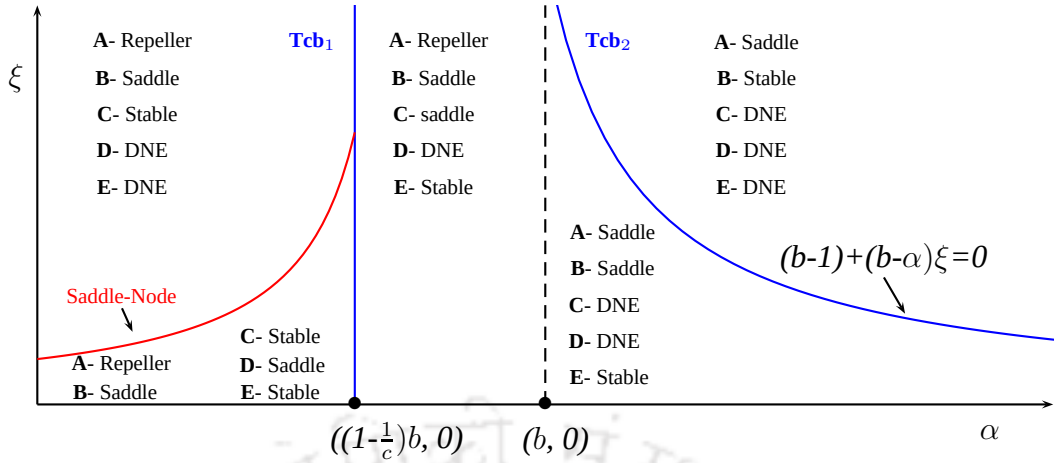

Figure 3.6: Stability region of the equilibria of system (2.1.3) in (α, ξ)-plane under Case 3. Here DNE stands for does not exist. In this case also, saddle-node bifurcation occurs along with two transcritical bifurcations, but no Hopf bifurcation occurs due to the unconditional stability of equilibrium $E(x_2, y_2)$.

Theorem 3.2.3. *Suppose that the interior equilibrium point $E(x_2, y_2)$ exists and it is locally asymptotically stable. If $\alpha\xi \geq 1$ and $\alpha > (1 - \frac{1}{c})b$, then (x_2, y_2) is globally stable.*

Proof. We consider the following function,

$$L_2(x, y) = \frac{\partial}{\partial x}\left(B_2(x, y) f_2(x, y)\right) + \frac{\partial}{\partial y}\left(B_2(x, y) g_2(x, y)\right),$$

where $f_2(x, y) = x\,(1 - x) - \frac{cxy}{x+y+\alpha\xi}$, $g_2(x, y) = m\left(\frac{b(x+\xi)}{x+y+\alpha\xi} - 1\right) y$ and $B_2(x, y) = \frac{x+y+\alpha\xi}{xy}$. Hence,

$$L_2(x, y) = \frac{(1 - \alpha\xi)}{y} - \frac{(2x + y)}{y} - \frac{m}{x}.$$

Now, if $\alpha\xi \geq 1$, then $L_2(x, y) < 0$ whenever $x > 0$ and $y > 0$. Therefore, by Dulac's criteria [49], we conclude that the system (2.1.3) does not have any non-trivial periodic orbit in $\mathbb{R}^2_+$. For the case $(1 - \frac{1}{c})b < \alpha < b$, the origin is a repeller and the two axial equilibria are both saddle, with the stable manifolds being the $x-$axis and $y-$axis respectively. For the case $\alpha > b$, both the points $(0, 0)$ and $(1, 0)$ (which always exist) are saddle in nature and their stable manifolds are the $y-$axis and $x-$axis respectively. Thus, this along with the Poincare-Bendixson Theorem [49] assures us that the interior equilibrium point (x_2, y_2) is globally stable. □

Theorem 3.2.4. *The axial equilibrium $B(1, 0)$ is globally stable, if either of the following results hold true,*

(a) $b \geq 1$ and the axial equilibrium point $B(1, 0)$ is locally asymptotically stable.

(b) $b < 1$ and the axial equilibrium point $B(1,0)$ is locally asymptotically stable in absence of any interior equilibrium point.

Proof. The above theorem will be proved using the simple flow analysis (on the lines of [7]). Let us first consider the case $b \geq 1$. Under the conditions for which $(1,0)$ is locally asymptotically stable we divide the region $\mathbb{R}^2_+$ into three subregions as follows,

$$\begin{aligned} R_1 &= \{(x,y) \in \mathbb{R}^2_+ | \overline{f}(x,y) < 0, \overline{g}(x,y) \geq 0\} \\ R_2 &= \{(x,y) \in \mathbb{R}^2_+ | \overline{f}(x,y) \leq 0, \overline{g}(x,y) < 0\} \\ R_3 &= \{(x,y) \in \mathbb{R}^2_+ | \overline{f}(x,y) > 0, \overline{g}(x,y) < 0\}, \end{aligned}$$

where $\overline{f}(x,y) = 1 - x - \frac{cy}{x+y+\alpha\xi}$ and $\overline{g}(x,y) = \frac{b(x+\xi)}{x+y+\alpha\xi} - 1$.

One can easily see that any trajectory that starts from a point in $\mathbb{R}^2_+$ will eventually converge to the axial equilibrium point $(1,0)$. Since there are no equilibrium point in this subregion, any trajectory that starts from subregion R_1 will enter subregion R_2. This entry will take place as a result of the trajectory crossing the predator isocline horizontally from right to left in finite time. Again, due to the non-existence of any equilibrium point in subregion R_2, we conclude that any trajectory in the subregion R_2 will either converge to the point $(1,0)$ or will enter subregion C in finite time by crossing the prey isocline vertically downwards. Once inside subregion R_3, the trajectory will remain inside this subregion for all subsequent times and hence it will eventually approach $(1,0)$ as $t \to \infty$.

One can easily prove the Theorem for the other case, $b < 1$, on similar lines. Hence the proof for this case is omitted. □

Theorem 3.2.5. *Suppose that the axial equilibrium point $C(0,(b-\alpha)\xi)$ is locally asymptotically stable and no interior equilibrium point exists, then $C(0,(b-\alpha)\xi)$ is globally stable.*

Proof. The above theorem can be proved on similar lines as Theorem 3.2.4. In this case, the region $\mathbb{R}^2_+$ is divided into three subregions as follows,

$$\begin{aligned} R_1' &= \{(x,y) \in \mathbb{R}^2_+ | \overline{f}(x,y) \geq 0, \overline{g}(x,y) > 0\} \\ R_2' &= \{(x,y) \in \mathbb{R}^2_+ | \overline{f}(x,y) < 0, \overline{g}(x,y) \geq 0\} \\ R_3' &= \{(x,y) \in \mathbb{R}^2_+ | \overline{f}(x,y) < 0, \overline{g}(x,y) < 0\}, \end{aligned}$$

where $\overline{f}(x,y) = 1 - x - \frac{cy}{x+y+\alpha\xi}$ and $\overline{g}(x,y) = \frac{b(x+\xi)}{x+y+\alpha\xi} - 1$.

A trajectory that starts from subregion R_1' enters subregion R_2' because there are no equilibrium points as well as no basin of attraction for $(0,0)$ and $(1,0)$ in subregion R_1'. This entry is a result of the trajectory crossing the prey isocline vertically upwards in finite time. Again, due to the non-existence of any interior equilibrium point and basin of attraction for $(1,0)$ in subregion R_2', any

trajectory in subregion R_2' will enter subregion R_3' in finite time by crossing the predator isocline horizontally from right to left. Once the trajectory is in subregion R_3', then it will remain inside this subregion for all subsequent times and hence will eventually converge to $(0, (b-\alpha)\xi)$ as $t \to \infty$. □

3.3 Observations, Ecological Interpretations and Justifications of the Results

In this section, we present some observations of the results obtained from the study of the modified ratio-dependent model in the last section under all three cases. Most of these observations are interpreted and justified ecologically, and are finally numerically illustrated.

Case 1(i)

Observation #1 : Taking the value of α in the range $0 < \alpha < \left(1 - \frac{1}{c}\right) b$ with any value of ξ leads to the equilibrium C being stable. This means that, if we supply high quality additional food to predators, then the prey population eventually gets extinct, while predator population will survive with low population of prey and eventually survive even without prey. A ecological justification could be given for that, provision of high quality of additional food to predators makes them survive and compete for it (better resource between the two). But due to limited supply of additional food, the predators naturally turn to their natural prey and also the predator's attack rate on prey is high and unbounded (*i.e.,* $c > 1$), which leads the prey towards extinction. The stability of equilibrium C is illustrated numerically in Figure 3.7 for parameter values $c = 2, m = 0.1, b = 2, \alpha = 0.5$ and $\xi = 1$.

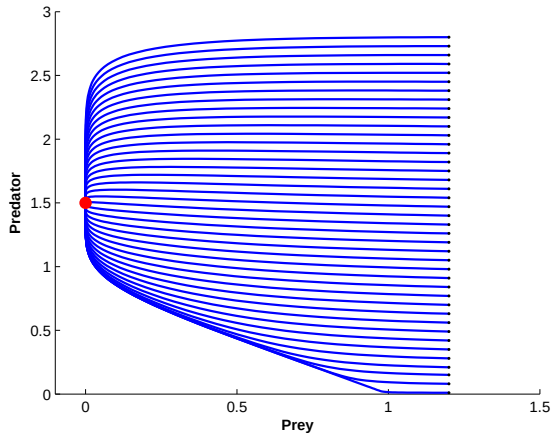

Figure 3.7: Figure illustrates that the predators can survive without prey *i.e.,* stability of equilibrium C, when $c = 2, m = 0.1, b = 2, \alpha = 0.5$ and $\xi = 1$.

Observation #2 : Fixing the value of α in range $0 < \alpha < \left(1 - \frac{1}{c}\right) b$, the value of ξ has a direct control over the future size of predators. This is because, the equilibrium level of predators is proportional to the quantity of additional food. Ecologically it can be interpreted and justified as, if we supply high quality additional food to predators, the predator will naturally go for it and their size will depend on the amount of additional food that is supplied. This observation is illustrated in Figure 3.8 for the parameter values $c = 2, m = 0.5, b = 2, \alpha = 0.5$ and $\xi = 0.3, 0.6$.

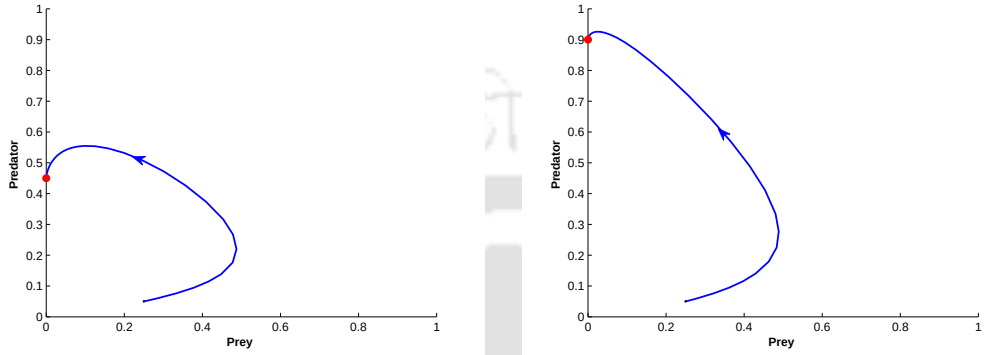

(a) Numerical simulations with parameters $c = 2, m = 0.5, b = 2, \alpha = 0.5$ and $\xi = 0.3$.

(b) Numerical simulations with parameters $c = 2, m = 0.5, b = 2, \alpha = 0.5$ and $\xi = 0.6$.

Figure 3.8: Figure shows control of predator's size by quantity of supplied additional food (with high quality) to predators.

Observation #3 : Though equilibrium A is a repeller in nature in range $0 < \alpha < \left(1 - \frac{1}{c}\right) b$, but supplying high quality additional food in low quantity leads both the predator and prey 'almost' towards extinction. It is interesting to note that, if we supply additional food with more quantity and reduce the amount of quantity after some time, then the prey population can go towards extinction at a much faster rate.

Observation #4 : For Case 1, we know that, there is no interior equilibrium that exist (in absence of additional food supply). Consequently there is no co-existence of populations. A choice of the value α in the range $\left(1 - \frac{1}{c}\right) b < \alpha < b$ with high ξ ($\xi > (1 - m(b-1))/b$) ensures that the interior equilibrium E is stable and when ξ is in the range $0 < \xi < (1 - m(b-1))/b$, there is a possibility of the existence of a limit cycle. This means that, if we supply the additional food with any quantity ξ and quality α, which falls in the range $\left(1 - \frac{1}{c}\right) b < \alpha < b$, then coexistence of both the population is possible. A lower amount of additional food supply can lead to their coexistence in oscillatory manner. This phenomena is illustrated in Figure 3.9 for the parameter values $c = 2, m = 0.1, b = 2, \alpha = 1.5$ with two values of quantity of additional food, namely, $\xi = 1$ and 0.135.

Observation #5 : If $\alpha > b$ (poor quality food) and $\xi < \frac{1-b}{b-\alpha}$, then coexistence of both the population is still possible despite the quality of additional food being poor. But if we increase the

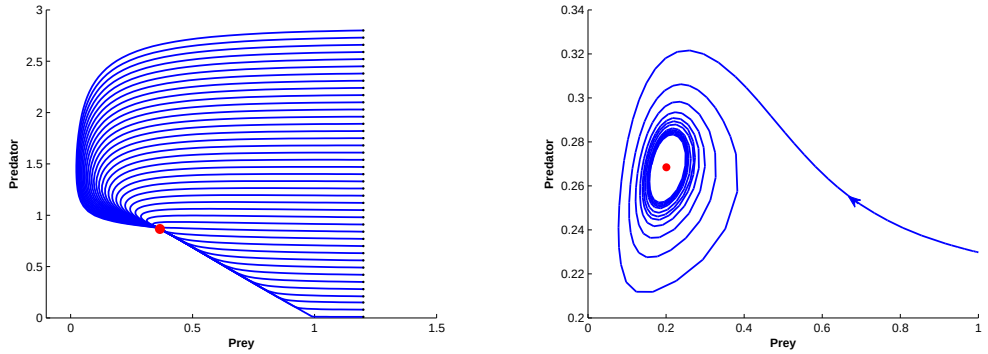

(a) Numerical simulations with parameters $c = 2, m = 0.1, b = 2, \alpha = 1.5$ and $\xi = 1$.

(b) Numerical simulations with parameters $c = 2, m = 0.1, b = 2, \alpha = 1.5$ and $\xi = 0.135$.

Figure 3.9: Figure illustrates the role of quantity of additional food in type of coexistence of both the population : (a) in stabilized form; (b) in oscillatory form.

quantity further, then predators can no longer survive. The reason for this is that providing poor quality food with higher quantity ($\xi > \frac{1-b}{b-\alpha}$), leads to the predator being distracted from the prey (with high nutrient value). This is illustrated in Figure 3.10(a), when parameter values are taken as $c = 2, m = 0.1, b = 2, \alpha = 6$ and $\xi = 1$.

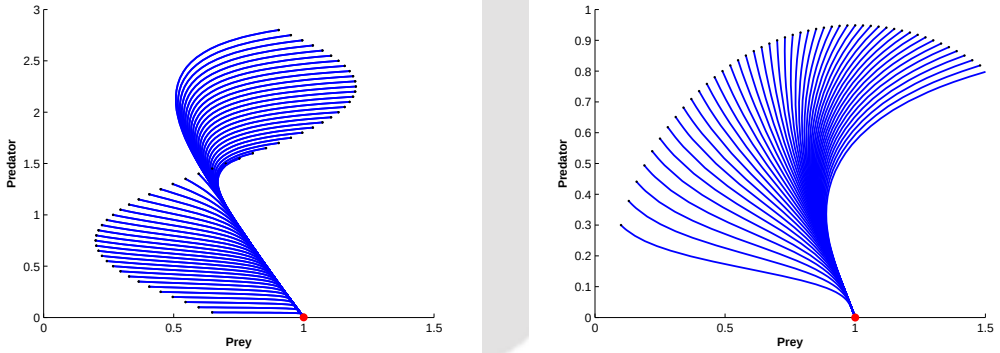

(a) Numerical simulations with parameters $c = 2, m = 0.1, b = 2, \alpha = 6$ and $\xi = 1$.

(b) Numerical simulations with parameters $c = 2, m = 1, b = .5, \alpha = 0.6$ and $\xi = 8$.

Figure 3.10: Figure illustrates the extinction of predator population due to poor quality additional food in high quantity: (a) when $b > 1$ (under Case 1(i)); (b) when $b < 1$ (under Case 1(ii)).

Case 1(ii) & (iii)

Observation #1 : When $bm \leq m$ (conversion efficiency of the predators is not more than their mortality rate), then the predator population will decline as time passes and will certainly go towards extinction, without the additional food supply. But, if we provide high quality food along with sufficient amount of quantity ($\xi > \frac{1-b}{b-\alpha}$), then the predator population will survive. If the

quantity is not sufficient ($\xi < \frac{1-b}{b-\alpha}$), even then, the predator's survival is possible, provided prey population is very low. Ecologically it can be justified as, if there is more prey (relatively low nutrition value), predators can get distracted from them in order to search high quality additional food in low quantity which ultimately leads them towards extinction, where as, if there is less number of prey, then there is no such distraction, and predators easily can survive on high quality additional food. Figure 3.11 illustrates this observation for parameters values $c = 2, m = 1, b = 0.5$ where the value for quality is $\alpha = 0.2$ and quantity are $\xi = 2, 1.8, 1.6$.

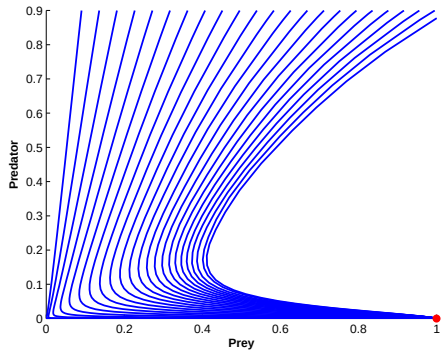

(a) Numerical simulations with parameters $c = 2, m = 1, b = 0.5$ and $\xi = 0$.

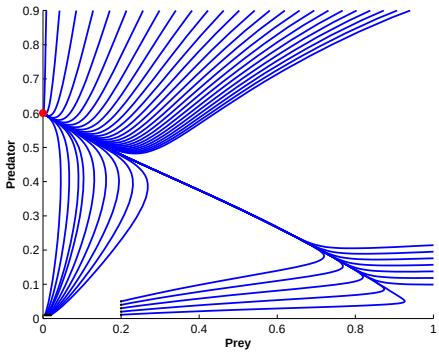

(b) Numerical simulations with parameters $c = 2, m = 1, b = 0.5, \alpha = 0.2$ and $\xi = 2$.

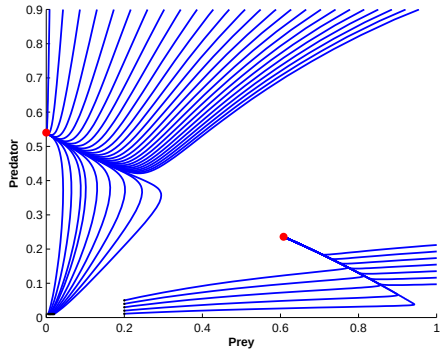

(c) Numerical simulations with parameters $c = 2, m = 1, b = 0.5, \alpha = 0.2$ and $\xi = 1.8$.

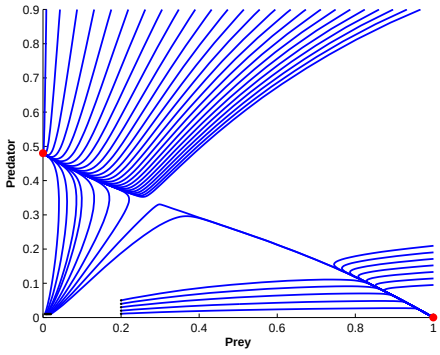

(d) Numerical simulations with parameters $c = 2, m = 1, b = 0.5, \alpha = 0.2$ and $\xi = 1.6$.

Figure 3.11: Figure illustrates the how quantity of additional food (with high quality) plays a role in predator's survival even when predator's mortality rate is more than their conversion efficiency : (a) predators are going towards extinction in absence of additional food; (b) and (c) predators can survive with sufficient amount of quantity of additional food ; (d) predators surviving with additional food (even when quantity is not sufficient) when prey is low in size.

Observation #2 : When α is in the range $\left(1 - \frac{1}{c}\right) b < \alpha < b$ with the quantity $\xi < \frac{1-b}{b-\alpha}$, then only B is stable. It means that, if we deteriorate the quality of additional food from high quality and supply it to the predators at low quantity ($\xi < \frac{1-b}{b-\alpha}$), then predator's survival is not possible. But if we supply same quality (deteriorated) additional food with sufficient amount of quantity

($\xi > \frac{1-b}{b-\alpha}$) then coexistence of both the populations is possible. This observation is described in Figure 3.12 for parameter values $c = 2, m = 1, b = 0.5, \alpha = 0.4$ and $\xi = 2, 8$.

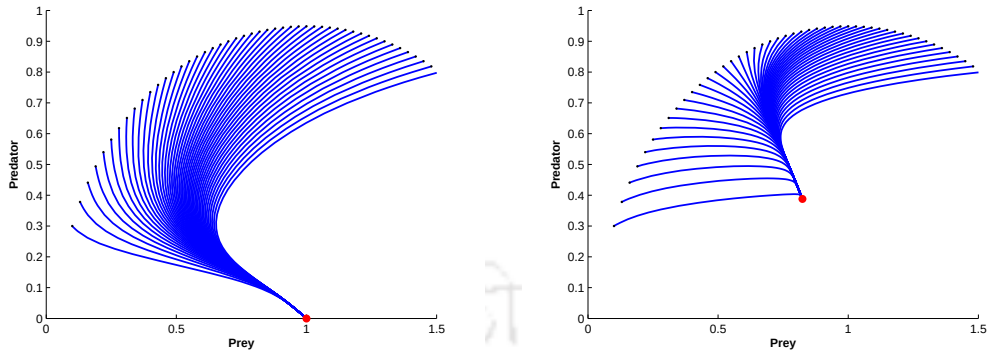

(a) Numerical simulations with parameters $c = 2, m = 1, b = 0.5, \alpha = 0.4$ and $\xi = 2$.

(b) Numerical simulations with parameters $c = 2, m = 1, b = 0.5, \alpha = 0.4$ and $\xi = 8$.

Figure 3.12: Figure illustrates the how quantity of additional food (with quality range $\left(1 - \frac{1}{c}\right) b < \alpha < b$) play a role in predator's survival : (a) with low quantity additional food supply predators are going towards extinction; (b) predators can survive with sufficient amount of quantity of additional food.

Observation #3 : When $\alpha > b$ (poor quality) then equilibrium B is stable for all value of ξ. This means, if we further deteriorate (from range $\left(1 - \frac{1}{c}\right) b < \alpha < b$ to range $\alpha > b$) the quality of additional food, then there is no way to prevent the predator's extinction. It is shown in Figure 3.10(b) with parameter values $c = 2, m = 1, b = 0.5, \alpha = 0.6$ and $\xi = 8$.

Observation #4 : When $c < 1$, the equilibrium C cannot be stabilized. It means that, when predator's attack rate (also called consumption rate of predators) is limited, then the prey population never goes towards extinction. Ecologically it is possible that, when predator population declines over time and also their consumption rate is limited, then there is no chance for decline in the prey population. Numerical simulation for this observation is shown in Figure 3.13(a) with parameters $c = 0.5, m = 1, b = 0.5, \alpha = 0.01$ and $\xi = 8$.

Case 2

Observation #1 : In comparison with Observation #1 under Case 1(i), here a choice of α in $0 < \alpha < \left(1 - \frac{1}{c}\right) b$ with ξ in such way that $\Delta > 0$ and $\xi > (1 - m(b-1))/b$ leads to the bi-stability of equilibrium C and E. If $\xi < (1 - m(b-1))/b$, then there is possibility of a small amplitude limit cycle around E. Ecologically, it means that, if conversion efficiency of predators is not much stronger than their mortality rate (*i.e.,* $0 < bm - m < 1$) and predator's attack rate on prey is high but bounded (*i.e.,* $1 + bm/(b+1) < c < b/(b-1)$), then providing high quality of additional food (with sufficiently low quantity) results in prey survival provided prey size is close to x_2 and predator

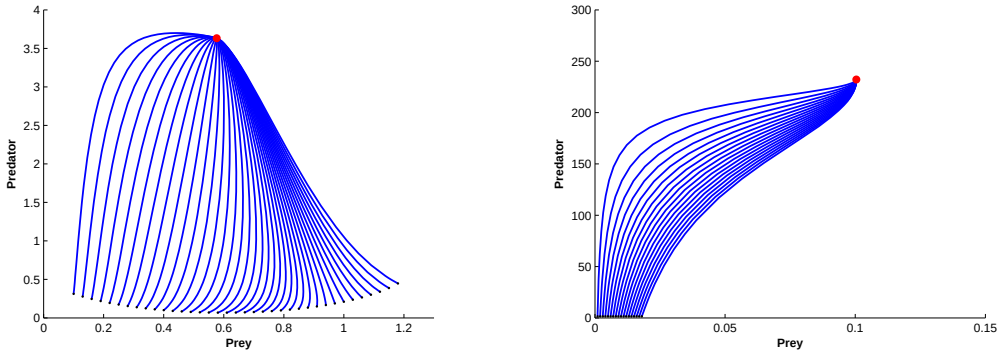

(a) Numerical simulations with parameters $c = 0.5, m = 1, b = 0.5, \alpha = 0.01$ and $\xi = 8$.

(b) Numerical simulations with parameters $c = 0.9, m = 0.05, b = 23, \alpha = 0.001$ and $\xi = 10$.

Figure 3.13: Figure illustrates the eradication of prey populations not possible when predator's attack rate is limited ($c < 1$), even with high quality and high quantity of additional food supply: (a) under Case 1(ii), where $b < 1$ (b) under Case 3, where $b > 1$.

size is close to y_2. If we increase the value of ξ s.t $\Delta < 0$, then prey's survival is not possible. Figure 3.14(a) illustrates the equilibrium C being stable and E being unstable and surrounded by a limit cycle when parameter values are $c = 1.163, m = 0.05, b = 3, \alpha = 0.1$ and $\xi = 0.005$.

Case 3

Observation #1 : Choosing α in $0 < \alpha < \left(1 - \frac{1}{c}\right) b$ and ξ in such way that $\Delta > 0$, shows the bi-stability for equilibrium C and E. This means that, if conversion efficiency of predators is much stronger than their mortality rate (*i.e.,* $bm - m \geq 1$) and predator's attack rate on prey is high but has more restrictive bound (*i.e.,* $1 < c < bm$) as compared with Case 2, then providing high quality of additional food (with sufficiently low quantity) can make the prey survive, provided, the prey and predator sizes are sufficiently close to the number x_2 and y_2 respectively. Taking a high value of ξ (s.t. $\Delta < 0$), leads the prey towards extinction. To distinguish between this observation and the observation obtained in Case 2, we found that, if the predator's attack rate on prey is relatively more restricted with the relation $bm - m \geq 1$, then oscillation in populations can be avoided. Numerical illustration is given in Figure 3.14(b) with parameters $c = 1.02, m = 0.05, b = 23, \alpha = 0.1$ and $\xi = 0.005$, where equilibria C and E are both stable. The corresponding basins of attractions are separated by the stable manifolds of equilibrium D.

Observation #2 : When $c < 1$, the equilibrium C is never stable. This means that, when predator's attack rate is bounded, then prey can not get extinct. Ecologically it can be justified as that, when both the populations are capable of surviving together, then additional food supply to predators results in the prey always benefiting. For example, if we supply high quality additional food, then it attracts the predators, which in turn increases the size of prey population. If we supply

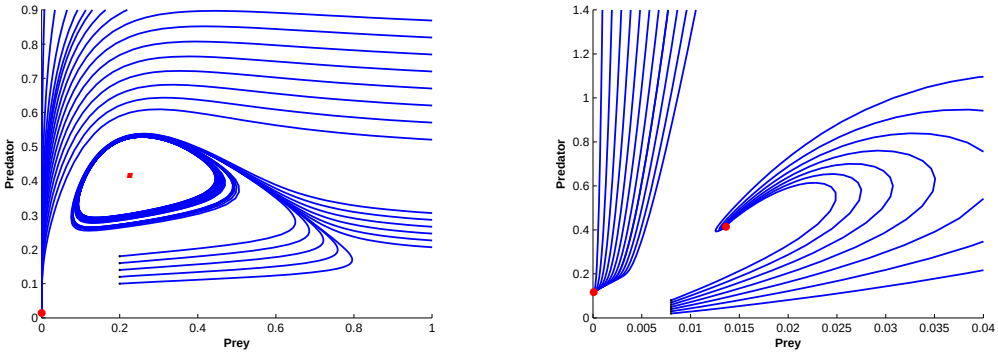

(a) Numerical simulations with parameters $c = 1.163, m = 0.05, b = 3, \alpha = 0.1$ and $\xi = 0.005$.

(b) Numerical simulations with parameters $c = 1.02, m = 0.05, b = 23, \alpha = 0.1$ and $\xi = 0.005$.

Figure 3.14: Figure illustrates the bi-stability of populations and the local coexistence of both the populations are (a) in oscillation form (under Case 2, where predator's attack rate on prey is high); (b) in stabilized form (under Case 3, where predator's attack on prey is relatively more restrictive).

poor quality additional food, then it distracts the predators from prey, which also benefits the prey. It is numerically illustrated in Figure 3.13(b) for parameters $c = 0.9, m = 0.05, b = 23, \alpha = 0.001$ and $\xi = 10$.

Note: The Observations $\#2, 3, 4$ and 5 made in Case 1(i) are also applicable for Case 2 and Case 3.

3.3.1 Some Other Observations

It is observed that when quality of additional food is high (lower value of α) then the equilibrium C is stable and ensures the survival of the predator population despite the absence of prey. Now, decreasing the quality of additional food results in the prey and predator populations converging towards carrying capacity and extinction respectively. Also, an appropriate choice of the quality of additional food $\left(i.e., \left(1-\frac{1}{c}\right)b < \alpha < \frac{b(1+\xi)-1}{\xi}\right)$ ensures the coexistence of both the species. Once this coexistence is ensured, the quality and quantity of additional food also can be used to control the densities of both the populations. For example, by fixing the value of ξ, as we increase α in the range $\left(1-\frac{1}{c}\right)b < \alpha < \frac{b(1+\xi)-1}{\xi}$, we observe that the prey population increases and the predator population decreases. Keeping the value of α close to $\left(1-\frac{1}{c}\right)b$ (with $\alpha > \left(1-\frac{1}{c}\right)b$), an increase in the value of ξ results in the increase of the predator population while the prey population is small (relative to population at the value α away from $\left(1-\frac{1}{c}\right)b$). We illustrate this in Figure 3.15 by presenting how the prey and predator density evolves for various values of α and ξ for the parameter values $c = 2$, $m = 0.1$ and $b = 2$.

Finally, we summarize the conclusion of our study in Table 3.4, which outlines as to how additional food should be supplied depending on the specific requirements and the predator's behaviour.

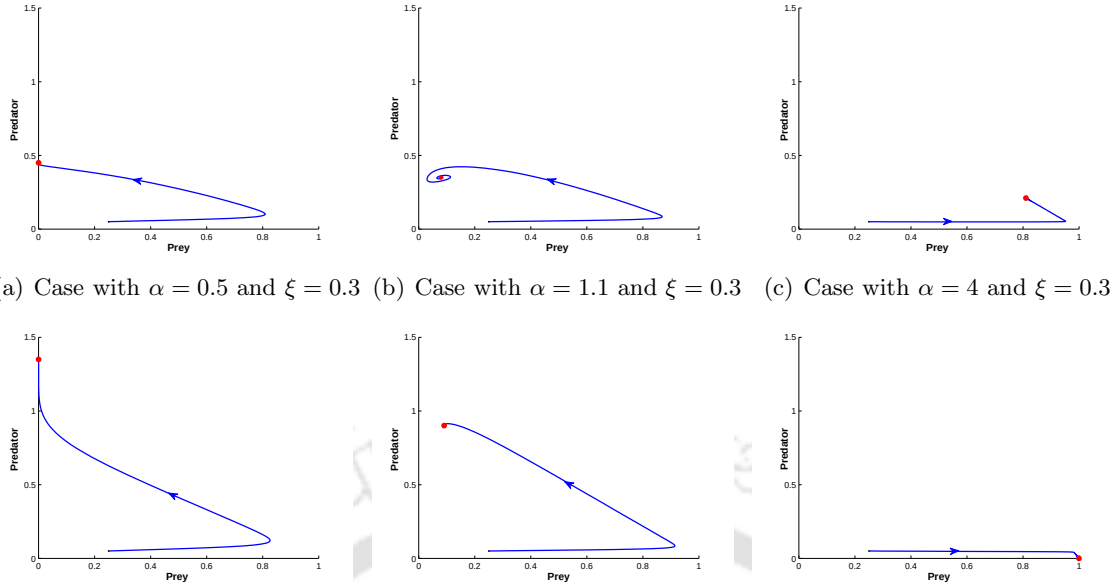

(a) Case with $\alpha = 0.5$ and $\xi = 0.3$ (b) Case with $\alpha = 1.1$ and $\xi = 0.3$ (c) Case with $\alpha = 4$ and $\xi = 0.3$

(d) Case with $\alpha = 0.5$ and $\xi = 0.9$ (e) Case with $\alpha = 1.1$ and $\xi = 0.9$ (f) Case with $\alpha = 4$ and $\xi = 0.9$

Figure 3.15: Evolution of prey and predator densities for various values of α and ξ, when $c = 2, m = 0.1, b = 2$. In Figure, $(a) \to (b) \to (c)$ or $(d) \to (e) \to (f)$, shows the stability of equilibrium C is going towards the stability of equilibrium B as we are increasing the value α for fixed ξ. $(a) \to (d)$ or $(b) \to (e)$, shows the predators size are increasing as we increasing the value ξ for fixed α.

3.4 Discussion and Conclusion

We study the dynamics of the modified ratio-dependent model under three possible scenarios arising from the nature of existential behaviour of the species as in the original model. These three scenarios resulting from the existence and stability of the interior equilibrium point of the original model are as follows: (a) extinction of both the species or predator alone, (b) either extinction of both the species or predator alone or co-existence in an oscillatory manner and (c) co-existence of both the species.

For the first case, corresponding to the extinction of both the species or predator alone, we first consider the range of high quality $0 < \alpha < \left(1 - \frac{1}{c}\right) b$. For this range, the predator population survives as a result of additional food supply, as opposed to extinction with no additional food. However, when $b \geq 1$ the prey population will still go to extinction. The reason for this is that the increase in the predator density results in high predation (due to limited quantity of additional food) causing the extinction of the prey population. When $b < 1$ this extinction can be avoided if the prey and predator's size are close to the number x_2 and y_2 respectively and value of ξ is chosen in such way that $\Delta > 0$ and $\xi > \frac{1-b}{b-\alpha}$. For the range $\left(1 - \frac{1}{c}\right) b < \alpha < \frac{b(1+\xi)-1}{\xi}$ both species can coexist due to the additional food supply. This case exemplifies how additional food can result in biological control of extinction. Finally when $\alpha > \frac{b(1+\xi)-1}{\xi}$, then the predator population becomes

Requirement	Predator's Behavior	Supply of Additional Food	
		Quality (α)	Quantity (ξ)
Coexistence (in stabilized form)	-	$\left(1-\frac{1}{c}\right)b < \alpha < \frac{b(1+\xi)-1}{\xi}$	$\xi > \frac{1-m(b-1)}{b}$
Coexistence with prey dominated (in stabilized form)	-	Nearest (possible) to $\frac{b(1+\xi)-1}{\xi}$	$\xi > \frac{1-m(b-1)}{b}$
Coexistence with predator dominated (in stabilized form)	-	Nearest (possible) to $\left(1-\frac{1}{c}\right)b$	Maximum (possible)
Coexistence (in oscillation form)	-	$\left(1-\frac{1}{c}\right)b < \alpha < \frac{b(1+\xi)-1}{\xi}$	$0 < \xi < \frac{1-m(b-1)}{b}$ provided $tr\ J_{(x_2,y_2)} > 0$
Coexistence (small oscillation form)	-	$\left(1-\frac{1}{c}\right)b < \alpha < \frac{b(1+\xi)-1}{\xi}$	Nearest (possible) to $\frac{1-m(b-1))}{b}$ provided $tr\ J_{(x_2,y_2)} > 0$
Coexistence (large oscillation form)	-	$\left(1-\frac{1}{c}\right)b < \alpha < \frac{b(1+\xi)-1}{\xi}$	Minimum (possible) provided $\xi > 0$ and $tr\ J_{(x_2,y_2)} > 0$
Prey's eradication	$bm > m,\ c \geq \frac{b}{b-1}$	$0 < \alpha < \left(1-\frac{1}{c}\right)b$	$\xi > 0$
	$1 < c < \frac{b}{b-1}$	$0 < \alpha < \left(1-\frac{1}{c}\right)b$	$\xi > 1-c+\frac{c}{b}$
	$bm \leq m,\ c > 1$	$0 < \alpha < \left(1-\frac{1}{c}\right)b$	$\xi > 1-c+\frac{c}{b}$
Predator's eradication	$bm \geq m$	$\alpha > b$	$\xi > \frac{b-1}{\alpha-b}$
	$bm < m$	$\left(1-\frac{1}{c}\right)b < \alpha < b$	Minimum (possible) with $\xi > 0$
		$\alpha > b$	$\xi > 0$

Table 3.4: Table gives the simple way, how to supply additional food to predators once we know the requirement and predator's behaviour.

extinct, whereas the prey survives. This happens due to the poor quality of food and the resulting distraction from predation, thereby benefiting the prey population. Next, we consider the second case with the range $0 < \alpha < \left(1-\frac{1}{c}\right)b$. For this range the predator will not get extinct due to the additional food supply. Also, coexistence of the two species is possible in this range of α, provided the prey and predator's size are close enough to x_2 and y_2 respectively and the quantity of food is low ($\xi < 1-c+c/b$). For the range $\left(1-\frac{1}{c}\right)b < \alpha < \frac{b(1+\xi)-1}{\xi}$, coexistence of both the species is possible, similar to the preceding sub-case. The implications for the range $\alpha > \frac{b(1+\xi)-1}{\xi}$ are akin to that of the first case. Finally, for the last case, the ecological consequences are the same as the

previous case, the only difference being that, when consumption rate of predators is limited ($c < 1$), then the prey population cannot be eradicated.

The work of Srinivasu et. al. [11] introduced the idea of control in a modified Holling type II model. In this Chapter we have presented and analyzed a modified ratio-dependent model. The analysis reveals the role of additional food in the control of prey population in a more explicit way in comparison to [11]. The modified Holling type II model predicts unbounded growth of predator density with limited quantity of additional food [11]. On the other hand, the analysis of the modified ratio-dependent model, shows the existence of globally stable equilibrium point $(0, (b-\alpha)\xi)$ explicitly and also here the predator growth is proportional to the quantity of additional food, which addresses this issue more realistically. The ratio-dependent functional response takes into account the intraspecific competition among the predators. This competition is not incorporated in a Holling type II model functional response, which is why the control of prey population (with additional food) for the modified Holling type II model is not as realistic as compared to the case of the modified ratio-dependent model, discussed in this Chapter.

In conclusion, we can say the modified ratio-dependent predator-prey model presents us with interesting ecological consequence and rich dynamics. This model provides us with a way of achieving greater control on the dynamics of the system, by way of appropriate handling of the quantity and quality of the additional food supplied to the predator in the system. Irrespective of the whether the original system (in absence of additional food) shows extinction or co-existence, it possible, by the choice of appropriate level of quantity and quality of additional food, to control the dynamics of the modified system as we desire. Of particular importance is the consequence of being able to conserve both the species by the additional food supply to the predator in a scenario where there is a possibility of extinction in absence of additional food. Another important consequence is the biological control of pest population by supply of additional food to the predator.

Chapter 4

Spatiotemporal Pattern for the Diffusion-Driven Modified Ratio-Dependent Model

In this chapter, we present the diffusion-driven modified ratio-dependent model and study its spatiotemporal dynamics. We explore the parametric conditions under which Turing instability can occur and reveal the spatiotemporal patterns by numerical simulations. Based on it, we observe that the quality and quantity of additional food plays a crucial role in Turing instability to occur, even for those parameter values for which the interior equilibrium point of the original ratio-dependent model either does not exist or is unstable.

4.1 The Model with Diffusion

We now present an extended model of the modified ratio-dependent model. This extension is due to the introduction of a diffusion term for the densities of both the predator and prey population, and is given by,

$$\begin{aligned}\frac{\partial N}{\partial T} &= D_1\nabla^2 N + rN\left(1-\frac{N}{K}\right) - \frac{e_1(\frac{N}{P})}{1+e_1h_1(\frac{N}{P})+e_2h_2(\frac{A}{P})}P,\\ \frac{\partial P}{\partial T} &= D_2\nabla^2 P + \frac{n_1e_1(\frac{N}{P})+n_2e_2(\frac{A}{P})}{1+e_1h_1(\frac{N}{P})+e_2h_2(\frac{A}{P})}P - m'P.\end{aligned} \tag{4.1.1}$$

over a spatial domain Ω with boundary $\partial\Omega$ and for $T > 0$. We will denote the spatial variable by $\mathbf{S} = (S_1, S_2)$. The additional food with a biomass of A is assumed to be uniformly available in the domain Ω. Here $N(\mathbf{S}, T)$ and $P(\mathbf{S}, T)$ denote the densities of prey and predator respectively at a point $\mathbf{S} \in \Omega$ and time T respectively. The parameters, D_1 and D_2 are the diffusivity of the densities of the prey and predator respectively. Also, the Laplacian operator $\nabla^2 = \frac{\partial^2}{\partial S_1^2} + \frac{\partial^2}{\partial S_2^2}$. The finite ecological domain Ω is taken to be $\Omega = [0, L] \times [0, M]$. The initial and boundary conditions

for the above system are taken to be

$$N(\mathbf{S},0)=\phi_1(\mathbf{S}), P(\mathbf{S},0)=\phi_2(\mathbf{S}),\ \text{for } \mathbf{S}\in\Omega.$$

and

$$\frac{\partial N}{\partial \mathbf{n}}=0, \frac{\partial P}{\partial \mathbf{n}}=0 \text{ for } \mathbf{S}\in\partial\Omega, T>0$$

respectively. The no-flux boundary condition is used in order to facilitate the study of the self-organizing patterns and this condition puts restriction on any inflow/outflow into/out of the domain [50].

We now non-dimensionalize the above system using the transformations, $x = N/K$, $y = P/Ke_1h_1$ and $t = rT$, to obtain,

$$\begin{aligned}\frac{\partial x}{\partial t} &= d_1\nabla^2 x + x\,(1-x) - \frac{cxy}{x+y+\alpha\xi},\\ \frac{\partial y}{\partial t} &= d_2\nabla^2 y + m\left(\frac{b\,[x+\xi]}{x+y+\alpha\xi}-1\right)y.\end{aligned} \tag{4.1.2}$$

subject to initial conditions

$$x(\mathbf{S},0)=\varphi_1(\mathbf{S}), y(\mathbf{S},0)=\varphi_2(\mathbf{S}),\ \mathbf{S}\in\Omega$$

and boundary conditions

$$\frac{\partial x}{\partial \mathbf{n}}=0, \frac{\partial y}{\partial \mathbf{n}}=0 \text{ for } \mathbf{S}\in\partial\Omega, t>0.$$

Here, $c = e_1/r$, $\alpha = n_1h_2/n_2h_1$, $\xi = \eta A/K$, $m = m'/r$, $b = n_1/m'h_1$, $\eta = n_2e_2/n_1e_1$, $d_1 = D_1/r$ and $d_2 = D_2/r$. Here the parameters that appear in the original ratio-dependent model, namely, c, m and b are ecological in nature. However, the parameters α and ξ appear because of additional food supply and can be viewed as parameters for biological control. While α is representative of the quality (nutritional value) of the additional food as compared to that of prey, ξ symbolizes the quantity of additional food being supplied to the predators.

4.2 The Model without Diffusion

In this section, we summarize the results of stability analysis of the interior equilibrium points of the system without diffusion ($d_1 = d_2 = 0$ in (4.1.2)), which is the modified ratio-dependent model (2.1.3). The detailed presentation of the results have been made in the previous chapter.

The stability conditions of the interior equilibrium point (x_2, y_2) under three cases, defined in last chapter, are summarized in Table 4.1. Note that the other interior equilibrium point (x_1, y_1), whenever it exists, is always saddle in nature.

Here we define $P = c-1-\frac{c}{b}+\xi$, $R = (b-\alpha)\xi+(b-1)$, and Δ, Δ_1, I_1, I_2 are same as defined earlier.

Conditions for (x_2, y_2) to be locally asymptotically stable	**Applicable Cases**
$0 < \alpha < \left(1 - \frac{1}{c}\right) b$	
(a) $P < 0,\ \Delta > 0$	
(i) $b < 1,\ R > 0$ and $x_2 \notin I_1$ or $\Delta_1 < 0$	Case 1
(ii) $x_2 \notin I_1$ or $\Delta_1 < 0$	Case 2, Case 3
$\left(1 - \frac{1}{c}\right) b < \alpha < b$	Case 3
(a) $R > 0,\ \Delta_1 > 0$ and $x_2 \notin I_1$	Case 1, Case 2, Case 3
(b) $R > 0,\ \Delta_1 < 0$	Case 1, Case 2, Case 3
$\alpha > b$	
(a) $b > 1,\ R > 0$ and $x_2 \notin I_2$	Case 1, Case 2, Case 3

Table 4.1: Conditions for stability of interior equilibrium point (x_2, y_2).

4.3 Turing Instability

In this section, we examine if Turing instability occurs for the interior equilibrium point of (4.1.2). We observe that the interior equilibrium point of the system (2.1.3) is a solution to the system with diffusivity (4.1.2) and satisfies the corresponding boundary conditions. We now make use of the definition of Turing instability given in [38]. The definition says that an interior equilibrium point of a system with diffusivity is Turing unstable if this equilibrium point is locally asymptotically stable for the system without diffusivity but is unstable for the system with diffusivity. While in many real life situations, diffusivity tends to have a stabilizing influence on the system, there are cases in which it can disturb the existent stability of the interior equilibrium point, thereby resulting in Turing instability.

We introduce the transformation $\mathbf{X} = (\overline{x}, \overline{y})^\top = (x - x_i, y - y_i)^\top$ and obtain the linearized system in the following form,

$$\mathbf{X}_t = D\nabla^2 \mathbf{X} + J_i \mathbf{X}, \tag{4.3.1}$$

with boundary conditions

$$\mathbf{X}_\mathbf{n}(\mathbf{S}, t) = 0,\ \mathbf{S} \in \partial\Omega,\ t > 0.$$

Here J_i has already been defined earlier as the linearization of

$$\left[f_1(x,y),\quad f_2(x,y)\right]^\top = \left[x\,(1-x) - \tfrac{cxy}{x+y+\alpha\xi},\quad m\left(\tfrac{b[x+\xi]}{x+y+\alpha\xi} - 1\right) y\right]^\top$$

and $D = \text{diag}(d_1, d_2)$. We use the separation of variables technique and assume the solution of (4.3.1) to be $\mathbf{X}(\mathbf{S}, t) = \psi(\mathbf{S})\rho(t)$, where $\rho : [0, \infty) \to \mathbb{R}^2$ and $\psi : \Omega \to \mathbb{R}$ [51], to obtain

$$\rho'(t) = (J_i - \lambda D)\rho \text{ and } \nabla^2\psi = -\lambda\psi,\ \mathbf{S} \in \Omega, \psi_\mathbf{n} = 0, \mathbf{S} \in \partial\Omega,$$

where λ is the eigenvalue of the operator $-\nabla^2$ and ψ be the corresponding eigenfunction on Ω with boundary conditions. More specifically, each eigenfunction ψ_j of $-\nabla^2$ corresponding to the

eigenvalue λ_j, satisfies the no-flux boundary condition. Thus we seek the solution of the form

$$\mathbf{X}(\mathbf{S},t) = \sum_{j=0}^{\infty}\sum_{k=1}^{2} b_{jk}\mathbf{c}_{jk}e^{\sigma_{jk}t}\psi_j,$$

where the constants b_{jk} are determined by a Fourier expansion of the initial conditions in terms of $\psi_j(\mathbf{S})$. Also, σ_{jk} is the eigenvalue for $J_i - \lambda_j D$, with $\mathbf{c}_{jk}$ being the corresponding eigenvector. Now, the eigenvalue σ_{jk} which determines temporal growth is given by the roots of the characteristic polynomial,

$$| \sigma_j I - J_i + \lambda_j D | = 0.$$

that is,

$$\sigma_j^2 + ((d_1+d_2)\lambda_j - (a_{11}+a_{22}))\,\sigma_j + (a_{11} - d_1\lambda_j)(a_{22} - d_2\lambda_j) - a_{12}a_{21} = 0,$$

where $J_i = (a_{ij})$. Since tr $J_i < 0, d_1, d_2 > 0$ and $\lambda_j \geq 0\ \forall j$, therefore $\text{tr}(J_i - \lambda_j D) = \text{tr}\ J_i - \lambda_j(d_1 + d_2) < 0$. So in order for Turing instability to occur, the condition $\det(J_i - \lambda_j D) \leq 0$ should be satisfied for some $j \geq 1$. Now,

$$\begin{aligned} H(\lambda_j) \equiv \det(J_i - \lambda_j D) &= (a_{11} - d_1\lambda_j)(a_{22} - d_2\lambda_j) - a_{12}a_{21} \\ &= d_1d_2\lambda_j^2 - (a_{22}d_1 + a_{11}d_2)\lambda_j + \det J_i. \end{aligned}$$

The necessary and sufficient condition for $H(\lambda_j) < 0$ are $a_{22}d_1 + a_{11}d_2 > 0$ and $(a_{22}d_1 + a_{11}d_2)^2 > 4d_1d_2 \det J_i$ respectively.

In summary, the necessary conditions for the system (4.1.2) to exhibit Turing instabilities are as follows:

(a) $a_{11} + a_{22} < 0$.

(b) $a_{11}a_{22} - a_{12}a_{21} > 0$.

(c) $a_{22}d_1 + a_{11}d_2 > 2\sqrt{d_1d_2 \det J_i}$.

These above three inequalities define the Turing space in which Turing instabilities occur and the following additional necessary conditions for Turing instability follow immediately:

(i) $a_{11}a_{22} < 0$ (from (a) and (c))

(ii) $a_{12}a_{21} < 0$ (from (b) and (i))

(iii) $d_1 \neq d_2$ (if $d_1 = d_2 = d, a_{22}d_1 + a_{11}d_2 \Rightarrow (a_{22} + a_{11})d < 0$ a contradiction).

In our case, we have $a_{22} < 0$. Now, from conditions $a_{22}d_1 + a_{11}d_2 > 0$ and $a_{11} + a_{22} < 0$, we get $d_1 < d_2$. Thus, a necessary condition for non-homogeneous spatial patterns is that the predators disperse faster than the prey. Also, since $a_{22} < 0$, then the condition $a_{11}a_{22} < 0$ means that $a_{11} > 0$, must hold for Turing instability. The conditions $a_{11} > 0, a_{22} < 0$ implies that $\frac{\partial f_1}{\partial x} > 0$ and $\frac{\partial f_2}{\partial y} < 0$. This means that the prey population is activated by it's own rate of production, whereas the predator population is inhibited by it's own rate of production [52]. In other words the prey and the predator play the role of activator and inhibitor respectively. Also, since $a_{12} < 0$ is satisfied, the system becomes an activator-inhibitor system, whenever Turing instability occurs [52, 53].

4.4 Bifurcations and Turing Space

In this section, we present the bifurcation analysis and diagrams for the interior equilibrium point (x_2, y_2) for all the three specified cases. These diagrams are in the (α, ξ) space for fixed parameter values c, m, b and fixed ratio d_2/d_1. We observe that the quality and quantity of additional food plays a crucial role in the determination of Turing instability. Before proceeding to the discussion on bifurcations, we give various expression and conditions required for the study of such bifurcations. The trace tr J_2 and determinant $\det J_2$ for our problem have already been defined earlier. The conditions for bifurcations are as follows:

1. Transcritical bifurcation:
   (a) Tcb_1: $\alpha = \left(1 - \frac{1}{c}\right) b$, provided $c > 1$.
   (b) Tcb_2: $m\,(b - 1 + (b - \alpha)\xi) = 0$.
2. Hopf bifurcation: tr $J_2 = 0$ provided $\det J_2 > 0$.
3. Saddle-node bifurcation: $(c - 1 - \frac{c}{b} + \xi)^2 = 4\xi(c - 1 - \frac{\alpha c}{b})$.
4. Turing bifurcation: The condition $a_{22}d_1 + a_{11}d_2 = 2\sqrt{d_1 d_2 \det J_2}$. In terms of the model parameters,
$$-\frac{bm(x_2 + \xi)y_2}{(x_2 + y_2 + \alpha\xi)^2} d_1 + x_2 \left(-1 + \frac{cy_2}{(x_2 + y_2 + \alpha\xi)^2}\right) d_2 = 2\sqrt{d_1 d_2 \det J_2},$$
provided, $d_2 > d_1 > 0$, tr $J_2 < 0$ and $\det J_2 > 0$. (This is the necessary conditions for Turing bifurcation. For sufficient condition please refer to Theorem B.0.5).

The behaviour of the equilibria changes across the (α, ξ) plane as we move through the various possible bifurcation curves. For the purpose of illustrating these bifurcation curves we choose representative parameter values for all the cases. We first consider the parameter values $c = 2, m =$

$0.5, b = 2$ and $d_2/d_1 = 25$. For these values the interior equilibrium point of the classical ratio-dependent model does not exist. However the point (x_2, y_2) for these values turn out to be stable for the allowable values of $\alpha > 1, \xi > 0$ and $\alpha\xi - 2\xi - 1 < 0$ (using results in Table 4.1). In this case we have the transcritical bifurcations curves Tcb_1 and Tcb_2, Hopf bifurcation curve as well as the Turing bifurcation curve Tb as given in Figure 4.1. The equilibrium point (x_2, y_2) becomes stable and $(0, (b-\alpha)\xi)$ loses its stability and vice versa as we move from one region to another by crossing Tcb_1. The axial equilibrium point $(1, 0)$ gains its stability, while the existence of (x_2, y_2) is lost when passing through the curve Tcb_2. As for the Turing bifurcation curve Tb, in the region above Tb and bounded by Tcb_1 and Tcb_2 in Figure 4.1, (x_2, y_2) is Turing stable. On the other hand, in the region between Tb curve and the Hopf bifurcation curve, (x_2, y_2) may exhibit Turing instability. In that case, this region will be the Turing space.

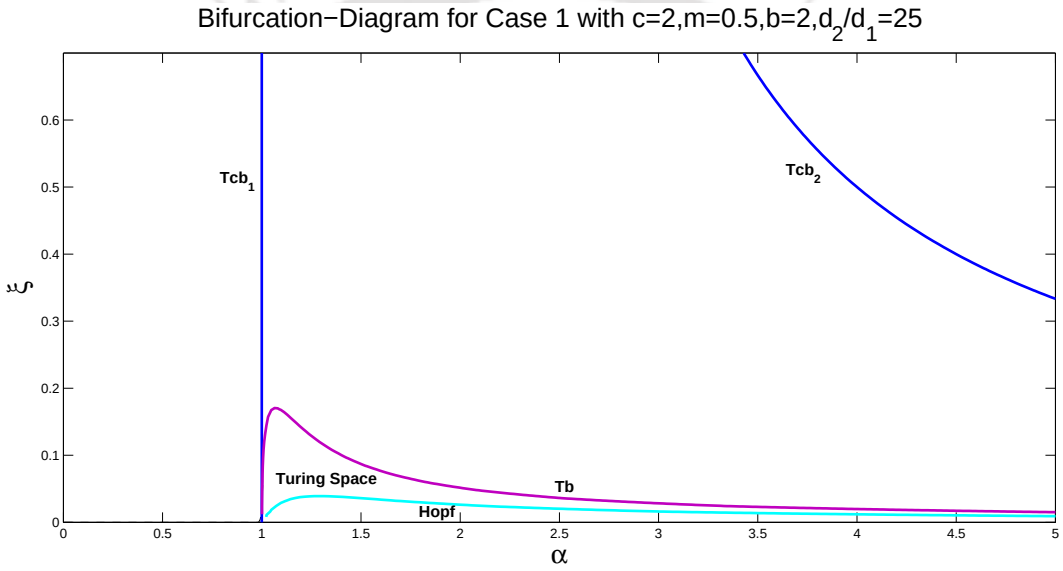

Figure 4.1: Bifurcation diagram for Case 1

Next, we make use of the parameter values $c = 1.2, m = 0.05, b = 3$ and $d_2/d_1 = 16$, in which case the interior equilibrium point of the original ratio-dependent model exist but is unstable. This point, however is stable for the modified model, provided all the conditions for such stability as given for Case 2 in Table 4.1 are satisfied. The bifurcations for this case are illustrated in Figure 4.2. In addition to the bifurcations, Tcb_1, Tcb_2, Hopf and Tb, we also now have saddle-node bifurcation. As with the preceding case, the nature of stability of (x_2, y_2) and $(0, (b-\alpha)\xi)$ changes as one moves from one region to another across the curve Tcb_1. The behaviour of (x_2, y_2) and $(1, 0)$ change across Tcb_2 is the same way as in the previous case. Similarly the changes in the Turing stability of (x_2, y_2) across Tb are identical to the earlier case. The point (x_2, y_2) loses or gains it stability across the Hopf bifurcation curve. The appearance/disappearance of the two interior equilibria

happen across the saddle-node bifurcation curve. The Turing space is the region bounded by the bifurcation curves Tb and Hopf, as well as the saddle-node curve.

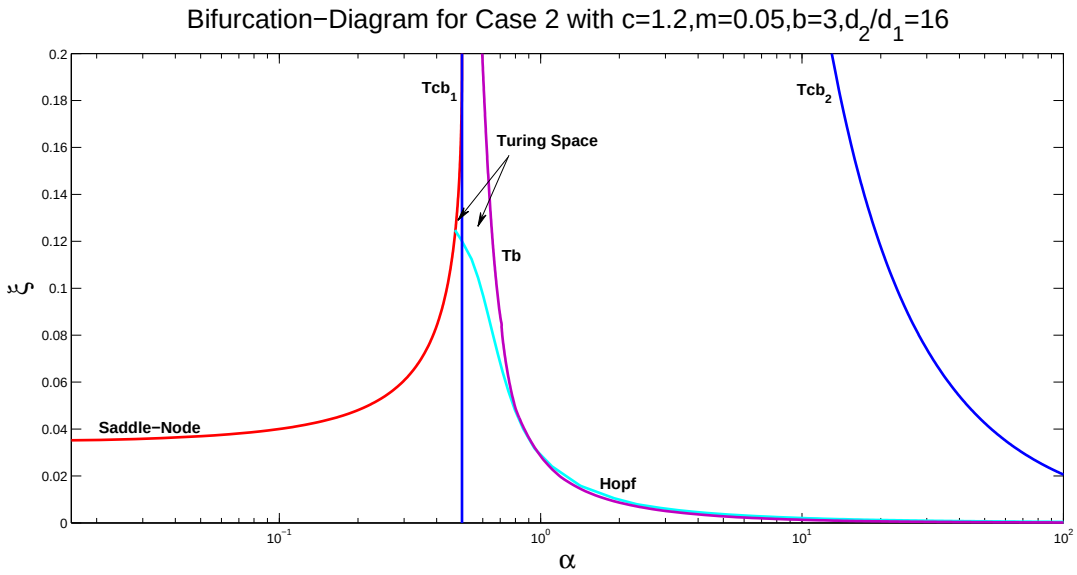

Figure 4.2: Bifurcation diagram for Case 2

Finally, the system is studied under the parameter values of $c = 1.1, m = 0.25, b = 5$ and $d_2/d_1 = 25$. This is the scenario where the original ratio-dependent model, admits a stable interior equilibrium point. The changes in the stability of the interior and axial equilibria, (x_2, y_2), $(0, (b-\alpha)\xi)$ and $(1, 0)$ across the bifurcation curves Tcb_1, Tcb_2, Tb, Hopf and saddle-node are similar to the ones on the preceding scenario. In this case, as seen in Figure 4.3, the Turing space is the region bounded by the curves Tb and saddle-node.

4.5 Turing Patterns

In this section, we will carry out the numerical simulation and observe the Turing patterns emerging from the spatially extended model (4.1.2). We have already discussed the various bifurcations for the interior equilibrium point (x_2, y_2) and have determined the Turing space as illustrated in Figures 4.1, 4.2 and 4.3.

For the purpose of numerical simulations with no-flux boundary condition, we considered a square domain of size 100×100. The numerical integration of the partial differential equations (4.1.2) was performed using the Euler explicit scheme. While a forward time approximation was used for the temporal derivative, a central space finite difference approximation was applied for the spatial derivatives, with the time and space intervals being $\Delta t = 0.1$ and $\Delta s_1 = \Delta s_2 = 2$ respectively. The temporal and spatial intervals chosen for the numerical simulations satisfy the

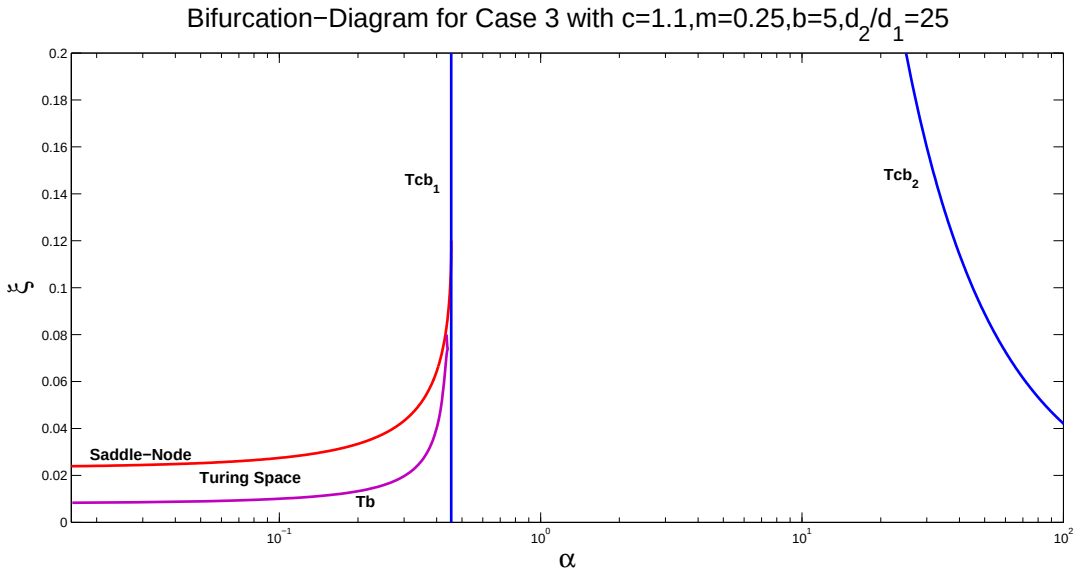

Figure 4.3: Bifurcation diagram for Case 3

numerical stability criterion of the linear approximation of the concerned model (4.1.2). For the no-flux condition a forward space approximation was used and set to zero to obtain boundary conditions. The initial population distribution (small perturbations around the interior equilibrium point (x_2, y_2)) was taken to be the absolute values of $x(s_{1,i}, s_{2,j}, 0) = x_2 + 0.001 \times Z_{i,j}^{(1)}$ and $y(s_{1,i}, s_{2,j}, 0) = y_2 + 0.001 \times Z_{i,j}^{(2)}$, where $Z_{i,j}^{(1)}$ and $Z_{i,j}^{(2)}$ are Gaussian white noise. The simulation were run for a large number of time steps, until a steady state Turing pattern was reached. The patterns emerging from the various cases discussed in the preceding section are illustrated in Figures 4.4,4.5,4.6,4.7,4.8 and 4.9.

For the first case, the parameter values used are $c = 2, m = 0.5, b = 2$ and $d_2/d_1 = 25$. We choose the values of $\alpha = 1.1$ and $\xi = 0.07$ from the Turing space for this case as illustrated in Figure 4.1. We take the initial population distribution to be the perturbations around the equilibrium point $x_2 = 0.0557$ (first figure of Figure 4.4) and $y_2 = 0.1187$ (first figure of Figure 4.5). We ran the simulations for a large number of time points. We however, present the prey and predator patterns that emerge at times $t = 1000, 3000$ and 5000 in Figures 4.4 and 4.5. We see a steady state emerging at time $t = 1000$ which regions of high (red) and low densities (blue). This pattern remains more or less unchanged for the subsequent times points of $t = 3000$ and 5000. These patterns are similar for both the prey and the predator even though the level of densities differ as indicated by the contour sidebar.

For the second case, we take the same parameters as in the preceding section, namely, $c = 1.2, m = 0.05, b = 3$ and $d_2/d_1 = 16$. Observing the Turing space for this case in Figure 4.2, we choose $\alpha = 0.62$ and $\xi = 0.09$ from the Turing space. The initial condition is set to be perturbations

around $x_2 = 0.1407, y_2 = 0.4956$. The emergence of prey and predator patterns from this initial condition are given in Figures 4.6 and 4.7. In this case, however the simulations had to be run for a longer time period before attaining a steady state. Staring from $t = 0$, the pattern emerges through $t = 5000$ before showing steady states at $t = 8000$ and 10000, for both the prey and predator population. In this case also the patterns that emerge are similar for both the populations with regions of high (red) and low (blue) densities, with the level of densities, however, being different for the two species.

Finally, we observe the patterns for the third case under the parameter values $c = 1.1, m = 0.25, b = 5$ and $d_2/d_1 = 25$. We choose the point $(\alpha, \xi) = (0.4, 0.06)$ from the Turing space (Figure 4.3). The emergence of patterns is similar to that of preceding case except that the steady state Turing pattern is reached much later. The initial (perturbations about $x_2 = 0.1537, y_2 = 0.5394$) and subsequent patterns at times $t = 10000, 15000$ and 20000 can be seen from Figures 4.8 and 4.9, with the steady state in the regions of both high and low densities being seen at time $t = 15000$ and 20000.

4.6 Conclusion

The nature of spatiotemporal dynamics and patterns for a diffusive modified ratio-dependent model (4.1.2) under supply of additional food to the predators is investigated in this Chapter. The supply of additional food was incorporated with the ratio-dependent functional response. The local stability results for the interior equilibrium point of the modified model without diffusion is presented in parametric form . Parametric conditions for Turing instability of the interior equilibrium point, upon addition of diffusivity are obtained by way of linearization of the spatiotemporal system. We discuss the various bifurcations resulting from these conditions. These are illustrated by considering particular values of the parameters $c, m,$ and b, with each set corresponding to various cases of existential and stability conditions of the interior equilibrium point of the original model. All these sets satisfy the conditions of existence and stability of the interior equilibrium point of the modified ratio-dependent model.

The bifurcation diagrams for these sets of parameter values illustrate the Turing space in the $\alpha - \xi$ plane. Values taken from the Turing space for all the three cases exhibit Turing patterns for the modified model. In absence of additional food one observes that the ratio-dependent spatiotemporal model does not exhibit Turing instability for the specific parameter values where the interior equilibrium point does not exist, where its exists but is unstable and where it exists and is stable. While the former two is due to the definition of Turing instability not being satisfied, the latter is due to the condition $\hat{a}_{22}\hat{d}_1 + \hat{a}_{11}\hat{d}_2 > 2\sqrt{\hat{d}_1\hat{d}_2 \det \hat{J}_*}$ not being satisfied in case of diffusion being added to the original model. Here $(\hat{a}_{ij}), i, j = 1, 2$ are entries of community matrix $\hat{J}_*$ of this model

at it's interior equilibrium point with $\hat{d}_k, k = 1, 2$ being the corresponding diffusion coefficients. Thus additional food plays a role in the Turing instability and consequently in formation of Turing patterns in the study of diffusive modified ratio-dependent model under these three cases.

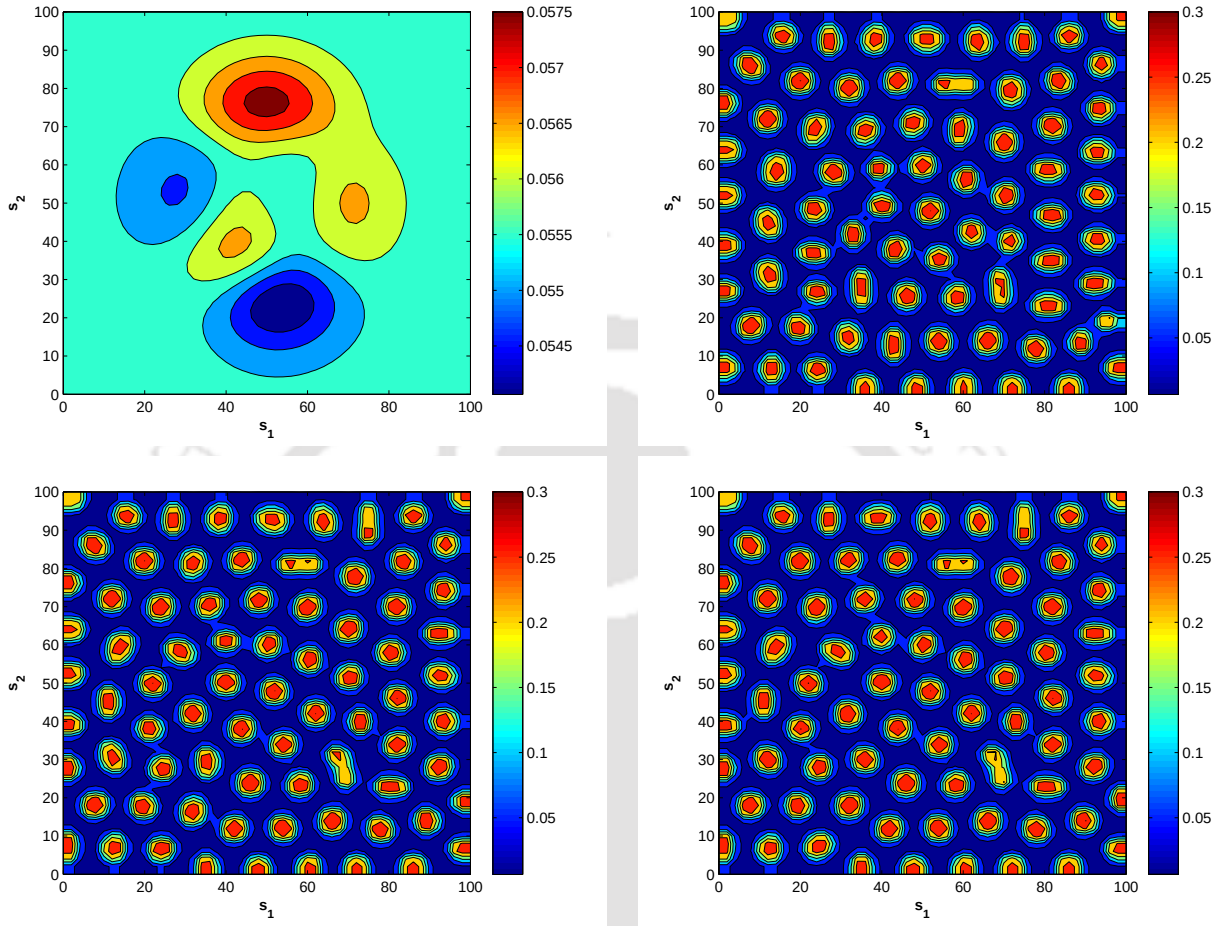

Figure 4.4: Snapshot of prey population at $t = 0, 1000, 3000$ and 5000 under Case 1 with $c = 2, m = 0.5, b = 2, d_2/d_1 = 25$ and $(\alpha, \xi) = (1.1, 0.07)$. Here, the left and right figures in the top followed by the left and right figures in the bottom are for $t = 0$, $t = 1000$, $t = 3000$ and $t = 5000$ respectively. The figure illustrates that for a randomly distributed initial prey population the patterns emerge as time progresses and eventually reaches the steady state. The red and blue colour signifies the high and low prey density area respectively.

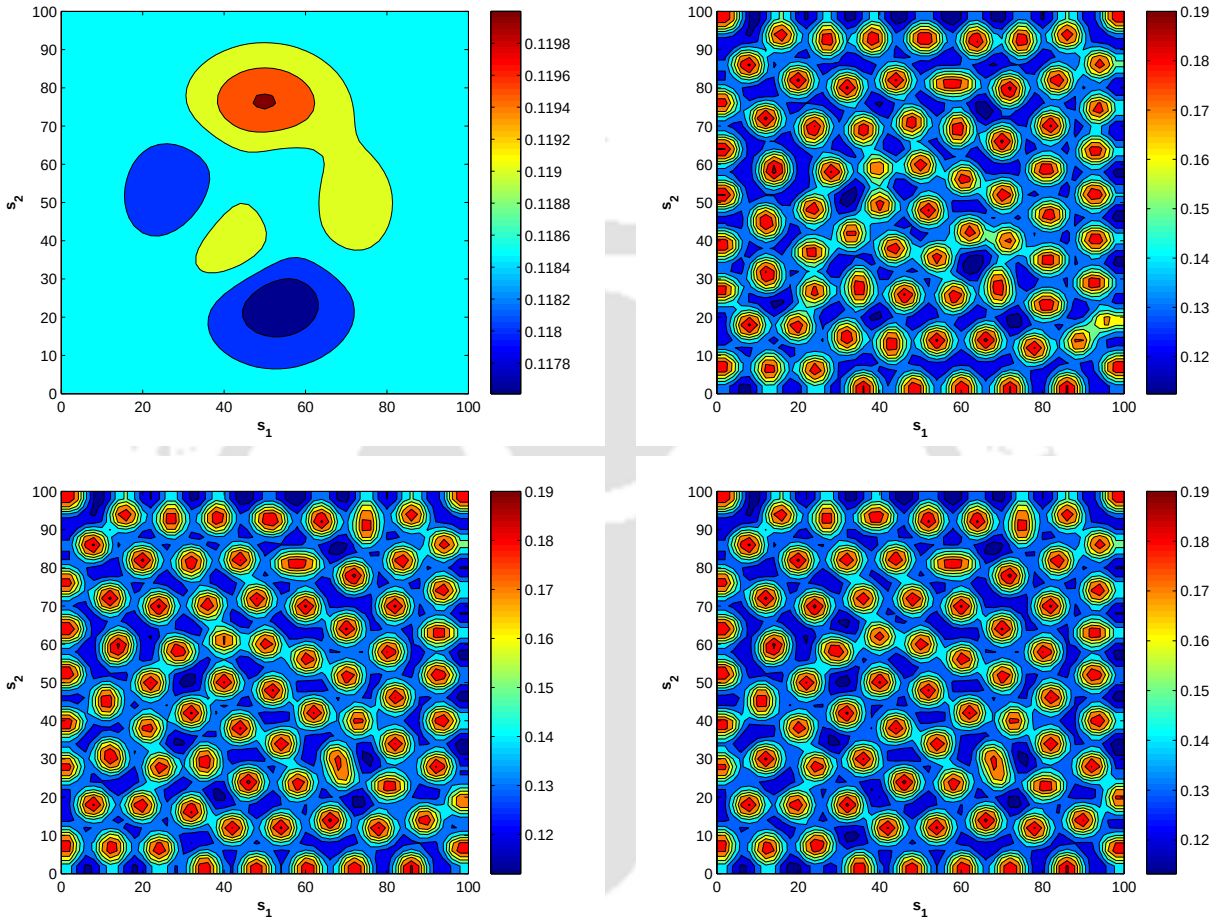

Figure 4.5: Snapshot of predator population at $t = 0, 1000, 3000$ and 5000 under Case 1 with $c = 2, m = 0.5, b = 2, d_2/d_1 = 25$ and $(\alpha, \xi) = (1.1, 0.07)$. Here, the left and right figures in the top followed by the left and right figures in the bottom are for $t = 0$, $t = 1000$, $t = 3000$ and $t = 5000$ respectively. The figure illustrates that for a randomly distributed initial predator population the patterns emerge as time progresses and eventually reaches the steady state. The red and blue colour signifies the high and low predator density area respectively.

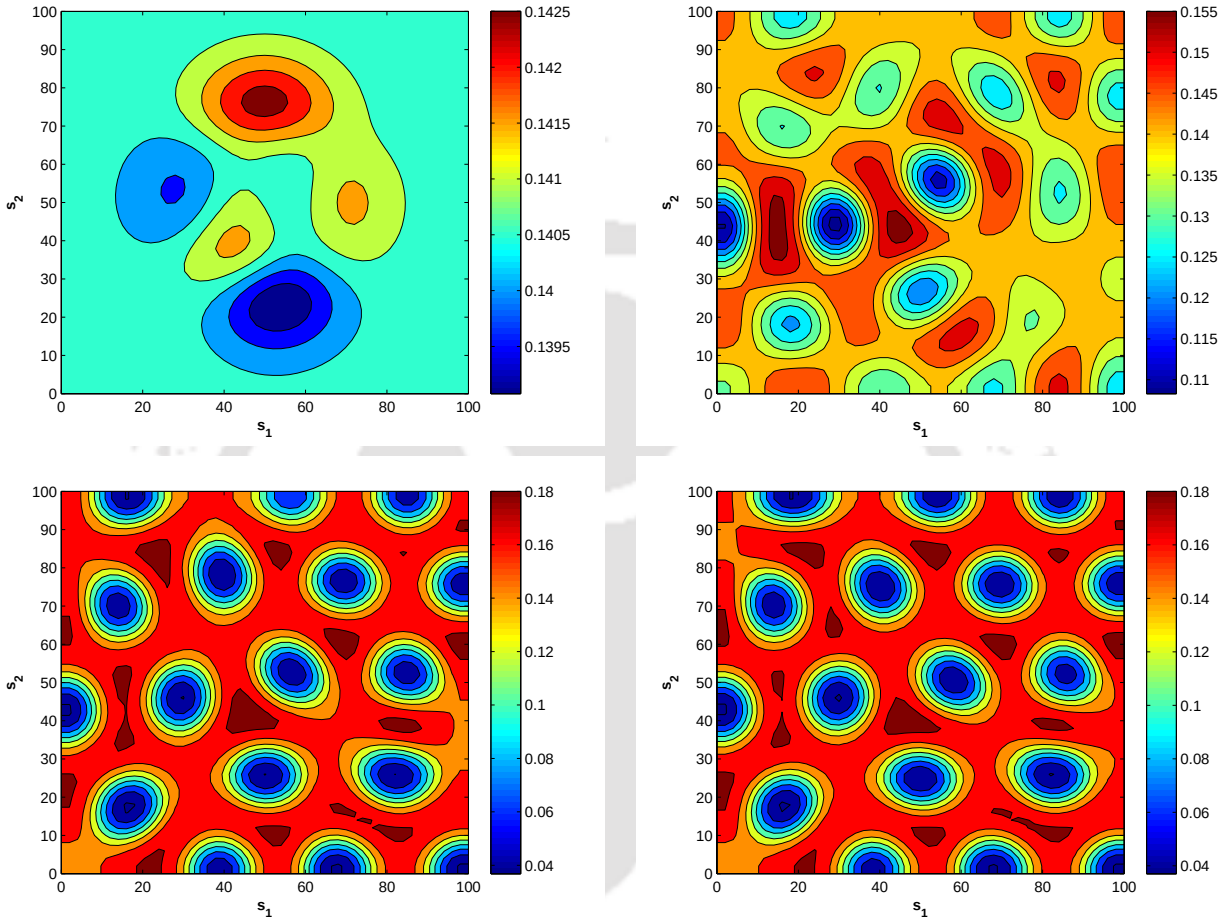

Figure 4.6: Snapshot of prey population at $t = 0, 5000, 8000$ and 10000 under Case 2 with $c = 1.2, m = 0.05, b = 3, d_2/d_1 = 16$ and $(\alpha, \xi) = (0.62, 0.09)$. Here, the left and right figures in the top followed by the left and right figures in the bottom are for $t = 0$, $t = 5000$, $t = 8000$ and $t = 10000$ respectively. The figure illustrates that for a randomly distributed initial prey population the patterns emerge as time progresses and eventually reaches the steady state. The red and blue colour signifies the high and low prey density area respectively.

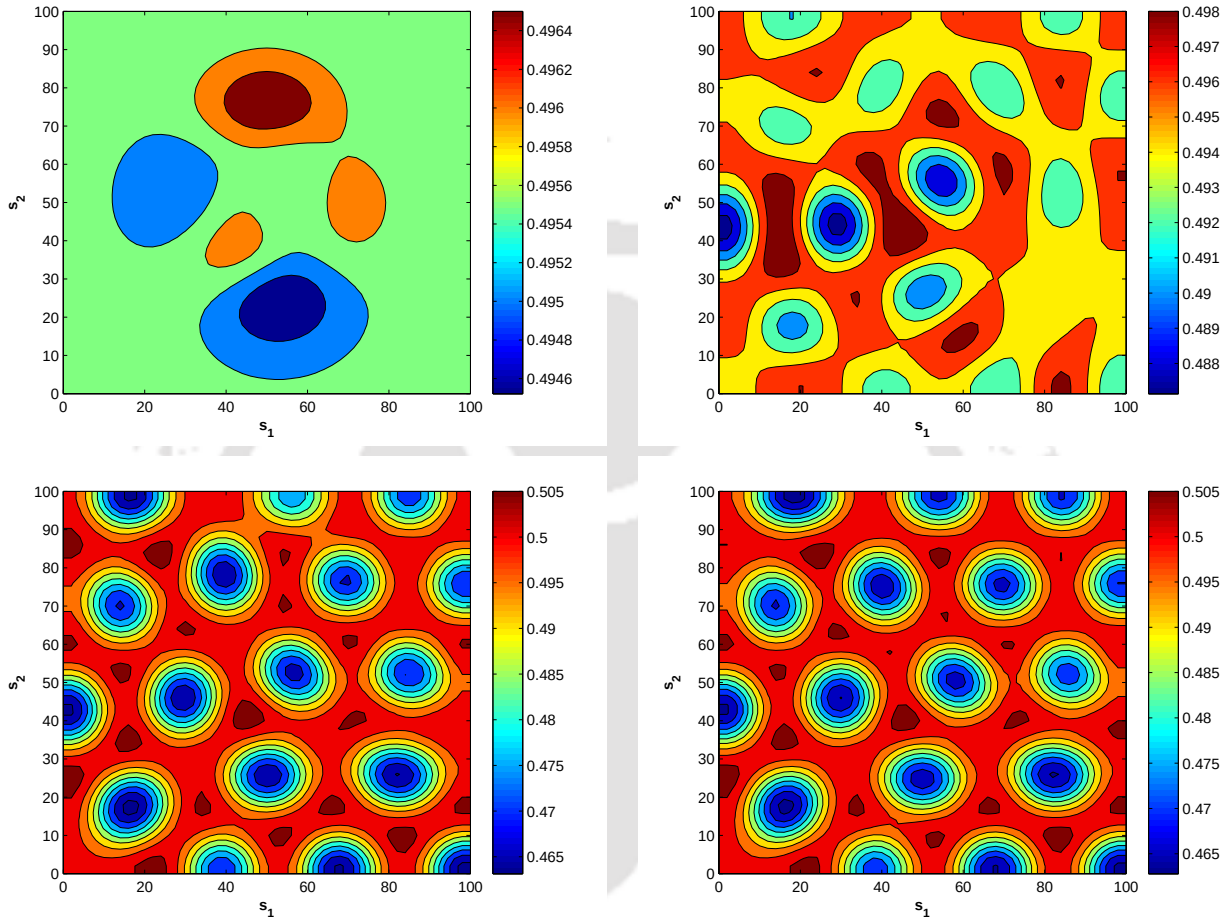

Figure 4.7: Snapshot of predator population at $t = 0, 5000, 8000$ and 10000 under Case 2 with $c = 1.2, m = 0.05, b = 3, d_2/d_1 = 16$ and $(\alpha, \xi) = (0.62, 0.09)$. Here, the left and right figures in the top followed by the left and right figures in the bottom are for $t = 0$, $t = 5000$, $t = 8000$ and $t = 10000$ respectively. The figure illustrates that for a randomly distributed initial predator population the patterns emerge as time progresses and eventually reaches the steady state. The red and blue colour signifies the high and low predator density area respectively.

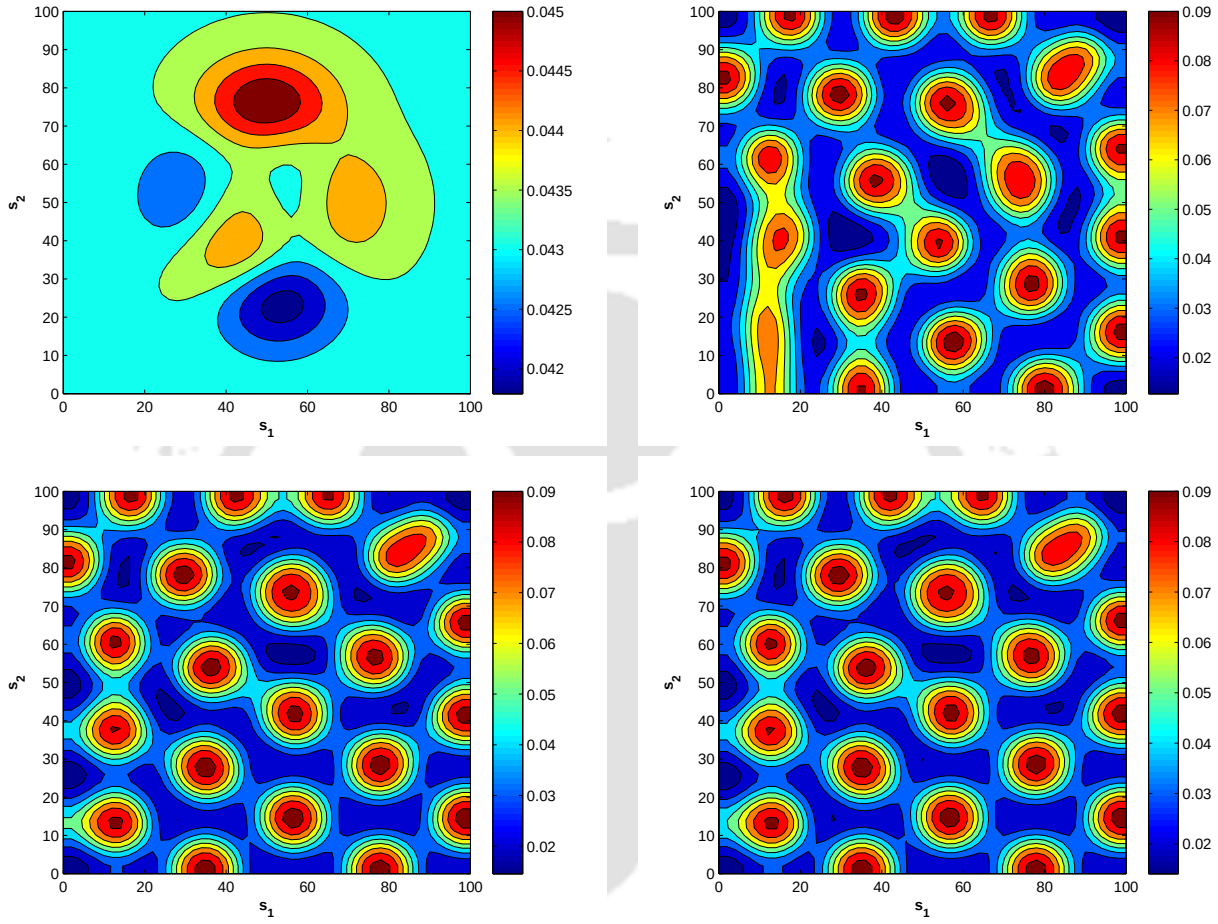

Figure 4.8: Snapshot of prey population at $t = 0, 10000, 15000$ and 20000 under Case 3 with $c = 1.1, m = 0.25, b = 5, d_2/d_1 = 25$ and $(\alpha, \xi) = (0.4, 0.06)$. Here, the left and right figures in the top followed by the left and right figures in the bottom are for $t = 0$, $t = 10000$, $t = 15000$ and $t = 20000$ respectively. The figure illustrates that for a randomly distributed initial prey population the patterns emerge as time progresses and eventually reaches the steady state. The red and blue colour signifies the high and low prey density area respectively.

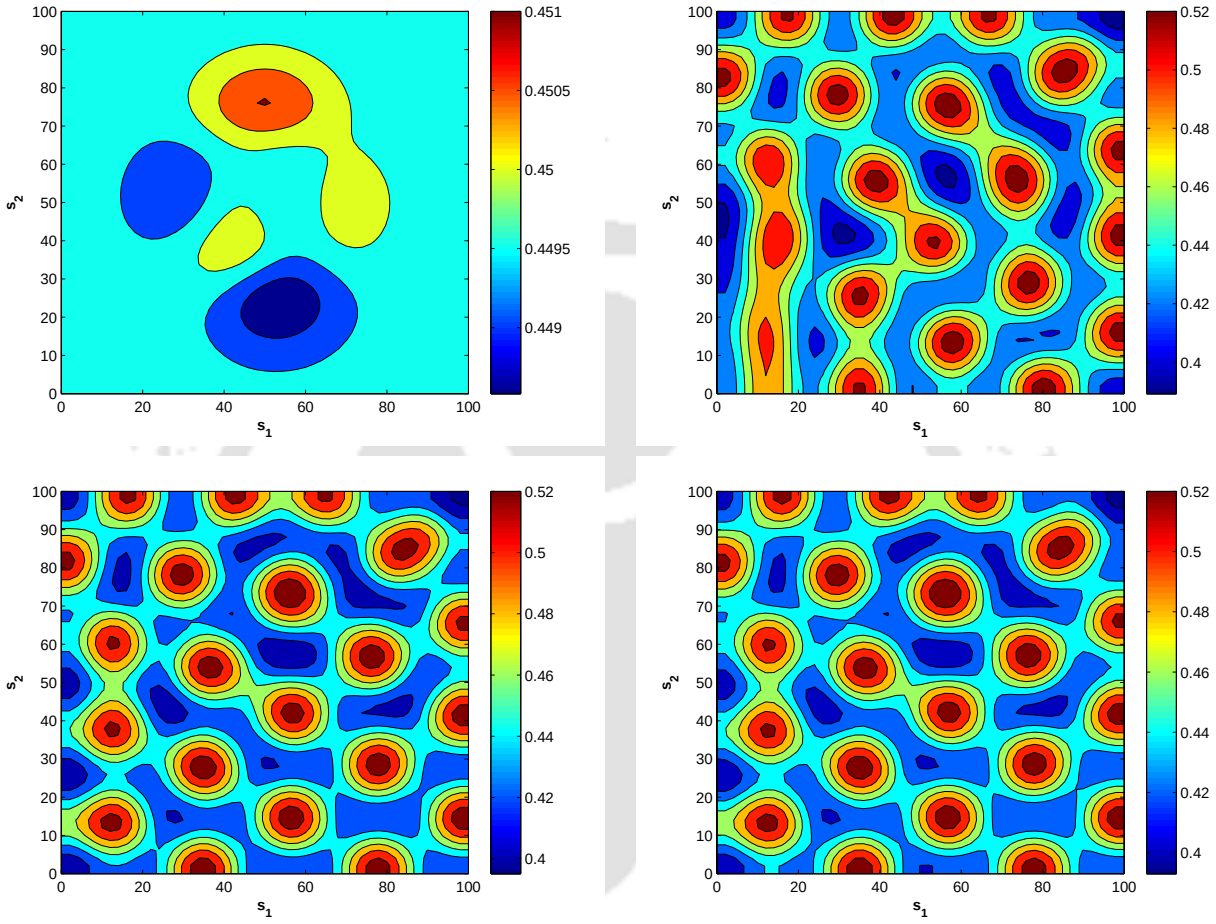

Figure 4.9: Snapshot of predator population at $t = 0, 10000, 15000$ and 20000 under Case 3 with $c = 1.1, m = 0.25, b = 5, d_2/d_1 = 25$ and $(\alpha, \xi) = (0.4, 0.06)$. Here, the left and right figures in the top followed by the left and right figures in the bottom are for $t = 0$, $t = 10000$, $t = 15000$ and $t = 20000$ respectively. The figure illustrates that for a randomly distributed initial predator population the patterns emerge as time progresses and eventually reaches the steady state. The red and blue colour signifies the high and low predator density area respectively.

Chapter 5

Models with Prey Harvesting

In this chapter, we present two models which incorporate prey harvesting to the classical and the modified ratio-dependent predator-prey model. We analyze the existence and stability of the equilibrium points of both the models and determine the range for sustainable harvesting effort. The optimal harvesting policy is determined by using Pontryagin's maximum principle. The results obtained are numerically illustrated. We examine the consequences of providing additional food (as a part of the total harvest effort) to predators in prey harvesting.

5.1 Boundedness of the Solution for a Class of Predator-Prey Systems

To begin with, we consider a general class of predator-prey system, which will include all the three predator-prey systems to be discussed in this chapter, namely, the ratio-dependent system with prey harvesting and the modified (by way of supply of additional food to the predators) ratio-dependent system with prey harvesting. We will show that the solution for this class of predator-prey system (as given below) is bounded in the first quadrant of $\mathbb{R}^2$.

$$\begin{aligned} \frac{dx}{dt} &= x\,(1-x) - h(x,y), \\ \frac{dy}{dt} &= m\left(\frac{b(x+\kappa)}{x+y+\upsilon} - 1\right) y, \end{aligned} \tag{5.1.1}$$

where the function $h(x,y)$ includes following form:

(i) $h(x,y) = \frac{cxy}{x+y} + qEx$, with $c, q, E > 0$,

(ii) $h(x,y) = \frac{cxy}{x+y+\alpha\xi} + qEx$, with $c, q, \alpha, \xi, E > 0$.

Also, parameters m, b are positive and κ, υ are non-negative.

Theorem 5.1.1. *If $(x(t), y(t))$ are the solution of system (5.1.1), then $x(t)$ will be bounded for any initial condition $x(0) \geq 0,\ y(0) \geq 0$.*

Proof. It can be shown, by vector field analysis, that the solutions of the general class of system (5.1.1) are non-negative. It can be seen from the first equation of (5.1.1) that,

$$\frac{dx}{dt} \leq x(1-x) \;\Rightarrow\; \lim_{t\to+\infty} \sup x(t) \leq 1.$$

Thus we conclude that $x(t)$ will be bounded for any non-negative initial condition. □

Theorem 5.1.2. *If $(x(t), y(t))$ are the solution of system (5.1.1) and $x(t)$ is bounded above, then $y(t)$ will also be bounded above for any initial condition $x(0) \geq 0$, $y(0) \geq 0$.*

Proof. We have already proved that $\lim_{t\to+\infty} \sup x(t) \leq 1$. Therefore for any $\epsilon > 0$ there exist a $T > 0$, s.t. $x(t) \leq 1 + \epsilon/b \;\; \forall\, t \geq T$. Thus, from the second equation of (5.1.1)

$$\begin{aligned} \frac{dy}{dt} &= m\left(\frac{b(x+\kappa)}{x+y+\upsilon} - 1\right) y \leq m\left(b\left(1+\frac{\epsilon}{b}+\kappa\right) - y\right),\; t \geq T \\ &\Rightarrow \lim_{t\to+\infty} \sup y(t) \leq b(1+\kappa) + \epsilon \end{aligned}$$

Since $\epsilon > 0$ is arbitrary, therefore we get, $\lim_{t\to+\infty} \sup y(t) \leq b(1+\kappa)$. Hence $y(t)$ is bounded for any non-negative initial condition. □

5.2 Stability of the Classical Ratio-Dependent Model with Prey Harvesting

First, we formulate a model to incorporate prey harvesting to the classical ratio-dependent model as follows,

$$\begin{aligned} \frac{dx}{dt} &= x\,(1-x) - \frac{cxy}{x+y} - qEx \\ \frac{dy}{dt} &= m\left(\frac{bx}{x+y} - 1\right) y. \end{aligned} \tag{5.2.1}$$

where q and E represent the prey catchability coefficient and harvesting effort respectively.

5.2.1 Existence of Equilibrium Points

This system (5.2.1), admits three equilibrium points, namely

- $(0, 0)$,
- $(1 - qE, 0)$ and
- the interior equilibrium point $(\bar{x}, \bar{y})$,

which are obtained by solving the prey and predator isoclines given by $x(1-x) - \frac{cxy}{x+y} - qEx = 0$ and $\frac{bxy}{x+y} - y = 0$ respectively. The equilibrium $(0,0)$ represents the extinction of both the species and $(1,0)$ represents the extinction of the predator population with the prey population being at its carrying capacity. The co-existence of both the species is represented by the interior equilibrium point $(\bar{x}, \bar{y})$, where

$$\bar{x} = 1 - c + \frac{c}{b} - qE$$

and $\bar{y} = (b-1)\bar{x}$. One can easily observe from interior equilibria of the system (2.1.2) and (5.2.1), that prey harvesting results in the reduction of the equilibrium level of both prey and predator, due to the increase in the mortality rate of the prey population and the consequent decrease in the availability of prey to predators. In order for the interior equilibrium point to exist we need $1-c+\frac{c}{b}-qE > 0$ which implies $E < \frac{1}{q}\left(1 - c + \frac{c}{b}\right)$. Also note that in this case $E < \frac{1}{q}\left(1 - c + \frac{c}{b}\right) < \frac{1}{q}$. So whenever the interior equilibrium point of the system (5.2.1) exists, then axial equilibrium point $(1 - qE, 0)$ will also exist.

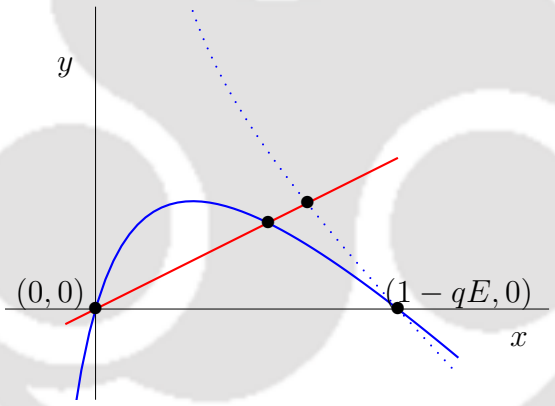

Geometrically, it is easy to see that as E increases, the point of intersection $(1 - qE, 0)$ of prey isocline with the x-axis moves towards the origin. Consequently, the interior equilibrium point, moves towards the y-axis (*i.e.,* there is a decrease in prey population density).

The conditions for the existence of the three equilibrium points are summarized in Table 5.1:

Equilibrium point	Existential Conditions
$(0,0)$	-
$(1-qE,0)$	$E<\frac{1}{q}$
$(\bar{x},\bar{y})=\left(1-c+\frac{c}{b}-qE,(b-1)\bar{x}\right)$	$b>1$ and $E<\frac{1}{q}\left(1-c+\frac{c}{b}\right)$

Table 5.1: Conditions on parameters for existence of equilibrium points of the classical ratio-dependent system with prey harvesting.

5.2.2 Local Stability Analysis

We now present the local asymptotic stability analysis of system (5.2.1). The Jacobian matrix for (5.2.1) is given by,

$$J=\begin{bmatrix}(1-x)-\frac{cy}{x+y}-qE+x\left[-1+\frac{cy}{(x+y)^2}\right] & -\frac{cx^2}{(x+y)^2}\\ \frac{bmy^2}{(x+y)^2} & m\left(\frac{bx}{x+y}-1\right)-\frac{bmxy}{(x+y)^2}\end{bmatrix}.$$

This matrix evaluated at the point $(1-qE,0)$ is,

$$J_{(1-qE,0)}=\begin{bmatrix}-(1-qE) & -c\\ 0 & m(b-1)\end{bmatrix}.$$

We observe that $(1-qE,0)$ is stable whenever $b<1$. The interior equilibrium point $(\bar{x},\bar{y})$ will not exist whenever this happens. Consequently, when the interior equilibrium point exists, then $(1,0)$ will be a saddle.

Finally, the Jacobian matrix at $(\bar{x},\bar{y})$ is given by

$$J_{(\bar{x},\bar{y})}=\begin{bmatrix}\bar{x}\left[-1+\frac{c\bar{y}}{(\bar{x}+\bar{y})^2}\right] & -\frac{c\bar{x}^2}{(\bar{x}+\bar{y})^2}\\ \frac{bm\bar{y}^2}{(\bar{x}+\bar{y})^2} & -\frac{bm\bar{x}\bar{y}}{(\bar{x}+\bar{y})^2}\end{bmatrix}$$

The condition for the interior equilibrium point (provided it exists) to be stable is

$$E<\frac{1}{q}\left(1-c+m+\frac{c-bm}{b^2}\right).$$

The Jacobian is not defined at equilibrium point $(0,0)$. To analyze the behaviour around $(0,0)$ we use a transformed system after Jost et al. [9]. Using transformation $u=\frac{x}{y},y=y$, results in the following $u-y$ system,

$$\begin{aligned}\frac{du}{dt} &= u\left(1-qE+m-uy\right)-\frac{u(c+bmu)}{u+1},\\ \frac{dy}{dt} &= m\left(\frac{bu}{u+1}-1\right)y.\end{aligned}$$

The corresponding Jacobian for the $u-y$ system is given by

$$J^{(u,y)} = \begin{bmatrix} (1-qE+m-uy) - \frac{(c+bmu)}{u+1} + u\left[-y - \frac{bm-c}{(u+1)^2}\right] & -u^2 \\ \frac{mby}{(u+1)^2} & m\left(\frac{bu}{u+1} - 1\right) \end{bmatrix},$$

which evaluated at $(0,0)$ gives,

$$J^{(u,y)}_{(0,0)} = \begin{bmatrix} 1-qE+m-c & 0 \\ 0 & -m \end{bmatrix}.$$

The point $(0,0)$ in this system is a saddle for $E < \frac{1}{q}(1+m-c)$ and an attractor for $E > \frac{1}{q}(1+m-c)$. We similarly obtain the $x-v$ system by using transformation $x = x, v = \frac{y}{x}$ as,

$$\begin{aligned} \frac{dx}{dt} &= x\left[(1-qE-x) - \frac{cv}{v+1}\right], \\ \frac{dv}{dt} &= v(x-1+qE-m) + \frac{v(bm+cv)}{v+1}. \end{aligned}$$

The corresponding Jacobian for the $x-v$ system is given by

$$J^{(x,v)} = \begin{bmatrix} \left[(1-qE-x) - \frac{cv}{v+1}\right] - x & x\left[-\frac{(v+1)c-cv}{(v+1)^2}\right] \\ v & v\left[\frac{(v+1)c-(bm+cv)}{(v+1)^2}\right] + (x-1+qE-m) + \frac{(bm+cv)}{v+1} \end{bmatrix},$$

whose value at $(0,0)$ is,

$$J^{(x,v)}_{(0,0)} = \begin{bmatrix} 1-qE & 0 \\ 0 & -1+qE-m+bm \end{bmatrix}.$$

Thus $(0,0)$ is a saddle when $E < \frac{1-m(b-1)}{q}$. On the other hand when $E > \frac{1-m(b-1)}{q}$, then $(0,0)$ is a repeller. Thus, in this case $(0,0)$ cannot be stable.

Reasoning on the lines of Jost et al. [9], we see that in the $u-y$ system, $(0,0)$ is an attractor when $E > \frac{1}{q}(1+m-c)$ and saddle when $E < \frac{1}{q}(1+m-c)$. The ramification of this for $(0,0)$ in the original $x-y$ system is that a trajectory will approach to $(0,0)$ only when the approach rate of x towards 0 is more rapid than the approach rate of y.

5.2.3 Global Stability Analysis

Theorem 5.2.1. *Suppose that the interior equilibrium point $(\bar{x},\bar{y})$ is locally asymptotically stable and the condition $m(b-1) \geq 1$ holds, then $(\bar{x},\bar{y})$ is also globally stable.*

Proof. We first define the following function,

$$L_1(x,y) = \frac{\partial}{\partial x}\left(B_1(x,y)f_1(x,y)\right) + \frac{\partial}{\partial y}\left(B_1(x,y)g_1(x,y)\right),$$

where $f_1(x,y) = x\left(1-qE-x\right) - \frac{cxy}{x+y}$, $g_1(x,y) = m\left(\frac{bx}{x+y} - 1\right)y$ and $B_1(x,y) = \frac{x+y}{xy^2}$. After simplification, we obtain,

$$L_1(x,y) = \frac{1-qE-(b-1)m-2x-y}{y^2}.$$

Now, $L_1(x,y) < 0$ whenever $x > 0$ and $y > 0$, since $m(b-1) \geq 1$. Thus, by using the Dulac's criterion [49], the system (5.2.1) will not have any non-trivial periodic orbit in $\mathbb{R}^2_+$. Note that both the trivial and the axial equilibrium points are saddle and have $y-$axis and $x-$axis as their respective stable manifolds. Using this in conjunction with the Poincare-Bendixson Theorem [49] gives us that the interior equilibrium point $(\bar{x}, \bar{y})$ will be globally stable. □

In order to determine a suitable harvesting effort ensuring the conservation of both the prey and predator populations, we need the equilibria $(0,0)$ and $(1-qE, 0)$ to be saddle and the interior equilibrium $(\bar{x}, \bar{y})$ to be stable in nature.

It can be seen that the axial equilibrium point $(1-qE, 0)$ is a saddle if $b > 1$ and the interior equilibrium $(\bar{x}, \bar{y})$ will be asymptotically stable when $E < \frac{1}{q}\left(1 - c + m + \frac{c-bm}{b^2}\right)$. Also $\frac{1}{q}\left(1-c+\frac{c}{b}\right) < \frac{1}{q}\left(1-c+m+\frac{c-bm}{b^2}\right) < \frac{1}{q}(1-c+m) \iff c < bm$. So as long as the condition $c < bm$ holds, the non-trivial equilibrium point for the system (5.2.1) is locally stable whenever it exists. It can be proven that $c < bm \iff c < 1+m$, whenever $m(b-1) \geq 1$. Thus under Case 3, $(\bar{x}, \bar{y})$ is locally stable (if it exists).

Finally, we summarize all the conditions (for the three cases defined in Table 3.2) on effort E in order to achieve ecologically sustainable harvesting (for the system (5.2.1)) in Table 5.2.

Conditions	**Ensures**	**Applicable Cases**
$E < \frac{1}{q}(1-c+m)$	$(0,0)$ is saddle	Case 3
$E < \frac{1}{q}\left(1-c+\frac{c}{b}\right)$	$(\bar{x}, \bar{y})$ exists and $(1-qE, 0)$ is saddle	Case 2, Case 3
$E < \frac{1}{q}\left(1-c+\frac{c}{b}\right)$	$(\bar{x}, \bar{y})$ is globally stable	Case 3

Table 5.2: Conditions on harvesting effort for the system (5.2.1).

This table indicates that prey harvesting should not be initiated with a random effort level E. Stability analysis gives us the way of determining an appropriate effort level since a randomly chosen effort level may lead to population extinction. For example, we choose the parameter values $c = 1.1, m = 1$ and $b = 3$ for which the interior equilibrium point of the system (2.1.2) is globally stable (as seen in Figure 5.1). With this same set of parameters and choosing $q = 1$ (for example), the interior equilibrium points $(\bar{x}, \bar{y})$ of the system (5.2.1) will not be globally stable for any choice of $E > 0.2667$. Thus, in this case, ecological conservation requires that the effort level E be kept below 0.2667. This is illustrated by the phase portraits in Figures 5.2 and 5.3. In Figure 5.2, $E = 0.2 < 0.2667$ resulting in conservation of both the species, whereas in Figure 5.3 we take $E = 0.5 > 0.2667$ and observe the extinction of both the species.

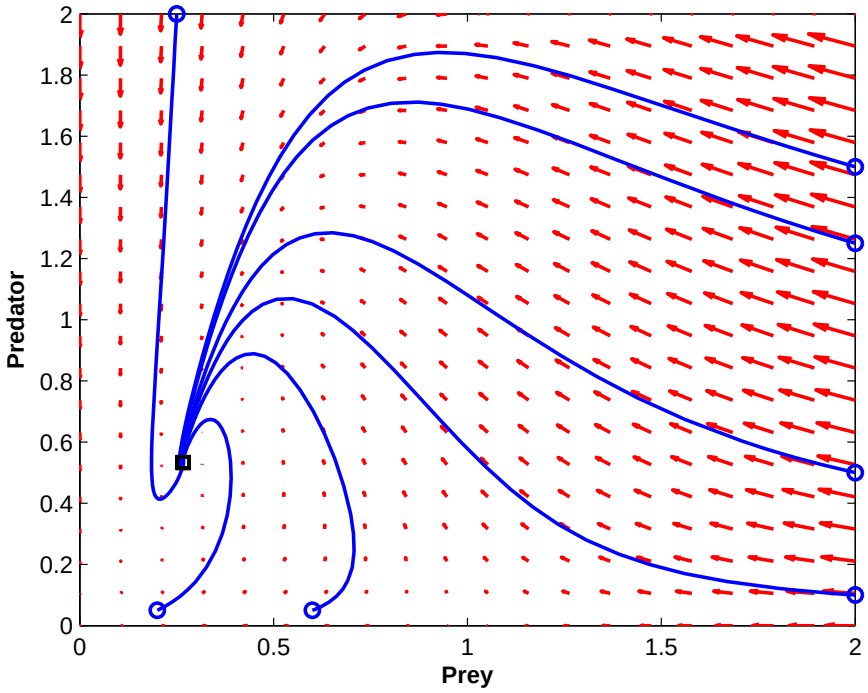

Figure 5.1: Phase-portrait for the system (2.1.2) with parameter values $c = 1.1, m = 1$ and $b = 3$.

5.3 Stability of the Modified Ratio-Dependent Model with Prey Harvesting

We now consider the model which incorporates prey harvesting to the modified ratio-dependent model (2.1.3). Accordingly we have,

$$\begin{aligned} \frac{dx}{dt} &= x\,(1-x) - \frac{cxy}{x+y+\alpha\xi} - qEx, \\ \frac{dy}{dt} &= m\left(\frac{b\,[x+\xi]}{x+y+\alpha\xi} - 1\right) y. \end{aligned} \tag{5.3.1}$$

Note that this model incorporates prey harvesting as well as the supply of additional food to the predators. Thus the model comprises of two economic components, namely the harvesting effort and the supply of additional food.

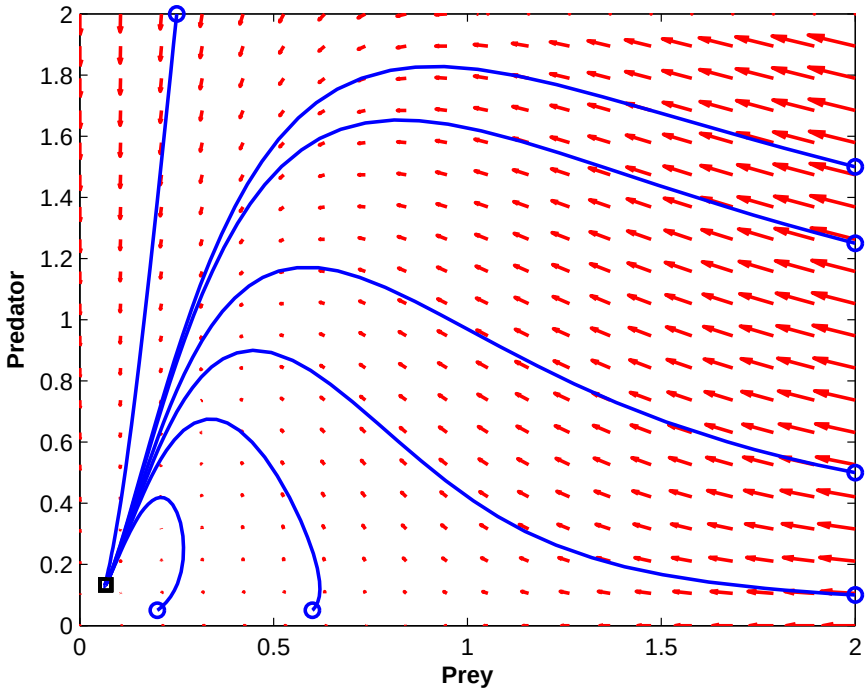

Figure 5.2: Phase-portrait for the system (5.2.1) with parameter values $c = 1.1, m = 1, b = 3, q = 1$ and $E = 0.2$.

5.3.1 Existence of Equilibrium Points

The system (5.3.1) admits the trivial equilibrium point $(0, 0)$, two axial equilibria, $(1 - qE, 0)$ and $(0, (b-\alpha)\xi)$ and two interior equilibria $(x_i, y_i),\ i = 1, 2$ given by the solution of following equations,

$$\begin{aligned} 1 - x - \frac{cy}{x + y + \alpha\xi} - qE &= 0 \\ \frac{b\,[x + \xi]}{x + y + \alpha\xi} - 1 &= 0. \end{aligned} \tag{5.3.2}$$

Solving (5.3.2) we obtain $(x_i, y_i),\ i = 1, 2$ where each $x_i \in (0, 1 - qE)$ is the root of quadratic equation $x^2 + (c - 1 - \frac{c}{b} + \xi + qE)x + \xi(qE + c - 1 - \frac{\alpha c}{b}) = 0$ (see Appendix C), which is given by

$$\begin{aligned} x_i &= \frac{1 - qE - c + \frac{c}{b} - \xi}{2} + \frac{(-1)^i}{2}\sqrt{\left(qE + c - 1 - \frac{c}{b} + \xi\right)^2 - 4\xi\left(qE + c - 1 - \frac{\alpha c}{b}\right)} \\ \text{and } y_i &= (b-1)x_i + (b-\alpha)\xi. \end{aligned}$$

The following relation can be derived from (5.3.2) (see Appendix C),

$$x_i = 1 - c + \frac{c}{b} - qE + \frac{c(\alpha - 1)\xi}{b(x_i + \xi)}.$$

This relation is satisfied by the interior equilibria (x_i, y_i) when they exist. From this relation we can conclude that whenever $\alpha > 1$, the supply of additional food to predators, reduces the pressure of

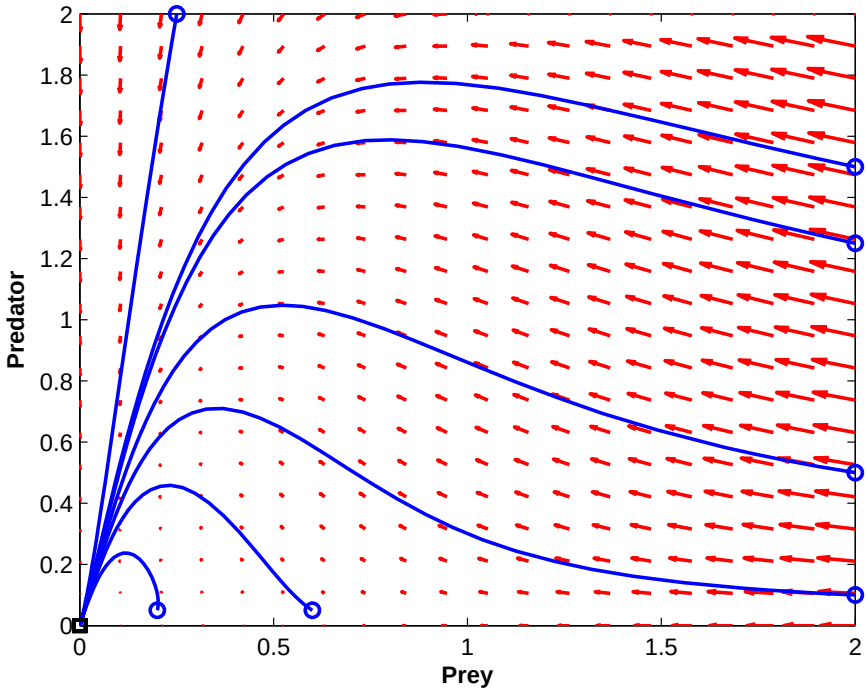

Figure 5.3: Phase-portrait for the system (5.2.1) with parameter values $c = 1.1, m = 1, b = 3, q = 1$ and $E = 0.5$.

predation (on prey) as well as the pressure (on both prey and predator) resulting from harvesting. Defining Δ as the expression under the square root term of x_i, we obtain the conditions (see Table 5.3) on the model parameters, required for the existence of the above equilibrium points.

Under the condition $0 < x_i < 1-qE$, we have $y_i > 0$. To see this, consider $y_i = \frac{(1-qE-x_i)(x_i+\alpha\xi)}{x_i+c-1+qE}$. Observe that if $c \geq 1-qE$, then $y_i > 0$. For the case when $c < 1-qE$ and noting that $x_i = 1-c-qE$ is an asymptote to the prey isocline $y_i = \frac{(1-qE-x_i)(x_i+\alpha\xi)}{x_i+c-1+qE}$, we obtain $x_i > 1-c-qE$. Thus $y_i > 0$ for $c < 1-qE$ also.

5.3.2 Local Stability Analysis

The Jacobian matrix for (5.3.1) is given by

$$J = \begin{bmatrix} (1-x) - \frac{cy}{x+y+\alpha\xi} - qE + x\left[-1 + \frac{cy}{(x+y+\alpha\xi)^2}\right] & -\frac{cx(x+\alpha\xi)}{(x+y+\alpha\xi)^2} \\ \frac{bmy(y+\alpha\xi-\xi)}{(x+y+\alpha\xi)^2} & m\left(\frac{b[x+\xi]}{x+y+\alpha\xi} - 1\right) - \frac{bm(x+\xi)y}{(x+y+\alpha\xi)^2} \end{bmatrix}.$$

Equilibrium point	Existential conditions
$(0,0)$	-
$(1-qE,0)$	$qE<1$
$(0,(b-\alpha)\xi)$	$b>\alpha$
(x_1,y_1)	$qE+c-1-\frac{c}{b}+\xi<0,\ qE+c-1-\frac{\alpha c}{b}>0,\ \Delta>0,\ x_1<1-qE$ or $qE+c-1-\frac{c}{b}+\xi<0,\ \Delta=0,\ x_1<1-qE$
(x_2,y_2)	$qE+c-1-\frac{c}{b}+\xi<0,\ qE+c-1-\frac{\alpha c}{b}>0,\ \Delta>0,\ x_2<1-qE$ or $qE+c-1-\frac{c}{b}+\xi<0,\ qE+c-1-\frac{\alpha c}{b}=0,\ x_2<1-qE$ or $qE+c-1-\frac{c}{b}+\xi<0,\ \Delta=0,\ x_2<1-qE$ or $qE+c-1-\frac{\alpha c}{b}<0,\ x_2<1-qE$

Table 5.3: Conditions on parameters for existence of equilibrium points of the modified ratio-dependent system with prey harvesting

Hence the Jacobian matrix at the equilibria of the system (5.3.1) is of the following form,

$$
\begin{aligned}
J_{(0,0)} &= \begin{bmatrix} 1-qE & 0 \\ 0 & \frac{m}{\alpha}(b-\alpha) \end{bmatrix}, \\
J_{(1-qE,0)} &= \begin{bmatrix} -(1-qE) & -\frac{c(1-qE)}{1-qE+\alpha\xi} \\ 0 & \frac{m((b-1)(1-qE)+(b-\alpha)\xi)}{1-qE+\alpha\xi} \end{bmatrix}, \\
J_{(0,(b-\alpha)\xi)} &= \begin{bmatrix} 1-qE-c+\frac{c\alpha}{b} & 0 \\ \frac{m(b-\alpha)(b-1)}{b} & -\frac{m(b-\alpha)}{b} \end{bmatrix}, \\
J_{(x_i,y_i)} &= \begin{bmatrix} x_i\left[-1+\frac{cy_i}{(x_i+y_i+\alpha\xi)^2}\right] & -\frac{cx_i(x_i+\alpha\xi)}{(x_i+y_i+\alpha\xi)^2} \\ \frac{bmy_i(y_i+\alpha\xi-\xi)}{(x_i+y_i+\alpha\xi)^2} & -\frac{bm(x_i+\xi)y_i}{(x_i+y_i+\alpha\xi)^2} \end{bmatrix}.
\end{aligned}
$$

For population conservation (while harvesting) to be ensured, we need the equilibria $(0,0),(1-qE,0)$ and $(0,(b-\alpha)\xi)$ to be unstable in nature. The equilibrium $(0,0)$ is always unstable in nature provided the axial equilibrium point $(1-qE,0)$ exists. However, $(1-qE,0)$ always exists in order to ensure the existence of the interior equilibrium point. Thus $(0,0)$ is always unstable. The conditions $(b-1)(1-qE)+(b-\alpha)\xi>0$ and $1-qE-c+\frac{c\alpha}{b}>0$ ensures the saddle nature of $(1-qE,0)$ and $(0,(b-\alpha)\xi)$ respectively. Note that, the condition for the saddle nature of $(1-qE,0)$ is satisfied whenever any one of the interior equilibrium point exists. This is because $0<y_i=(b-1)x_i+(b-\alpha)\xi<(b-1)(1-qE)+(b-\alpha)\xi$.

The stability of interior equilibria (x_i, y_i) can be analyzed by using the determinant and trace of the Jacobian matrix $J_{(x_i,y_i)}$ given by

$$\det J_{(x_i,y_i)} = \frac{bcmx_iy_i}{(x_i+y_i+\alpha\xi)^3}\left[\xi(\alpha-1)+\frac{b}{c}(x_i+\xi)^2\right],$$

$$tr\ J_{(x_i,y_i)} = \frac{-(b+1)x_i^2-[(b\xi-1)+m(b-1)]\,x_i-m(b-\alpha)\xi}{b(x_i+\xi)}.$$

We study the stability of interior equilibrium points (for all the three cases defined in Table 3.2) when $(0,(b-\alpha)\xi)$ either exists with saddle nature or does not exist at all. Here, only interior equilibrium point (x_2, y_2) can exists, if $x_2 < 1-qE$ holds. We summarizes the conditions as follows,

Cases	**Interior equilibrium point exists**	**Stable**
Case 1	(x_2, y_2)	if $tr\ J_{(x_2,y_2)} < 0$
Case 2	(x_2, y_2)	if $tr\ J_{(x_2,y_2)} < 0$
Case 3	(x_2, y_2)	always

5.3.3 Global Stability Analysis

Theorem 5.3.1. *Suppose that the interior equilibrium point (x_2, y_2) is locally asymptotically stable and the conditions $\alpha\xi \geq 1-qE$ and $\alpha > \left(1-\frac{1-qE}{c}\right)b$ hold, then (x_2, y_2) is also globally stable.*

Proof. We first define the following function,

$$L_2(x,y) = \frac{\partial}{\partial x}\left(B_2(x,y)f_2(x,y)\right) + \frac{\partial}{\partial y}\left(B_2(x,y)g_2(x,y)\right),$$

where $f_2(x,y) = x\,(1-x) - \frac{cxy}{x+y+\alpha\xi} - qEx$, $g_2(x,y) = m\left(\frac{b(x+\xi)}{x+y+\alpha\xi} - 1\right)y$ and $B_2(x,y) = \frac{x+y+\alpha\xi}{xy}$. After simplification, we obtain,

$$L_2(x,y) = \frac{(1-qE-\alpha\xi)}{y} - \frac{(2x+y)}{y} - \frac{m}{x}.$$

Now, $L_2(x,y) < 0$ whenever $x > 0$ and $y > 0$, since $\alpha\xi \geq 1-qE$. Thus, by the Dulac's criterion [49] the system (5.3.1) will not have any non-trivial periodic orbit in $\mathbb{R}^2_+$. Note that, when $\left(1-\frac{1-qE}{c}\right)b < \alpha < b$, then the trivial equilibrium point is a repeller and the two axial equilibria, $(1-qE, 0)$ and $(0,(b-\alpha)\xi)$, are both saddle and have $x-$axis and $y-$axis as their respective stable manifolds. On the other hand, when $\alpha > b$, then both $(0,0)$ and $(1-qE,0)$ are saddle and have $y-$axis and $x-$axis as their respective manifolds. Using these, in conjunction with the Poincare-Bendixson Theorem [49] gives us that the interior equilibrium point (x_2, y_2) will be globally stable. □

Finally, we summarize in Table 5.4 the conditions on effort E in order to achieve ecologically sustainable harvesting for the system (5.3.1).

Conditions	**Ensures**	**Applicable Cases**
$E < \frac{1}{q}$	$(0,0)$ is saddle/repeller and $(1-qE,0)$ exists	Case 1, Case 2, Case 3
$E < \frac{1}{q}\left(1+\frac{(b-\alpha)\xi}{b-1}\right)$	$(1-qE,0)$ is saddle	Case 1, Case 2, Case 3
$E < \frac{1}{q}(1-c+\frac{\alpha c}{b})$	(x_2,y_2) exists provided $x_2 < 1-qE$ and $(0,(b-\alpha)\xi)$ is saddle (if it is exists)	Case 1, Case 2, Case 3
$\frac{1}{q}(1-\alpha\xi) \le E < \frac{1}{q}(1-c+\frac{\alpha c}{b})$ and $tr\ J_{(x_2,y_2)} < 0$	(x_2,y_2) is globally stable (if it exists)	Case 1, Case 2
$\frac{1}{q}(1-\alpha\xi) \le E < \frac{1}{q}(1-c+\frac{\alpha c}{b})$	(x_2,y_2) is globally stable (if it exists)	Case 3

Table 5.4: Conditions on harvesting effort for the system (5.3.1).

Clearly, here, one can see that ecologically sustainable harvesting is possible under all three cases whereas without additional food it possible only under Case 3. Also, one can observe that bounds on harvesting effort E depends on the additional food parameters, namely, α and ξ. A choice of $\alpha > 1$, results in an increase in the upper bound for ecologically sustainable harvesting effort (corresponding to the global stability of interior equilibrium point) as compared to the case without additional food. On the other hand, a choice of $\xi > 1/b$ ensures that the condition $tr\ J_{(x_2,y_2)} < 0$ (required for global stability of (x_2,y_2) under Case 1 and Case 2) is satisfied. This illustrates the advantage of providing additional food to the predators over the scenario of no additional food being provided. A consequence of this is that a higher effort level can be achieved with the choice of an appropriate level of additional food supply. For example, we choose the same parameter values, $c = 1.1, m = 1, b = 3$ and $q = 1$ as in Section 4. Recall that in this example, the ecological conservation required that the effort level E be kept below 0.2667. As an illustration, we choose $E = 0.5$, which results in the extinction of both the populations, when no additional food is provided. However an appropriate level of additional food (for example, $\alpha = 2$ and $\xi = 0.5$ for which coexistence is achieved for $0 < E < 0.633$) ensures the stability of the interior equilibrium point and hence conservation of both the species. The phase portrait for this example is given in Figure 5.4.

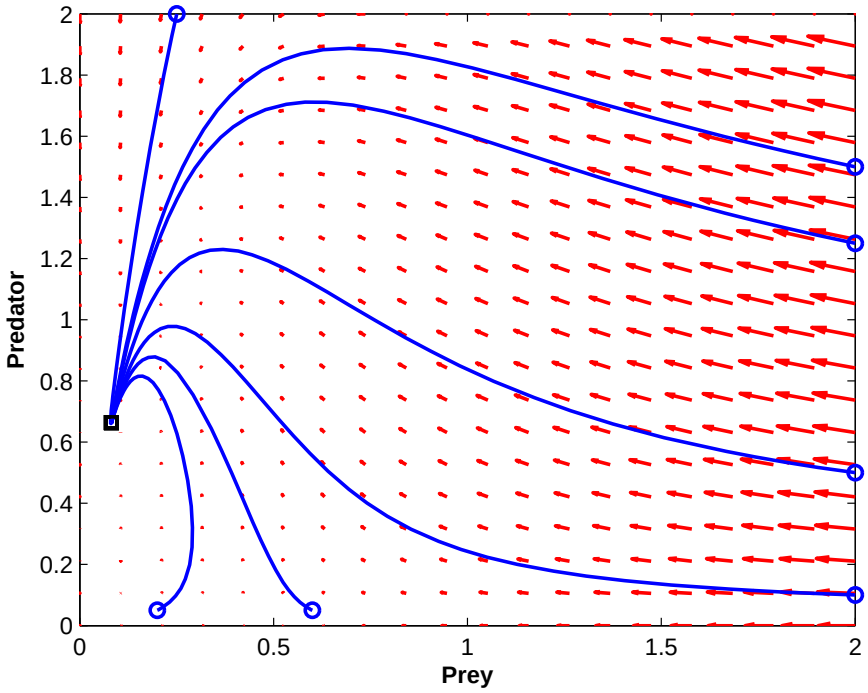

Figure 5.4: Phase-portrait for the system (5.3.1) with parameter values $c = 1.1, m = 1, b = 3, q = 1, E = 0.5, \alpha = 2$ and $\xi = 0.5$.

5.4 Optimal Harvesting Policy for the Ratio-Dependent Model

We now formulate the problem of optimal harvesting policy in case of the classical ratio-dependent model as follows:

$$\max_{0\leq E\leq E_{\max}} \int_0^\infty e^{-\delta t}\left[pqx - c_1\right] E dt \tag{5.4.1}$$

subject to the system (5.2.1)

$$\begin{aligned} \frac{dx}{dt} &= x\left(1-x\right) - \frac{cxy}{x+y} - qEx, \\ \frac{dy}{dt} &= m\left(\frac{bx}{x+y} - 1\right) y. \end{aligned}$$

and the effort constraint

$$E \in [0, E_{\max}],$$

with the initial and terminal conditions being $(x(0), y(0)) = (x_0, y_0)$ and $(x(\infty), y(\infty)) = (\bar{x}, \bar{y})$ respectively. Here p is the price per unit stock of the prey biomass, c_1 is the cost per unit effort for harvesting and $E_{\max}$ is the maximum effort capacity of the harvesting industry. Also, δ denotes the continuously compounded annual rate of discount. The objective of the problem is to find the

optimal harvesting effort *i.e.,* $E(t) \in [0, E_{\max}]$ for $t \geq 0$ so as to achieve the bioeconomic objective of maximizing the profits from harvesting while ensuring population conservation.

In order to use the Pontryagin's maximum principle [54] we define the Hamiltonian for this control problem as,

$$\mathcal{H} = e^{-\delta t}\left[pqx - c_1\right]E + \lambda_1\left[x\left(1-x\right) - \frac{cxy}{x+y} - qEx\right] + \lambda_2\left[m\left(\frac{bx}{x+y} - 1\right)y\right].$$

Using the maximum principle results in the state equation being given by (5.2.1) while the co-state equations are given by

$$\begin{aligned}
\frac{d\lambda_1}{dt} &= -\frac{\partial \mathcal{H}}{\partial x} = -e^{-\delta t}pqE - \lambda_1\left(1 - 2x - \frac{cy^2}{(x+y)^2} - qE\right) - \lambda_2\frac{bmy^2}{(x+y)^2}, \\
\frac{d\lambda_2}{dt} &= -\frac{\partial \mathcal{H}}{\partial y} = \lambda_1\frac{cx^2}{(x+y)^2} - m\lambda_2\left(\frac{bx^2}{(x+y)^2} - 1\right).
\end{aligned} \tag{5.4.2}$$

Since $\mathcal{H}$ is linear in control E, so the optimal control is combination of bang-bang and singular control [40]. The condition for the optimal control can be obtained from the relation

$$\frac{\partial \mathcal{H}}{\partial E} = e^{-\delta t}(pqx - c_1) - \lambda_1 qx = 0.$$

Chaudhuri [55] (citing Goh [40]) points out that the harvesting policy for a zero-discount rate (*i.e.,* $\delta = 0$) is more robust than the non-zero rate of discount. In order to obtain the singular optimal equilibrium solution $(\widetilde{x}, \widetilde{y})$, the interior equilibrium points of system (5.2.1) and (5.4.2) are substituted into $\frac{\partial H}{\partial E} = 0$ to get (see Appendix C),

$$x = \frac{1}{2}\left[\frac{c_1}{pq} + \left(1 - c + \frac{c}{b}\right)\right]. \tag{5.4.3}$$

The necessary conditions for the singular control to be optimal is that the generalized Legendre condition [40]

$$(\lambda_1 - 2p)x + (\lambda_1 - p)\left(-1 + \frac{c}{b^2}(b-1)^2 + qE\right) + \frac{(\lambda_1 c - \lambda_2 bm)}{b^3}(b-1)^2 \geq 0$$

is satisfied along singular solution (see Appendix C). Hence optimal harvesting policy will be,

$$E^{\,\mathrm{RD}}(t) = \begin{cases} E_{\max} & \text{if } \; x > \widetilde{x} \\ \widetilde{E} & \text{if } \; x = \widetilde{x} \\ 0 & \text{if } \; x < \widetilde{x}, \end{cases}$$

where $\widetilde{x}$ is the value of x in (5.4.3) (called the singular optimal equilibrium prey population size). Also, $\widetilde{E}$ is called the singular control of the system (5.2.1) corresponding to the singular solution $(\widetilde{x}, \widetilde{y})$.

We illustrate this with a numerical example. For this purpose, we choose the parameter values to be $c = 1.1, m = 1, b = 3, q = 1, p = 1$ and $c_1 = 0.005$. For this set of parameter values, $\widetilde{x} = 0.1358$

(from equation (5.4.3)). Recall that the interior equilibrium point of system (5.2.1) is globally asymptotically stable if $E \in [0, 0.2667)$. So we can take $E_{\max}$ to be 0.2667. Thus, according to the optimal harvest policy, if at time t the prey population size is greater than the optimal equilibrium prey population size $\widetilde{x} = 0.1358$ *i.e.,* $x(t) > 0.1358$, then the harvesting effort is chosen to be $E_{\max} = 0.2667$ until the prey size reduces to $\widetilde{x}$. Once this happens, *i.e.,* $x(t) = 0.1358$, then we will adopt the singular optimal control $\widetilde{E}$, given in this case by $\widetilde{E} = \frac{1}{q}\left(1 - \widetilde{x} - \frac{c}{b}(b-1)\right) = 0.1308$. When $x(t) < \widetilde{x}$, the harvesting is stopped *i.e.,* $E = 0$ and remains so until the prey population density is restored at least to the level of $\widetilde{x}$ again. The optimal trajectory for system (5.2.1) with initial population densities $(x_0, y_0) = (0.9, 0.4)$ is shown in Figure 5.5. The optimal trajectory is a combination of two trajectories, one (dashed) corresponding to the maximum harvesting effort $E_{\max} = 0.2667$ while the second one corresponds to the singular effort $\widetilde{E} = 0.1308$. The switch from maximum harvesting effort $E_{\max}$ to singular effort $\widetilde{E}$ happens at time $t = 5.3$.

The optimal harvesting policy will thus be,

$$E^{\,\mathrm{RD}}(t) = \begin{cases} E_{\max} = 0.2667 & \text{if } t \leq 5.3, \\ \widetilde{E} \quad = 0.1308 & \text{if } t > 5.3. \end{cases}$$

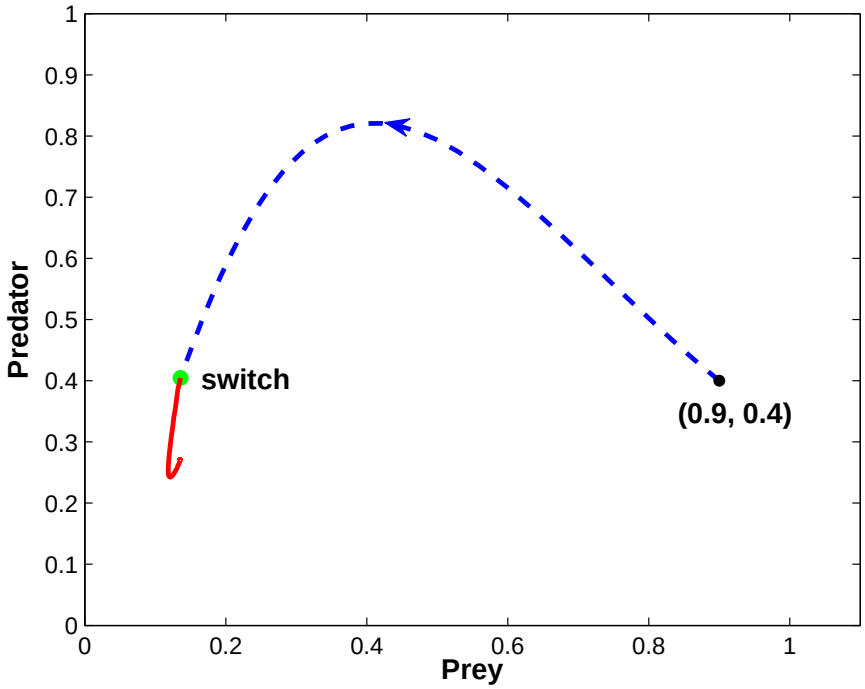

Figure 5.5: Optimal path emanating from point $(0.9, 0.4)$ subject to the system (5.2.1) with parameter values $c = 1.1, m = 1, b = 3, q = 1, p = 1$ and $c_1 = 0.005$.

5.5 Optimal Harvesting Policy for the Modified Ratio-Dependent Model

For the modified ratio-dependent model, the problem of optimal harvesting policy is formulated as follows:

$$\max_{0\le E\le E_{\max}} \int_0^\infty e^{-\delta t}\left[(pqx-c_1)\,E-c_2\xi\right]dt \tag{5.5.1}$$

subject to the system (5.3.1)

$$\begin{aligned}\frac{dx}{dt} &= x\,(1-x)-\frac{cxy}{x+y+\alpha\xi}-qEx,\\ \frac{dy}{dt} &= m\left(\frac{b\,[x+\xi]}{x+y+\alpha\xi}-1\right)y.\end{aligned}$$

and the effort constraint

$$E\in[0,E_{\max}]\,,$$

with the initial and terminal conditions $(x(0),y(0))=(x_0,y_0)$ and $(x(\infty),y(\infty))=(x_2,y_2)$ respectively. The parameters p, c_1, $E_{\max}$ and δ have the same interpretation as in the case of harvesting for classical ratio-dependent model discussed in the previous section. The new parameter c_2 is the cost per unit quantity biomass of additional food with some fixed nutrition value. As before, the objective of the problem is to find the optimal harvesting effort *i.e.,* $E(t)\in[0,E_{\max}]$ for $t\ge 0$ so as to achieve the bioeconomic objective of maximizing the profits from harvesting while ensuring population conservation. The Hamiltonian for this control problem is defined as

$$\begin{aligned}\mathcal{H} &= e^{-\delta t}\left[(pqx-c_1)\,E-c_2\xi\right]+\lambda_1\left[x\,(1-x)-\frac{cxy}{x+y+\alpha\xi}-qEx\right]+\\ &\quad \lambda_2\left[m\left(\frac{b\,[x+\xi]}{x+y+\alpha\xi}-1\right)y\right].\end{aligned}$$

Using Pontryagin's maximum principle results in the state equations for this problem being given by (5.3.1) while the co-state equations are given by,

$$\begin{aligned}\frac{d\lambda_1}{dt} &= -\frac{\partial\mathcal{H}}{\partial x}=-e^{-\delta t}pqE-\lambda_1\left(1-2x-\frac{cy(y+\alpha\xi)}{(x+y+\alpha\xi)^2}-qE\right)-\lambda_2\frac{bmy(y+\alpha\xi-\xi)}{(x+y+\alpha\xi)^2},\\ \frac{d\lambda_2}{dt} &= -\frac{\partial\mathcal{H}}{\partial y}=\lambda_1\frac{cx(x+\alpha\xi)}{(x+y+\alpha\xi)^2}-m\lambda_2\left(\frac{b\,(x+\xi)\,(x+\alpha\xi)}{(x+y+\alpha\xi)^2}-1\right).\end{aligned} \tag{5.5.2}$$

Note that, here $\mathcal{H}$ is linear in control E. Therefore, the optimal control will be a combination of bang-bang and singular control [40]. The optimal control follows from the condition,

$$\frac{\partial\mathcal{H}}{\partial E}=e^{-\delta t}(pqx-c_1)-\lambda_1 qx=0.$$

To determine the singular optimal equilibrium solution (x^*, y^*) we take $\delta = 0$ and substitute the interior equilibrium points of the systems (5.3.1) and (5.5.2) into $\frac{\partial \mathcal{H}}{\partial E} = 0$ which results in the following cubic equation (see Appendix C),

$$\begin{aligned} & (-2bpq)x^3 + (bc_1 + (-4b\xi + b + c - bc)pq)x^2 + 2(bc_1 + pq(b + c - bc - b\xi))\xi)x \\ + \quad & \xi(-c(1-\alpha)c_1 + bc_1\xi + pq(b - c(b-\alpha))\xi) = 0. \end{aligned} \tag{5.5.3}$$

When sign of the coefficient of x^3 and constant term in a cubic equation are opposite, then the equation has atleast one positive root. Thus, in the above case, if $(\frac{c\alpha}{b} - \frac{c}{b} + \xi)c_1 + pq\xi(1 - c + \frac{c\alpha}{b}) > 0$ then above cubic equation has at least one positive root. Let x^* be the positive root of this cubic equation. Then x^* is called the singular optimal equilibrium prey-population level. The necessary conditions for the singular control to be optimal is that the generalized Legendre condition [40]

$$(2\lambda_1 - p)\left(1 - \frac{cy}{(x + y + \alpha\xi)^2}\right) + (\lambda_1 cx + \lambda_2 bm(y + \alpha\xi - \xi))\frac{y}{(x + y + \alpha\xi)^3} \geq 0$$

is satisfied along singular solution (see Appendix C). Hence the optimal harvesting policy will be,

$$E^{\text{MRD}}(t) = \begin{cases} E_{\max} & \text{if } x > x^* \\ E^* & \text{if } x = x^* \\ 0 & \text{if } x < x^*. \end{cases}$$

Note that, in order to ensure an economically better harvesting policy with the additional food as compared to harvesting without additional food being supplied to the predators in the system, the integrand in (5.5.1) must be greater than the integrand in (5.4.1). This can be ensured as long as the cost per unit quantity biomass of additional food satisfies,

$$c_2 \quad < \quad \frac{1}{\xi}(pqx - c_1)\left(E^{\text{MRD}} - E^{\text{RD}}\right).$$

It can be shown that equation (5.5.3) reduces to (see Appendix C)

$$2bpq(x^* + \xi)^2(x^* - \widetilde{x}) = c\xi(c_1 + pq\xi)(\alpha - 1).$$

Consequently, $x^* < (>)\widetilde{x} \iff \alpha < (>)1$. This means that in order to undertake prey harvesting with additional food at a level, x^* below (above) $\widetilde{x}$ (the level without additional food), the predators need to be supplied with good (poor) quality of additional food. There is no benefit in terms of harvesting stock level, by providing same quality of additional food relative to the prey, *i.e.,* $\alpha = 1$, since this results in $x^* = \widetilde{x}$ and $E^* = \widetilde{E}$. Apart from this, there is added financial burden arising from supply of additional food in this case.

One can observe from the cubic equation (5.5.3) that the singular optimal prey-equilibrium level x^* is dependent on the biological control parameters α and ξ. We will now illustrate through

numerical examples, that for the modified model with additional food, the optimal harvesting policy can be more effectively decided by an appropriate choice of α and ξ. For this purpose, we refer to the example on prey harvesting without additional food case, as given in the previous section. Recall that for the parameter values $b = 3, c = 1.1, m = 1, p = 1, q = 1$ and $c_1 = 0.005$, no prey harvesting can be done until the prey size reaches a level of $\widetilde{x} = 0.1358$. However, for this set of parameter values, the system supported by additional food to the predators results in bioeconomically sustainable harvesting policy for some $x(t) < \widetilde{x}$. In fact in this case, the harvesting effort can be more than the corresponding harvesting effort for the system without additional food.

To begin with, we set $x^* = 0.0001$. Then, in this case α and ξ has to satisfy the relation $(-0.2856 + 1.1\alpha)\xi^2 + (-0.00533712 + 0.0055\alpha)\xi + 0.8144 \times 10^{-8} = 0$. By choosing $\alpha = 0.94$ and $\xi = 0.0001515$ (which satisfies this relation), one can harvest at the maximum effort level $E_{\max} = 0.2447$, for all time, provided $x(0) > x^*$. Clearly, the economic returns here is better than the returns without the additional food. Now, choosing $\alpha = 0.9, 0.8, 0.7$ with corresponding $\xi = 0.0005277, 0.001569, 0.003065$ respectively, one can prey harvest at the maximum harvest rate of $0.23, 0.1933, 0.1567$ respectively, provided $x(0) > x^*$. These numerical values of α suggest that, as we decreases the α value (improvement in the quality of additional food) maximum harvest rate is keeps decreasing. This phenomenon is possibly due to the increase in the predator population level (resulting from better quality of additional food) but the quantity being fixed, thereby resulting in more predation of prey by the predators. This can also be mathematically justified, by recalling that $y_2 = (b-1)x_2 + (b-\alpha)\xi$. As we decrease the value of α (for fixed ξ), y_2 (predator equilibrium level) will increase, while prey equilibrium level x_2 will decrease. For the parameter values $\alpha = 0.94$ and $\xi = 0.0001515$, the optimal trajectory for system (5.3.1) with initial population densities $(x_0, y_0) = (0.9, 0.4)$ is shown in Figure 5.6.

We now consider a second example, when $\widetilde{x} < x^*$, with same parameters values chosen earlier, namely, $b = 3, c = 1.1, m = 1, p = 1, q = 1$ and $c_1 = 0.005$. In this case, for some $x(t) > \widetilde{x}$, harvesting cannot be undertaken till the prey population reaches a level of atleast x^*. But, whenever harvesting is possible, $E_{\max}$ and E^* can be increased by increasing the value of α and ξ. This may be possible from an ecological point of view, since supply of poor quality additional food could result in the predators being distracted, thereby easing the predation pressure on the prey, whose size consequently increases. Thus, the harvest effort can be increased in such a scenario. We set $x^* = 0.2$, in which case α and ξ has to satisfy the relation $(-1.485+1.1\alpha)\xi^2+(-0.1595+0.0055\alpha)\xi-0.0154 = 0$. By choosing $\alpha = 2$ and $\xi = 0.2836$ and if $x(0) > x^*$ one can start harvesting at the maximum effort level $E_{\max} = 0.6333$, till x reduces to $x^* = 0.2$. After reaching $x^* = 0.2$, we switch to the singular effort level $E^* = 0.2817$.

For the parameter values $\alpha = 2$ and $\xi = 0.2836$, the optimal trajectory for system (5.3.1) with initial population densities $(x_0, y_0) = (0.9, 0.4)$ is shown in Figure 5.7. The optimal trajectory is

a combination of two trajectories, one (dashed) corresponding to the maximum harvesting effort $E_{\max} = 0.6333$ while the second one corresponds to the singular effort $E^* = 0.2817$. The switch from maximum harvesting effort $E_{\max}$ to singular effort $\widetilde{E}$ happens at time $t = 2.9$.

$$E^{\,\mathrm{MRD}}(t) = \begin{cases} E_{\max} = 0.6333 & \text{if } \ t \leq 2.9, \\ E^* \quad = 0.2817 & \text{if } \ t > 2.9. \end{cases}$$

Note that, in this case also, we get an improved harvesting policy, even with the low quality

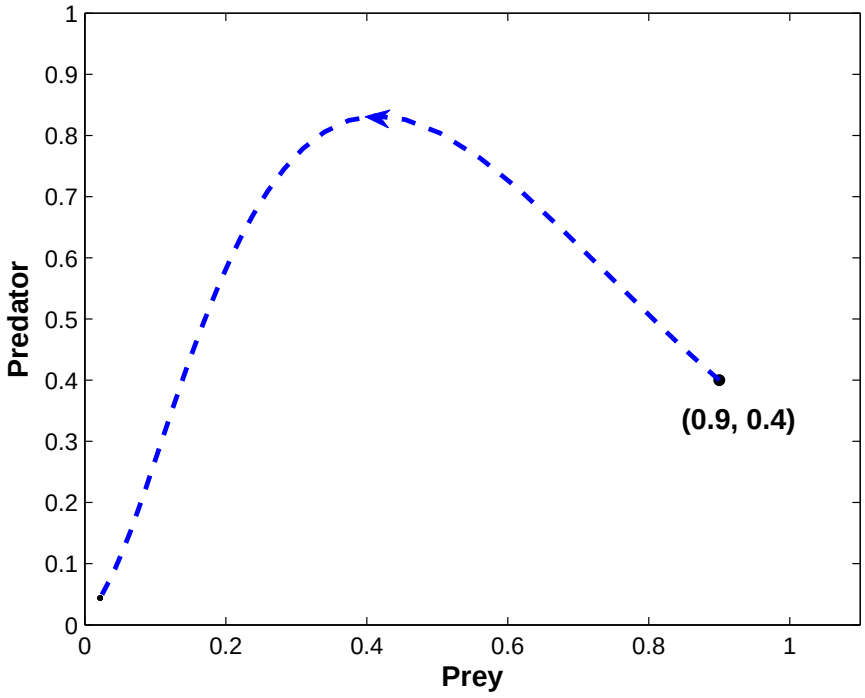

Figure 5.6: Optimal path emanating from point $(0.9, 0.4)$ subject to the system (5.3.1) with parameter values $c = 1.1, m = 1, b = 3, q = 1, p = 1, c_1 = 0.005,\ \alpha = 0.94$ and $\xi = 0.0001515$.

additional food as compared to prey nutrients, since $\alpha = 2 > 1$ and while keeping prey population level at a level higher than the level without the additional food case. This is illustrative of how the supply of additional food can play a critical role in formulating an efficient harvesting policy along with population conservation.

5.6 Conclusion

We undertake a comparative study between classical ratio-dependent and modified ratio-dependent predator-prey model by incorporating prey harvesting into both the models. While the classical ratio-dependent model has a ratio-dependent functional response, the modified model also has ratio-dependent functional response but with the additional food being made available to predators. The

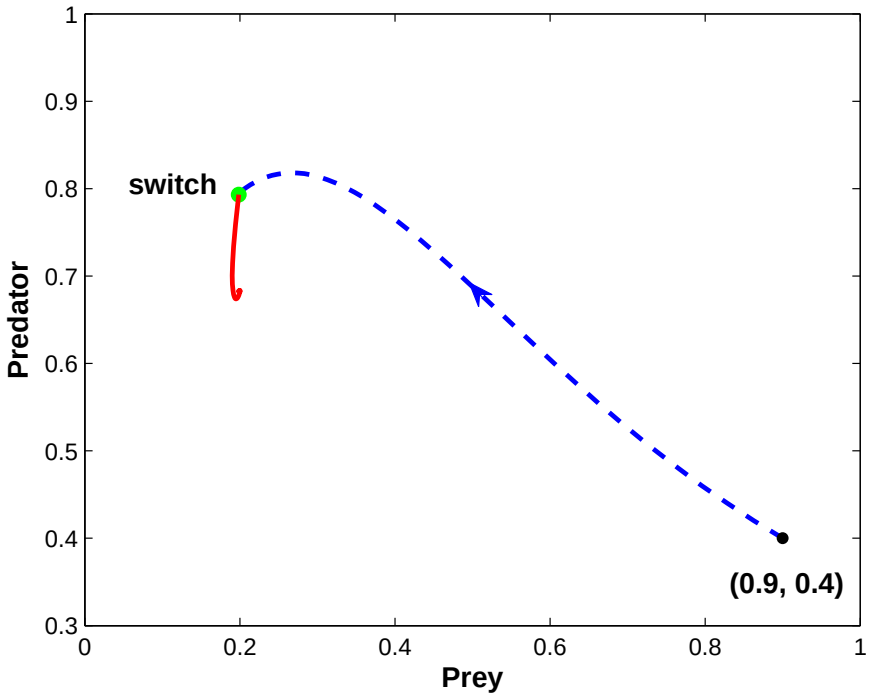

Figure 5.7: Optimal path emanating from point $(0.9, 0.4)$ subject to the system (5.3.1) with parameter values $c = 1.1, m = 1, b = 3, q = 1, p = 1, c_1 = 0.005, \alpha = 2$ and $\xi = 0.2836$.

comparison of the models is done from the perspective of how the additional food supply to the predators play a role in deciding the range of bioeconomically sustainable prey harvesting effort. This was accomplished by analyzing the existence and stability of the equilibrium points and also the optimal harvesting policy using the Pontryagin's maximum principle.

We analyzed both the bioeconomic models to determine the extent of ecologically sustainable harvesting effort. In particular, the conditions for existence and stability of the interior equilibrium point was studied since a stable interior equilibrium point represents the co-existence of both the species for all time. It was observed that the maximum sustainable effort level as a result of additional food supply is always greater than corresponding maximum sustainable effort level without additional food, provided $\alpha > 1$. We then formulated a bioeconomic control problem which seeks to maximize the profit from harvesting while ensuring population conservation. The resulting optimal harvesting policy was found to result in higher returns as well as better population conservation in case of additional food supply.

Chapter 6

Optimal Control of Pest Population

This chapter is devoted to the determination of an optimal strategy for pest (prey) population control, by taking the additional food supplied to the predator as the control variable. The problem is formulated as a minimum time optimal control problem with the objective of driving the pest population from a given initial state to a desired target state in the minimum possible time.

6.1 Modified Ratio-Dependent Model Revisited

We begin by recalling the modified ratio-dependent predator-prey model (2.1.3) with additional food (non-prey) being supplied to the predators, given by,

$$\begin{aligned} \frac{dx}{dt} &= x\,(1-x) - \frac{cxy}{x+y+\alpha\xi}, \\ \frac{dy}{dt} &= m\left(\frac{b\,[x+\xi]}{x+y+\alpha\xi} - 1\right) y. \end{aligned}$$

Here, the parameter α characterizes the quality of the additional food, since it is inversely proportional to the nutritional value of additional food. The other control parameter ξ characterizes the quantity of additional food. The system (2.1.3) has atmost five equilibria namely, trivial $(0,0)$, two axial $(1,0)$ and $(0,(b-\alpha)\xi)$ and two interior (x_i,y_i) for $i=1,2$, where each x_i is the root of,

$$x^2 + \left(c - 1 - \frac{c}{b} + \xi\right)x + \left(c - 1 - \frac{\alpha c}{b}\right)\xi = 0 \tag{6.1.1}$$

and $y_i = (b-1)x_i + (b-\alpha)\xi$. The dynamics of the system (2.1.3) has been studied in detail in Chapter 3 and the results are summarized here in Table 6.1 under three cases defined in Table 3.2.

Range of α	Conditions	$(0,0)$	$(1,0)$	$(0,(b-\alpha)\xi)$	(x_1,y_1)	(x_2,y_2)	Applicable Cases
$0<\alpha<\left(1-\frac{1}{c}\right)b$	$b\geq 1$	Repeller	Saddle	Stable	DNE	DNE	Case 1
	$P<0,\Delta>0$						
	(i) $b<1,\ R>0,\ x_2\notin I_1$ or $\Delta_1<0$	Repeller	Saddle	Stable	Saddle	Stable	Case 1
	(ii) $b<1,\ R>0$ and $x_2\in I_1$	Repeller	Saddle	Stable	Saddle	Unstable	Case 1
	(iii) $b<1,\ R<0$	Repeller	Stable	Stable	Saddle	DNE	Case 1
	(iv) $x_2\notin I_1$ or $\Delta_1<0$	Repeller	Saddle	Stable	Saddle	Stable	Case 2, Case 3
	(v) $b>1,\ x_2\in I_1$	Repeller	Saddle	Stable	Saddle	Unstable	Case 2
	$P>0$ or $\Delta<0$	Repeller	Saddle	Stable	DNE	DNE	Case 1, Case 2, Case 3
$\left(1-\frac{1}{c}\right)b<\alpha<b$		Repeller	Saddle	Saddle	DNE	Stable	Case 3
	$R>0,\ x_2\notin I_1$ or $\Delta_1<0$	Repeller	Saddle	Saddle	DNE	Stable	Case 1, Case 2
	$R>0\ x_2\in I_1$	Repeller	Saddle	Saddle	DNE	Unstable	Case 1, Case 2
	$R<0$	Repeller	Stable	Saddle	DNE	DNE	Case 1
$\alpha>b$							
	$b>1,\ R>0$						
	(i) $x_2\notin I_2$	Saddle	Saddle	DNE	DNE	Stable	Case 1, Case 2, Case 3
	(ii) $x_2\in I_2$	Saddle	Saddle	DNE	DNE	Unstable	Case 1, Case 2
	$R<0$	Saddle	Stable	DNE	DNE	DNE	Case 1, Case 2, Case 3

Table 6.1: Summary of stability results for the modified ratio-dependent system (2.1.3).

Here $P = c - 1 - c/b + \xi,\ R = (b-\alpha)\xi + (b-1)$,

$\Delta = (c - 1 - c/b + \xi)^2 - 4\xi(c - 1 - \frac{\alpha c}{b})$,

$\Delta_1 = ((b\xi - 1) + m(b-1))^2 - 4m(b-\alpha)(b+1)\xi$,

$I_1 = \left[-\frac{m(b-1)+(b\xi-1)+\sqrt{\Delta_1}}{2(b+1)}, -\frac{m(b-1)+(b\xi-1)-\sqrt{\Delta_1}}{2(b+1)}\right]$

$I_2 = \left(0, -\frac{m(b-1)+(b\xi-1)-\sqrt{\Delta_1}}{2(b+1)}\right]$ and

DNE: Does Not Exist.

From the results presented in Table 6.1, it can be observed that if α is from the range $0 < \alpha < \left(1 - \frac{1}{c}\right) b$, then $(0, (b-\alpha)\xi)$ is stable. If the value of α is increased to $\alpha > b$, such that $R < 0$, then $(1, 0)$ is stable. We infer that as the value of α increases (decreases), the prey size also increases (decreases). In other words, as the quality of additional food deteriorates (improves), the prey population keeps increasing (decreasing). Ecologically, this is plausible by observing that the provision of poor quality additional food distracts the predators from the prey. On the other hand, provision of good quality additional food to predators with quantity being kept fixed leads to an increase in the population of predators, resulting in more predation of their natural prey. This clearly indicates that the quality of additional food has a direct role in the control of prey (pest) population. Thus, for the problem considered in this Chapter, we treat α as a control variable while keeping ξ constant. Now, the interior equilibria of system (2.1.3) becomes a function of α only, *i.e.*,

$$\begin{aligned} x_i(\alpha) &= \frac{1 - c + \frac{c}{b} - \xi}{2} + \frac{(-1)^i}{2}\sqrt{\left(c - 1 - \frac{c}{b} + \xi\right)^2 - 4\xi\left(c - 1 - \frac{\alpha c}{b}\right)}, \\ y_i(\alpha) &= (b-1)x_i + (b-\alpha)\xi, \quad \text{for} \quad i = 1, 2. \end{aligned}$$

Using equation (A.0.1), y_i can be rewritten as,

$$y_i(\alpha) = \frac{b}{c}(x_i(\alpha) + \xi)(1 - x_i(\alpha)) \tag{6.1.2}$$

For $x_i(\alpha) < 1$, the curve (6.1.2) denotes the set of all admissible equilibrium in the state space of the system (2.1.3). The analysis of the system (2.1.3) in Chapter 3 shows that, (x_1, y_1) exists (with only saddle nature) provided (x_2, y_2) exists. Also the existence of (x_1, y_1) comes for some fixed range of α too. Therefore we are only interested in (x_2, y_2) as an interior equilibrium for the purpose of pest control.

6.2 Minimum Time Optimal Control Problem

We consider the prey population to be pest in nature and it is desirable that it's size is maintained at an appropriate constant level. It is also desirable that this constant level is attained in the minimum possible time from a given initial state. As we noted in the previous section, for each α, (x_2, y_2) represents the constant level. The quality of additional food is taken as the control variate, which is used to bring the pest population to the desired level. Let $\alpha(t)$ (which characterizes the quality of additional food) be the control variate at time t. Our goal is to find an admissible optimal control $\alpha(t) \in [\alpha_{\min}, \alpha_{\max}]$ such that it drives the system (2.1.3) from an arbitrary initial state (x_0, y_0) to the target state (x_2, y_2) in a minimum possible time T. The problem can now be formulated as follows,

$$\max_{\alpha(t)} \int_0^T -1 \, dt$$

subject to the system:

$$\frac{dx}{dt} = x\,(1-x) - \frac{cxy}{x+y+\alpha\xi},$$
$$\frac{dy}{dt} = m\left(\frac{b\,[x+\xi]}{x+y+\alpha\xi} - 1\right) y,$$

with the initial condition $(x(0), y(0)) = (x_0, y_0)$ and terminal condition $(x(T), y(T)) = (x_2(\bar{\alpha}), y_2(\bar{\alpha}))$, where the final time T is unspecified and $\bar{\alpha}$ is some fixed value of $\alpha \in [\alpha_{\min}, \alpha_{\max}]$. The Hamiltonian for this problem is defined as,

$$\mathcal{H} = -1 + \lambda_1 \left[x\,(1-x) - \frac{cxy}{x+y+\alpha\xi}\right] + \lambda_2 \left[m\left(\frac{b\,[x+\xi]}{x+y+\alpha\xi} - 1\right) y\right]. \tag{6.2.1}$$

From Pontryagin's maximum principle [40, 54], the optimal solution needs to satisfy the following co-state equations,

$$\begin{aligned}
\frac{d\lambda_1}{dt} &= -\lambda_1\left(1 - 2x - \frac{cy(y+\alpha\xi)}{(x+y+\alpha\xi)^2}\right) - \lambda_2 \frac{bmy(y+\alpha\xi-\xi)}{(x+y+\alpha\xi)^2}, \\
\frac{d\lambda_2}{dt} &= \lambda_1 \frac{cx(x+\alpha\xi)}{(x+y+\alpha\xi)^2} - m\lambda_2\left(\frac{b\,(x+\xi)\,(x+\alpha\xi)}{(x+y+\alpha\xi)^2} - 1\right).
\end{aligned} \tag{6.2.2}$$

The optimal control $\alpha^*(t)$ must maximize $\mathcal{H}$ along an optimal trajectory w.r.t. all admissible controls. Thus,

$$\alpha^*(t) = \alpha_{\min}, \text{ only if } \frac{\partial \mathcal{H}}{\partial \alpha} < 0,$$
$$\alpha^*(t) = \alpha_{\max}, \text{ only if } \frac{\partial \mathcal{H}}{\partial \alpha} > 0.$$

If for some interval $[t_1, t_2] \subseteq [0, \widetilde{T}]$,

$$\frac{\partial \mathcal{H}}{\partial \alpha} = \frac{y\xi}{(x+y+\alpha\xi)^2}\left[\lambda_1 cx - \lambda_2 mb\,(x+\xi)\right] = 0, \tag{6.2.3}$$

then $\alpha^*(t)$ is called the singular control [40]. This is possible because the second derivative of $\mathcal{H}$ w.r.t. α, results in the following form,

$$\frac{\partial^2 \mathcal{H}}{\partial \alpha^2} = \frac{-2\xi}{(x+y+\alpha\xi)}\frac{\partial \mathcal{H}}{\partial \alpha}.$$

Suppose that the optimal singular solution exists. Now, differentiating (6.2.3) w.r.t. t along singular solution and using (2.1.3) and (6.2.2), we get

$$\frac{d}{dt}\frac{\partial \mathcal{H}}{\partial \alpha} = \frac{\lambda_2 mby\xi}{(x+y+\alpha\xi)^2}\left(2x^2 + (\xi - m - 1)x - m\xi\right) = 0.$$

Similarly, along singular solution, we get,

$$\frac{d^2}{dt^2}\frac{\partial \mathcal{H}}{\partial \alpha} = \frac{\lambda_2 mbxy\,(4x+\xi-m-1)\,\xi}{(x+y+\alpha\xi)^2}\left(1 - x - \frac{cy}{x+y+\alpha\xi}\right) = 0.$$

So singular optimal solution is a point $(\hat{x}, \hat{y})$ in the state space, where $\hat{x}$ is the positive solution of the equation,

$$2x^2 + (\xi - m - 1)x - m\xi = 0 \tag{6.2.4}$$

and

$$\hat{y} = \frac{b}{c}(\hat{x} + \xi)(1 - \hat{x}). \tag{6.2.5}$$

Note that point $(\hat{x}, \hat{y})$, lies on the x-isocline of the system (2.1.3), whenever $\hat{x} < 1$. The singular optimal solution is atmost a single possible point $(\hat{x}, \hat{y})$ in the state space and unless $\hat{x} = x_2(\bar{\alpha})$, there does not exist any such interval $[t_1, t_2] \subseteq [0, \widetilde{T}]$ for which $\frac{\partial \mathcal{H}}{\partial \alpha} = 0$. Thus there does not exist any singular control. Therefore, the optimal solution of the considered problem is of bang-bang type only. Thus, the optimal control will be,

$$\alpha^*(t) = \begin{cases} \alpha_{\min}, & \text{if } \frac{\partial \mathcal{H}}{\partial \alpha} < 0, \\ \alpha_{\max}, & \text{if } \frac{\partial \mathcal{H}}{\partial \alpha} > 0. \end{cases}$$

6.3 Switching Regions

We are interested in the regions of state space, where trajectories can switch from one path to another in order to reach the target state. This switching happens when $\frac{\partial \mathcal{H}}{\partial \alpha}$ changes it's sign. Accordingly, we define the switching function as $\sigma(t) \equiv \lambda_1(t)cx(t) - \lambda_2(t)mb\,(x(t)+\xi)$. If τ denotes the switching time at which the switch occurs, then,

$$\sigma(\tau) \equiv \lambda_1(\tau)cx(\tau) - \lambda_2(\tau)mb\,(x(\tau)+\xi) = 0. \tag{6.3.1}$$

The transversality condition along an optimal solution trajectory gives $\mathcal{H}(t) = 0 \ \forall \ t \in [0, T]$. In particular $\mathcal{H}(\tau) = 0$, *i.e.*,

$$\lambda_1(\tau)x(\tau)\left(1 - x(\tau)\right) - \lambda_2(\tau)my(\tau) = 1.$$

Using the expression $\lambda_1(\tau)x(\tau) = \lambda_2(\tau)mb\left(x(\tau) + \xi\right)/c$ (from (6.3.1)) gives us

$$\lambda_2(\tau) = \frac{1}{m\left(\frac{b}{c}\left(x(\tau) + \xi\right)\left(1 - x(\tau)\right) - y(\tau)\right)}.$$

It can be easily seen that both $\lambda_1(\tau)$ and $\lambda_2(\tau)$ are positive when $y < \frac{b}{c}\left(x + \xi\right)\left(1 - x\right)$ and are both negative when $y > \frac{b}{c}\left(x + \xi\right)\left(1 - x\right)$. Also, we observe that if the control variable α changes from $\alpha_{\max}$ to $\alpha_{\min}$ ($\alpha_{\min}$ to $\alpha_{\max}$) then $\sigma'(t)|_{t=\tau} < 0$ (> 0). Here,

$$\sigma'(t) = \lambda_2 mb\left(2x^2 + (\xi - m - 1)x - m\xi\right).$$

From the above observation, we conclude that switch of the control variable α from $\alpha_{\max}$ to $\alpha_{\min}$ ($\alpha_{\min}$ to $\alpha_{\max}$) at time τ can happen only in the regions R_1 and R_3 (R_2 and R_4), where the regions are given by,

$$\begin{aligned}
R_1 &= \left\{(x, y)\middle| x < \hat{x},\ y < \frac{b}{c}\left(x + \xi\right)\left(1 - x\right)\right\},\\
R_2 &= \left\{(x, y)\middle| x > \hat{x},\ y < \frac{b}{c}\left(x + \xi\right)\left(1 - x\right)\right\},\\
R_3 &= \left\{(x, y)\middle| x > \hat{x},\ y > \frac{b}{c}\left(x + \xi\right)\left(1 - x\right)\right\},\\
R_4 &= \left\{(x, y)\middle| x < \hat{x},\ y > \frac{b}{c}\left(x + \xi\right)\left(1 - x\right)\right\}.
\end{aligned}$$

6.4 Numerical Illustration and Discussion

As discussed in Section 6.2, the optimal control is only bang-bang in nature. That is, the optimal strategy will comprise of the control $\alpha = \alpha_{\min}$ or $\alpha = \alpha_{\max}$. The system being driven from the given arbitrary state to the target state in minimum possible time could involve multiple switching between the controls $\alpha = \alpha_{\min}$ and $\alpha = \alpha_{\max}$. The specific switching of these two controls is numerically determined under examples for all the three cases (defined in Section 6.1). This is accomplished by using the information about the switching regions $\{R_i\}_{i=1}^{4}$ and integrating the state equations (2.1.3) and costate equations (6.2.2) backwards in time. Each choice made for the set, $\{T, \lambda_1(T), \lambda_2(T)\}$, of constants of integration produces an initial state (x_0, y_0) in the state space.

In this problem, the target state is set as $P(x_2(T), y_2(T)) = (x_2(\bar{\alpha}), y_2(\bar{\alpha}))$, where $\bar{\alpha} = \alpha_{\max}$. As per the optimal control strategy, the control $\alpha = \alpha_{\min}$ will always be present as a part of the

strategy. The optimal feedback policy for Case 1, Case 2 and Case 3 are illustrated in Figure 6.1, 6.2 and 6.3 respectively. The curves PQ_1 and PQ_2 represent the switching curves. Typically, the system (2.1.3) with the initial state being P_1 evolves under the control $\alpha = \alpha_{\min}$ until the solution trajectory intersects the switching curve PQ_1. At the point of intersection on the curve PQ_1, the trajectory now evolves under the control $\alpha = \alpha_{\max}$ until it intersects the other switching curve PQ_2. At the point of intersection on PQ_2, the control again switches to $\alpha = \alpha_{\min}$ until the trajectory reaches it's target state. On the other hand, if the initial state of the system is at P_2 then the system (2.1.3) is driven under the control $\alpha = \alpha_{\max}$ until it reaches the switching curve PQ_2. At the intersection point on the switching curve, the control applied changes to $\alpha = \alpha_{\min}$ until the trajectory reaches it's target state. Note that, in order to remain at the target state $(x(T), y(T))$ forever, we need to switch to the control $\alpha = \bar{\alpha}$ once the target state has been reached.

Figure 6.1 is illustrative of Case 1, where parameter values are chosen as $c = 2, m = 0.5, b = 2$ and $\xi = 0.1$. We set $\alpha_{\min} = 0.5$ and $\alpha_{\max} = 2$ as an extreme values of control variable. Here the target state is $(0.2702, 0.2702)$, which is the equilibrium point of the system (2.1.3) for the $\bar{\alpha} = \alpha_{\max} = 2$. In order to reach the pest target below to 0.2702, $\bar{\alpha}$ has to be taken as less than the value 2. In other words, if we want the pest population lower than 0.2702 in minimum time, we need to increase the quality of additional food that being supplied to predators. Figure 6.2 is

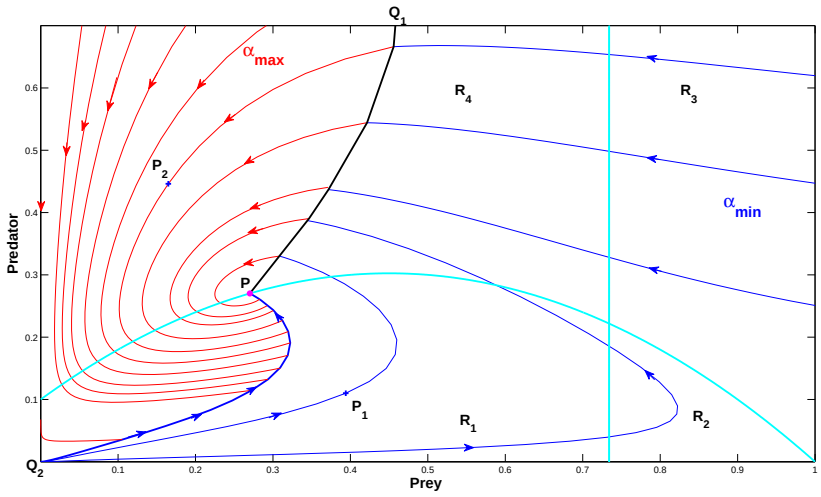

Figure 6.1: Optimal control of pest through quality of additional food under Case 1 with parameter values $c = 2, m = 0.5, b = 2, \xi = 0.1, \alpha_{\min} = 0.5$ and $\alpha_{\max} = 2$.

illustrative of Case 2, where value of parameters are chosen as $c = 1.2, m = 0.05, b = 3$ and $\xi = 0.1$. The extreme values of control variable, in this case, are taken as $\alpha_{\min} = 0.25$ and $\alpha_{\max} = 1$. The target state to be reached for this case is $(0.2, 0.6)$ (the equilibrium point of the system (2.1.3) with $\bar{\alpha} = \alpha_{\max} = 1$). In order for the pest size target to be kept below to 0.2, $\bar{\alpha}$ needs to be less than the

value 1. Finally, Figure 6.3 illustrates Case 3, with the parameters being $c = 1.1, m = 0.05, b = 3$

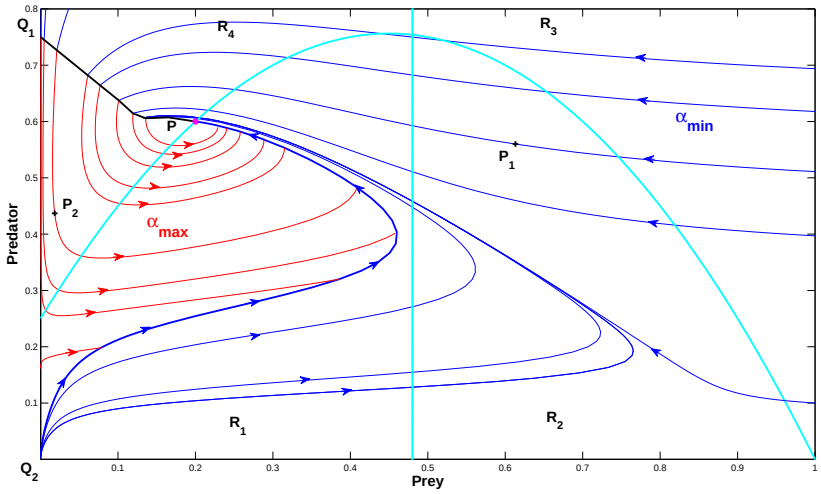

Figure 6.2: Optimal control of pest through quality of additional food under Case 2 with parameter values $c = 1.2, m = 0.05, b = 3, \xi = 0.1, \alpha_{\min} = 0.25$ and $\alpha_{\max} = 1$.

and $\xi = 0.1$. We set the extreme control variates as $\alpha_{\min} = 0.1$ and $\alpha_{\max} = 0.5$. The target state here is the equilibrium point $(0.2069, 0.6639)$ of the system (2.1.3) for $\bar{\alpha} = \alpha_{\max} = 0.5$. To ensure that the pest population level goes below to 0.2069, $\bar{\alpha}$ has to be set less than the value 0.5.

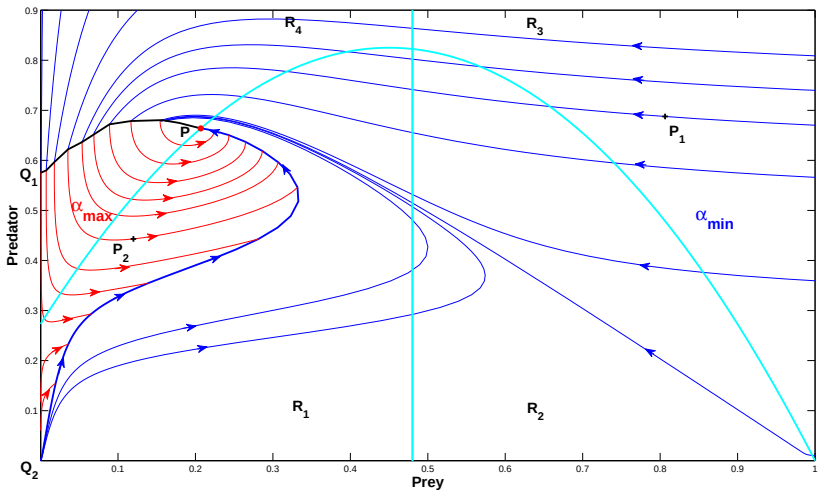

Figure 6.3: Optimal control of pest through quality of additional food under Case 3 with parameter values $c = 1.1, m = 0.05, b = 3, \xi = 0.1, \alpha_{\min} = 0.1$ and $\alpha_{\max} = 0.5$.

6.5 Conclusion

In Chapter 3, we studied the dynamics of a predator-prey system with additional food being supplied to the predators. The results obtained and observations made suggested that the quality and quantity of additional food played a significant role in controlling the system. For the purpose of pest (prey) management, we choose the quality of additional food as the control variable. It is imperative that the pest population is controlled through a desired manner and quick control mechanism. This motivated the formulation of the problem in this Chapter, as a minimum time optimal control for a predator-prey system with additional food to the predators. The necessary conditions (Pontryagins maximum principle) for optimal control, was used to obtain the optimal strategy of the time optimal control problem. Using the necessary conditions along with transversality condition we obtained two types of switching regions in the state space. Finally, we numerically illustrate how manipulation of the quality of additional food to predators can be effectively used for pest control in the minimum possible time.

Chapter 7

Conclusion and Future Directions

In this thesis we studied various aspects of a predator-prey system with additional food being supplied to the predators. In Chapter 2, we derived a modified ratio-dependent model with additional food supply to the predators, on the lines of derivation of functional response for a Holling type-II model. In this model, we assumed that the prey exhibits logistic growth in absence of predation. The predators have an additional food (non-prey) source apart from their natural prey. The rate of provision of additional food to predators is kept constant and is uniformly distributed in the predator's habitat.

In Chapter 3, we analyzed the modified ratio-dependent model. The model system can have atmost five equilibria. The existential and stability conditions are established for all the equilibrium points. The model exhibits transcritical, saddle-node and Hopf bifurcations. The role of additional food was particularly studied and discussed. It was observed that the supply of additional food to predators plays an important role in population conservation and pest management.

In Chapter 4, we presented a diffusive modified ratio-dependent model. The necessary conditions for Turing instability were derived. For the purpose of numerical illustration of patterns, the necessary conditions for Turing instability were used to determine the Turing space in the α-ξ plane, for specific ecological parameter values. Choosing some values of α and ξ in the Turing space, a number of numerical simulations were performed to capture the formation of spatiotemporal patterns.

In Chapter 5, we presented two bio-economic models, namely the classical ratio-dependent and modified ratio-dependent model by incorporating prey harvesting. To determine the role of additional food in the harvesting model, we derived existential and stability conditions for interior equilibria of both the models. We also analyzed the role of additional food supply in determining the optimal harvesting policy using optimal control theory. We found the necessary conditions for the optimal harvesting effort and observed the significant role of additional food in deciding the optimal harvesting policy.

Finally, in Chapter 6, a time optimal control was formulated, with the aim of pest control by way of driving the pest population to a desired level in minimum possible time. The quality of additional food is used as the control variable. The bang-bang control policy to achieve the desired target level of pest population was derived. Also the switching regions for the control variable was established. Finally, we numerically illustrated the role of additional food (quality) supplied, in the control of pest population.

We summarize the beneficial consequences of introducing additional food to the predators in the predator-prey system as follows,

- The additional food supplied plays an important role in populations conservation and in pest management.
- It plays a crucial role in the formation of spatiotemporal patterns for both the prey and predator population.
- The level of ecologically sustainable prey harvesting effort is dependent on the additional food supply.
- It plays a vital role in determining an optimal prey harvesting policy in conjunction with the population conservation, which is more efficient as compared to the case without additional food supply.

Some of the future directions of this work would be motivated by the relaxation of the assumptions made for the modified ratio-dependent model. Two such possible directions are briefly outlined below,

1. *A delay model:*
   We will study the following modified ratio-dependent model with two delays, τ_1(delay in hunting) and τ_2 (delay in positive feedback) [56, 57],
   $$\begin{aligned} \frac{dx}{dt} &= x(t)\left(1-x(t)\right) - \frac{cx(t)y(t-\tau_1)}{x(t-\tau_1)+y(t-\tau_1)+\alpha\xi}, \\ \frac{dy}{dt} &= m\left(\frac{b\left[x(t-\tau_2)+\xi\right]}{x(t-\tau_2)+y(t-\tau_2)+\alpha\xi} - 1\right) y(t). \end{aligned}$$
2. *A stochastic model :*
   We will modify the model to incorporate environmental fluctuations like natural disasters. The perturbations around the interior equilibrium point (x_i, y_i) will be assumed to be Gaussian white noise and proportional to the distances of $x(t)$ and $y(t)$ from the interior equilibrium point (x_i, y_i). The resulting model in terms of stochastic differential equations obtained by

the inclusion of a Wiener process driven term [2] will be as follows,

$$\begin{aligned} dx &= \left(x\left(1-x\right) - \frac{cxy}{x+y+\alpha\xi} \right) dt + \sigma_1 (x - x_i) dW^{(1)}(t), \\ dy &= \left(m\left(\frac{b\left[x+\xi\right]}{x+y+\alpha\xi} - 1 \right) y \right) dt + \sigma_2 (y - y_i) dW^{(2)}(t). \end{aligned}$$

Here $dW^{(i)}(t),\ i = 1:2$ represent two independent Wiener processes and $\sigma_i > 0,\ i = 1:2$ are the respective stochastic intensities.

Appendix A

Existential Conditions for the Interior Equilibria of the System (2.1.3)

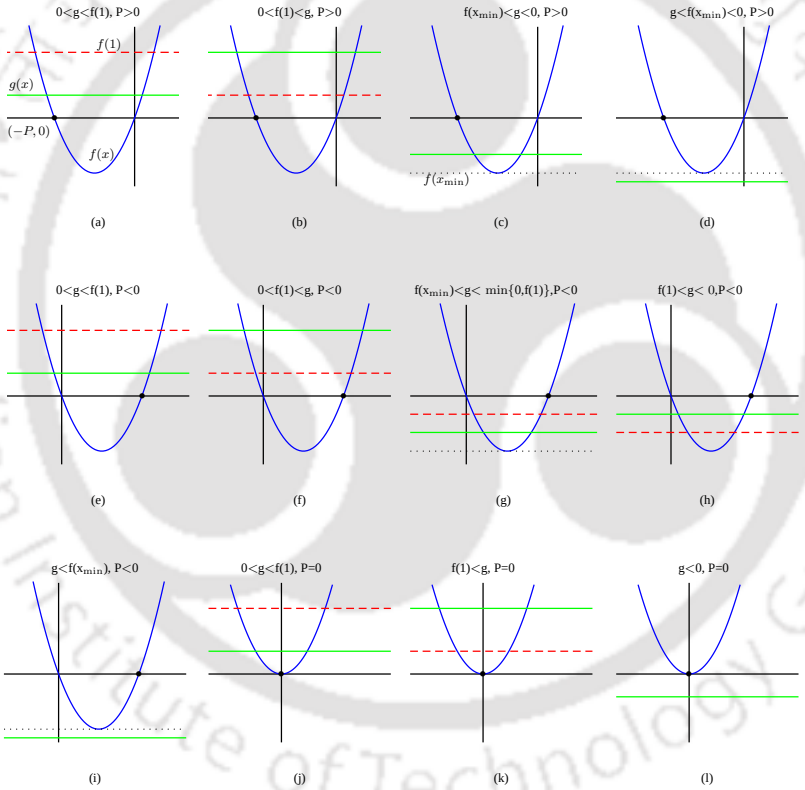

Figure A.1: Figure illustrates the existential condition for abscissa of interior equilibria of the system (2.1.3) under all possible behavior of the functions $f(x)$ and $g(x)$. Figure (g) gives the condition for which both the abscissa of interior equilibria exist (*i.e.*, $x_i \in (0,1)$) simultaneously. The condition of existence of only x_1 is illustrated in Figure (h) and the existence of only x_2 are illustrated by the Figures (a), (e) and (j).

The two interior equilibria are $(x_i, y_i),\ i = 1, 2$, where each $x_i \in (0, 1)$ is a root of

$$x^2 + \left(c - 1 - \frac{c}{b} + \xi\right) x + \left(c - 1 - \frac{\alpha c}{b}\right) \xi = 0. \tag{A.0.1}$$

Let $f(x) = x^2 + Px$ and $g(x) = -\left(c - 1 - \frac{\alpha c}{b}\right) \xi$, where $P = c - 1 - \frac{c}{b} + \xi$. The possible behavior of the functions $f(x)$ and $g(x)$ can be seen from Figure A.1. The graph immediately suggests the conditions under which abscissa of interior equilibrium points exist.
Also $y_i = (b-1)x_i + (b-\alpha)\xi$. It is easy to see that whenever $x_i \in (0, 1)$, $b > 1$ and $(b-1)+(b-\alpha) < 0$ which implies that $y_i < 0$.

Determinant and Trace for the Interior Equilibria for the System (2.1.3)

$$\begin{aligned}
\det J_{(x_i,y_i)} &= -x\left(-1 + \frac{cy_i}{(x_i + y_i + \alpha\xi)^2}\right) \times \frac{bm(x_i + \xi)y_i}{(x_i + y_i + \alpha\xi)^2} + \\
&\quad \frac{bmy_i(y_i + \alpha\xi - \xi)}{(x_i + y_i + \alpha\xi)^2} \times \frac{cx(x_i + \alpha\xi)}{(x_i + y_i + \alpha\xi)^2} \\
&= -x_i\left(-1 + \frac{cy_i}{(x_i + y_i + \alpha\xi)^2}\right) \times \frac{bm(x_i + \xi)y_i}{(x_i + y_i + \alpha\xi)^2} + \\
&\quad \frac{b(b-1)my_i(x_i + \xi)}{(x_i + y_i + \alpha\xi)^2} \times \frac{cx(x_i + \alpha\xi)}{(x_i + y_i + \alpha\xi)^2} \\
&= \frac{bmx_i(x_i + \xi)y_i}{(x_i + y_i + \alpha\xi)^4}\left[(x_i + y_i + \alpha\xi)^2 - cy_i + (b-1) \times c(x_i + \alpha\xi)\right] \\
&= \frac{bmx_i(x_i + \xi)y_i}{(x_i + y_i + \alpha\xi)^4}\left[b^2(x_i + \xi)^2 - cy_i + (b-1) \times c(x_i + \alpha\xi)\right] \\
&= \frac{bmx_i(x_i + \xi)y_i}{(x_i + y_i + \alpha\xi)^4}\left[b^2(x_i + \xi)^2 - c((b-1)x_i + (b-\alpha)\xi) + (b-1) \times c(x_i + \alpha\xi)\right] \\
&= \frac{bmx_i(x_i + \xi)y_i}{(x_i + y_i + \alpha\xi)^4}\left[b^2(x_i + \xi)^2 - c(b-1)x_i - cb\xi + c\alpha\xi + c(b-1)x_i + c(b-1)\alpha\xi\right] \\
&= \frac{bmx_i(x_i + \xi)y_i}{(x_i + y_i + \alpha\xi)^4}\left[b^2(x_i + \xi)^2 - cb\xi + c\alpha\xi + cb\alpha\xi - c\alpha\xi\right] \\
&= \frac{bmx_i(x_i + \xi)y_i}{(x_i + y_i + \alpha\xi)^4}\left[b^2(x_i + \xi)^2 - cb\xi + cb\alpha\xi\right] \\
&= \frac{bmx_i(x_i + \xi)y_i}{(x_i + y_i + \alpha\xi)^4}\left[b^2(x_i + \xi)^2 + cb\xi(\alpha - 1)\right] \\
&= \frac{b^2cmx_i(x_i + \xi)y_i}{(x_i + y_i + \alpha\xi)^4}\left[\frac{b}{c}(x_i + \xi)^2 + \xi(\alpha - 1)\right] \\
&= \frac{bcmx_iy_i}{(x_i + y_i + \alpha\xi)^3}\left[\xi(\alpha - 1) + \frac{b}{c}(x_i + \xi)^2\right].
\end{aligned}$$

$$
\begin{aligned}
tr\ J_{(x_i,y_i)} &= x_i\left[-1+\frac{cy_i}{(x_i+y_i+\alpha\xi)^2}\right]-\frac{bm(x_i+\xi)y_i}{(x_i+y_i+\alpha\xi)^2}\\
&= -x_i+\frac{cx_iy_i}{(x_i+y_i+\alpha\xi)^2}-\frac{bm(x_i+\xi)y_i}{(x_i+y_i+\alpha\xi)^2}\\
&= -x_i+\frac{x_i(1-x_i)}{(x_i+y_i+\alpha\xi)}-\frac{my_i}{(x_i+y_i+\alpha\xi)}\\
&= -x_i+\frac{x_i(1-x_i)}{b(x_i+\xi)}-\frac{my_i}{b(x_i+\xi)}\\
&= -x_i+\frac{x_i(1-x_i)}{b(x_i+\xi)}-\frac{m[(b-1)x_i+(b-\alpha)\xi]}{b(x_i+\xi)}\\
&= -x_i\left[1+\frac{(x_i-1)}{b(x_i+\xi)}+\frac{m(b-1)}{b(x_i+\xi)}\right]-\frac{m(b-\alpha)\xi}{b(_i+\xi)}\\
&= -x_i\left[\frac{b(x_i+\xi)+(x_i-1)+m(b-1)}{b(x_i+\xi)}\right]-\frac{m(b-\alpha)\xi}{b(x_i+\xi)}\\
&= -x_i\left[\frac{(b+1)x_i+(b\xi-1)+m(b-1)}{b(x_i+\xi)}\right]-\frac{m(b-\alpha)\xi}{b(x_i+\xi)}\\
&= \frac{-(b+1)x_i^2-[(b\xi-1)+m(b-1)]\,x_i-m(b-\alpha)\xi}{b(x_i+\xi)}.
\end{aligned}
$$

We have

$$
\begin{aligned}
x_1 &= \frac{1}{2}\left[1-c+\frac{c}{b}-\xi-\sqrt{(1-c+\frac{c}{b}-\xi)^2-4\xi(c-1-\frac{\alpha c}{b})}\ \right]\\
x_1+\xi &= \frac{1}{2}\left[1-c+\frac{c}{b}+\xi-\sqrt{(1-c+\frac{c}{b}-\xi)^2-4\xi(c-1-\frac{\alpha c}{b})}\ \right]\\
&= \frac{1}{2}\left[1-c+\frac{c}{b}+\xi-\sqrt{(1-c+\frac{c}{b}-\xi)^2-4\xi((c-1-\frac{c}{b})+\frac{c}{b}-\frac{\alpha c}{b})}\ \right]\\
&= \frac{1}{2}\left[1-c+\frac{c}{b}+\xi-\sqrt{(1-c+\frac{c}{b}+\xi)^2-\frac{4c\xi}{b}(1-\alpha)}\ \right]\\
&= \frac{1}{2}\left[\frac{(1-c+\frac{c}{b}+\xi)^2-(1-c+\frac{c}{b}+\xi)^2+\frac{4c\xi}{b}(1-\alpha)}{1-c+\frac{c}{b}+\xi+\sqrt{(1-c+\frac{c}{b}+\xi)^2-\frac{4c\xi}{b}(1-\alpha)}}\right]\\
&= \frac{1}{2}\left[\frac{\frac{4c\xi}{b}(1-\alpha)}{1-c+\frac{c}{b}+\xi+\sqrt{(1-c+\frac{c}{b}+\xi)^2-\frac{4c\xi}{b}(1-\alpha)}}\right]\\
&\le \frac{1}{2}\left[\frac{\frac{4c\xi}{b}(1-\alpha)}{1-c+\frac{c}{b}+\xi}\right]\\
&= \frac{\frac{2c\xi}{b}(1-\alpha)}{1-c+\frac{c}{b}+\xi}\\
&= \frac{2\sqrt{\frac{c\xi}{b}(1-\alpha)}\sqrt{\frac{c\xi}{b}(1-\alpha)}}{1-c+\frac{c}{b}+\xi}\\
&\le \sqrt{\frac{c\xi}{b}(1-\alpha)}.
\end{aligned}
$$

Thus $\xi(\alpha-1)+\frac{b}{c}(x_1+\xi)^2 \leq 0 \Longrightarrow \det J_{(x_1,y_1)} \leq 0$, where equality holds when

$$\frac{4c\xi}{b}(1-\alpha) = (1-c+\frac{c}{b}+\xi)^2.$$

We will now prove $\det J_{(x_2,y_2)} \geq 0$ whenever $c < \frac{b}{b-1}$, $\alpha < \left(1-\frac{1}{c}\right)b$ and $\xi < 1-c+\frac{c}{b}$. The proof is as follows,

Since (x_2, y_2) exists, so we have

$$\begin{aligned}
\frac{4c\xi}{b}(1-\alpha) &\leq (1-c+\frac{c}{b}+\xi)^2 \\
\sqrt{\frac{c\xi}{b}(1-\alpha)} &\leq \frac{(1-c+\frac{c}{b}+\xi)}{2} \\
-\xi+\sqrt{\frac{c\xi}{b}(1-\alpha)} &\leq \frac{(1-c+\frac{c}{b}-\xi)}{2}+\frac{1}{2}\sqrt{(1-c+\frac{c}{b}-\xi)^2-4\xi(c-1-\frac{\alpha c}{b})} \\
&= x_2
\end{aligned}$$

The equality sign holds when $\frac{4c\xi}{b}(1-\alpha) = (1-c+\frac{c}{b}+\xi)^2$ *i.e.*, $x_1 = x_2$. When $x_2 = -\xi+\sqrt{\frac{c\xi}{b}(1-\alpha)}$ then $\det J_{(x_2,y_2)} = 0$, which also implies that the discriminant of x_2 is $(1-c+\frac{c}{b}-\xi)^2-4\xi(c-1-\frac{\alpha c}{b})$ and is equal to zero. Hence the existential curve of x_i and the curve $\det J_{(x_i,y_i)} = 0$, $i = 1 = 2$, both coincide in the (α,ξ)-plane.

For the case $c < \frac{b}{b-1}$, $\left(1-\frac{1}{c}\right)b < \alpha < 1$, we have

$$\left(1-\frac{1}{c}\right)b < \alpha \Rightarrow c-1-\frac{c\alpha}{b} < 0 \Rightarrow \frac{c}{b}(1-\alpha) < 1-c+\frac{c}{b}$$

Now

$$\begin{aligned}
-\xi+\sqrt{\frac{c\xi}{b}(1-\alpha)} &= \sqrt{\frac{c\xi}{b}(1-\alpha)}-\xi\times\frac{\sqrt{\frac{c\xi}{b}(1-\alpha)}+\xi}{\sqrt{\frac{c\xi}{b}(1-\alpha)}+\xi} \\
&= \frac{\frac{c\xi}{b}(1-\alpha)-\xi^2}{\sqrt{\frac{c\xi}{b}(1-\alpha)}+\xi} \\
&= \frac{\xi\left[\frac{c}{b}(1-\alpha)-\xi\right]}{\sqrt{\frac{c\xi}{b}(1-\alpha)}+\xi} \\
&< \frac{c}{b}(1-\alpha)-\xi \\
&< 1-c+\frac{c}{b}-\xi \\
&= \frac{1-c+\frac{c}{b}-\xi}{2}+\frac{1-c+\frac{c}{b}-\xi}{2} \\
&< \frac{1-c+\frac{c}{b}-\xi}{2}+\frac{1}{2}\sqrt{(1-c+\frac{c}{b}-\xi)^2-4\xi(c-1-\frac{\alpha c}{b})} \\
&= x_2.
\end{aligned}$$

Thus we conclude that $\det J_{(x_2,y_2)} > 0$.

Bifurcations

Theorem A.0.1. *Suppose $\xi > \frac{1}{b}$. Then the system (2.1.3) undergoes transcritical bifurcation at the axial equilibrium point $\mathbf{x}_1(0,(b-\alpha)\xi)$ as the parameter α passes through the bifurcation value $\alpha = \alpha_0$ where $\alpha_0 = \left(1-\frac{1}{c}\right)b$.*
Note that the condition $\xi > \frac{1}{b}$ certainly ensures that tr $J_{(x_2,y_2)} < 0$ whenever (x_2,y_2) exists.

Proof. We will prove this theorem by verifying the following conditions due to Sotomayor (as given in [49]):

(i) $\mathbf{w}^T\mathbf{f}_\alpha(\mathbf{x}_0,\alpha_0) = 0.$

(ii) $\mathbf{w}^T\left[D\mathbf{f}_\alpha(\mathbf{x}_0,\alpha_0)\mathbf{v}\right] \neq 0.$

(iii) $\mathbf{w}^T\left[D^2\mathbf{f}(\mathbf{x}_0,\alpha_0)(\mathbf{v},\mathbf{v})\right] \neq 0.$

where $\mathbf{v}$ and $\mathbf{w}$ are eigenvectors of a matrix $A \equiv D\mathbf{f}(\mathbf{x}_0,\xi_0)$ and A^T respectively, corresponding to simple eigenvalue $\lambda = 0$. In this case we have the following,

$$\mathbf{f}(x,y) = \left[f_1(x,y),\quad f_2(x,y)\right]^\top = \left[x\,(1-x) - \tfrac{cxy}{x+y+\alpha\xi},\quad m\left(\tfrac{b[x+\xi]}{x+y+\alpha\xi} - 1\right)y\right]^\top$$

$$\mathbf{f}_\alpha(x,y) = \left[\tfrac{c\xi xy}{(x+y+\alpha\xi)^2},\quad -\tfrac{bm\xi(x+\xi)y}{(x+y+\alpha\xi)^2}\right]^\top$$

$$D\mathbf{f}(\mathbf{x},\alpha) = \begin{bmatrix} (1-x) - \frac{cy}{x+y+\alpha\xi} + x\left[-1 + \frac{cy}{(x+y+\alpha\xi)^2}\right] & -\frac{cx(x+\alpha\xi)}{(x+y+\alpha\xi)^2} \\ \frac{bmy(y+\alpha\xi-\xi)}{(x+y+\alpha\xi)^2} & m\left(\frac{b[x+\xi]}{x+y+\alpha\xi} - 1\right) - \frac{bm(x+\xi)y}{(x+y+\alpha\xi)^2} \end{bmatrix}$$

$$D^2\mathbf{f}(\mathbf{x},\alpha) = \begin{bmatrix} \left(-2 + 2\frac{cy(y+\alpha\xi)}{(x+y+\alpha\xi)^3}, -\frac{c(x+\alpha\xi)(y+\alpha\xi)+cxy}{(x+y+\alpha\xi)^3}\right)^\top & \left(-\frac{c(x+\alpha\xi)(y+\alpha\xi)+cxy}{(x+y+\alpha\xi)^3}, 2\frac{cx(x+\alpha\xi)}{(x+y+\alpha\xi)^3}\right)^\top \\ \left(-2\frac{bmy(y+\alpha\xi-\xi)}{(x+y+\alpha\xi)^3}, bm\frac{(x+\alpha\xi)(y+\alpha\xi-\xi)+(x+\xi)y}{(x+y+\alpha\xi)^3}\right)^\top & \left(bm\frac{(x+\alpha\xi)(y+\alpha\xi-\xi)+(x+\xi)y}{(x+y+\alpha\xi)^3}, -2bm\frac{(x+\xi)(x+\alpha\xi)}{(x+y+\alpha\xi)^3}\right)^\top \end{bmatrix}$$

$$D\mathbf{f}_\alpha(\mathbf{x},\alpha) = \begin{bmatrix} \frac{(x+y+\alpha\xi)^2c\xi y - 2c\xi xy(x+y+\alpha\xi)}{(x+y+\alpha\xi)^4} & \frac{(x+y+\alpha\xi)^2c\xi x - 2c\xi xy(x+y+\alpha\xi)}{(x+y+\alpha\xi)^4} \\ -\frac{(x+y+\alpha\xi)^2bm\xi y - 2bm\xi(x+\xi)y(x+y+\alpha\xi)}{(x+y+\alpha\xi)^4} & -\frac{(x+y+\alpha\xi)^2bm\xi(x+\xi) - 2bm\xi(x+\xi)y(x+y+\alpha\xi)}{(x+y+\alpha\xi)^4} \end{bmatrix}$$

$$= \begin{bmatrix} c\xi y\frac{(-x+y+\alpha\xi)}{(x+y+\alpha\xi)^3} & c\xi x\frac{(x-y+\alpha\xi)}{(x+y+\alpha\xi)^3} \\ -bm\xi y\frac{(x+y+\alpha\xi)-2(x+\xi)}{(x+y+\alpha\xi)^3} & -bm\xi(x+\xi)\frac{(x+y+\alpha\xi)-2y}{(x+y+\alpha\xi)^3} \end{bmatrix}$$

Hence

$$
\begin{aligned}
D\mathbf{f}(\mathbf{x}_1,\alpha_0) &= \begin{bmatrix} 0 & 0 \\ \frac{m(b-1)}{c} & \frac{-m}{c} \end{bmatrix}, \ \mathbf{f}_\alpha(\mathbf{x}_1,\alpha_0) = \begin{bmatrix} 0 \\ -\frac{m\xi}{c} \end{bmatrix} \\
D\mathbf{f}_\alpha(\mathbf{x}_1,\alpha_0) &= \begin{bmatrix} \frac{1}{b} & 0 \\ -\frac{m(b-2)}{bc} & -\frac{m(c-2)}{bc} \end{bmatrix} \\
D^2\mathbf{f}(\mathbf{x}_1,\alpha_0) &= \begin{bmatrix} \left(2(\frac{1}{b\xi}-1), \frac{-c\alpha_0}{b^2\xi}\right)^\top & \left(\frac{-c\alpha_0}{b^2\xi}, 0\right)^\top \\ \left(-\frac{2m(b-1)}{bc\xi}, m\frac{b(\alpha_0+1)-2\alpha_0}{b^2\xi}\right)^\top & \left(m\frac{b(\alpha_0+1)-2\alpha_0}{b^2\xi}, -\frac{2m\alpha_0}{b^2\xi}\right)^\top \end{bmatrix}
\end{aligned}
$$

Also $\mathbf{v} = (1,\ b-1)^\top$, $\mathbf{w} = (1,0)^\top$. Hence

$$\mathbf{w}^T\mathbf{f}_\alpha(\mathbf{x}_1,\alpha_0) = 0, \mathbf{w}^T\left[D\mathbf{f}_\alpha(\mathbf{x}_1,\alpha_0)\mathbf{v}\right] = \frac{1}{b} \neq 0$$

and

$$\mathbf{w}^T\left[D^2\mathbf{f}(\mathbf{x}_1,\alpha_0)(\mathbf{v},\ \mathbf{v})\right] = -\frac{2(b\xi-1)}{b\xi} + \frac{-2c(b-1)\alpha_0}{b^2\xi} \neq 0.$$

□

Theorem A.0.2. *The system (2.1.3) undergoes Hopf bifurcation at the interior equilibrium point (x_2, y_2) as the parameter α passes through the bifurcation value $\alpha = \alpha_0$ s.t.*

$$tr\ \ J_{(x_2,y_2)}\Big|_{\alpha=\alpha_0} = 0.$$

Proof. We know that

$$
\begin{aligned}
tr\ \ J_{(x_2,y_2)} &= \frac{-(b+1)x_2^2 - \left[(b\xi-1)+m(b-1)\right]x_2 - m(b-\alpha)\xi}{b(x_2+\xi)} \\
&= \frac{-(b+1)x_2^2 - (b\xi-1)x_2 - my_2}{b(x_2+\xi)}.
\end{aligned}
$$

Also we have $x_2 + y_2 + \alpha\xi = b(x_2+\xi)$ which gives

$$\frac{\partial y_2}{\partial\alpha} = (b-1)\frac{\partial x_2}{\partial\alpha}.$$

Now

$$
\begin{aligned}
\frac{\partial}{\partial\alpha}tr\ \ J_{(x_2,y_2)} &= \frac{-2(b+1)x_2\frac{\partial x_2}{\partial\alpha} - (b\xi-1)\frac{\partial x_2}{\partial\alpha} - m\frac{\partial y_2}{\partial\alpha}}{b(x_2+\xi)} \\
&= \frac{-2(b+1)x_2\frac{\partial x_2}{\partial\alpha} - (b\xi-1)\frac{\partial x_2}{\partial\alpha} - m(b-1)\frac{\partial x_2}{\partial\alpha}}{b(x_2+\xi)} \\
&= \frac{1}{b(x_2+\xi)}\frac{\partial x_2}{\partial\alpha}\left(-2(b+1)x_2 - (b\xi-1) - m(b-1)\right).
\end{aligned}
$$

This is non-zero unless x_2 is a repeated root of the equation $-(b+1)x^2 - \left[(b\xi-1)+m(b-1)\right]x - m(b-\alpha)\xi = 0$. □

Theorem A.0.3. *The system (2.1.3) undergoes transcritical bifurcation at the axial equilibrium point* $\mathbf{x}_0 = (1, 0)$ *as the parameter* ξ *passes through the bifurcation value* $\xi = \xi_0$ *where* $\xi_0 = \frac{b-1}{\alpha-b}$.

Proof. In this case we have Sotomayor's conditions as follows:

(i) $\mathbf{w}^T \mathbf{f}_\xi(\mathbf{x}_0, \xi_0) = 0.$

(ii) $\mathbf{w}^T \left[D\mathbf{f}_\xi(\mathbf{x}_0, \xi_0)\mathbf{v}\right] \neq 0.$

(iii) $\mathbf{w}^T \left[D^2\mathbf{f}(\mathbf{x}_0, \xi_0)(\mathbf{v}, \mathbf{v})\right] \neq 0.$

where $\mathbf{v}$ and $\mathbf{w}$ are eigenvectors of a matrix $A \equiv D\mathbf{f}(\mathbf{x}_0, \xi_0)$ and A^T respectively, corresponding to simple eigenvalue $\lambda = 0$. We thus have,

$$\mathbf{f}(x,y) = \left[f_1(x,y), \quad f_2(x,y)\right]^\top = \left[x\,(1-x) - \tfrac{cxy}{x+y+\alpha\xi}, \quad m\left(\tfrac{b[x+\xi]}{x+y+\alpha\xi} - 1\right) y\right]^\top$$

$$\mathbf{f}_\xi(x,y) = \left[\tfrac{c\alpha xy}{(x+y+\alpha\xi)^2}, \quad bmy\tfrac{(x+y+\alpha\xi)-(x+\xi)\alpha}{(x+y+\alpha\xi)^2}\right]^\top = \left[\tfrac{c\alpha xy}{(x+y+\alpha\xi)^2}, \quad bm\tfrac{xy(1-\alpha)+y^2}{(x+y+\alpha\xi)^2}\right]^\top$$

$$D\mathbf{f}(\mathbf{x},\xi) = \begin{bmatrix} (1-x) - \frac{cy}{x+y+\alpha\xi} + x\left[-1 + \frac{cy}{(x+y+\alpha\xi)^2}\right] & -\frac{cx(x+\alpha\xi)}{(x+y+\alpha\xi)^2} \\ \frac{bmy(y+\alpha\xi-\xi)}{(x+y+\alpha\xi)^2} & m\left(\frac{b[x+\xi]}{x+y+\alpha\xi} - 1\right) - \frac{bm(x+\xi)y}{(x+y+\alpha\xi)^2} \end{bmatrix}$$

$$D^2\mathbf{f}(\mathbf{x},\xi) = \begin{bmatrix} \left(-2 + 2\frac{cy(y+\alpha\xi)}{(x+y+\alpha\xi)^3}, -\frac{c(x+\alpha\xi)(y+\alpha\xi)+cxy}{(x+y+\alpha\xi)^3}\right)^\top & \left(-\frac{c(x+\alpha\xi)(y+\alpha\xi)+cxy}{(x+y+\alpha\xi)^3}, 2\frac{cx(x+\alpha\xi)}{(x+y+\alpha\xi)^3}\right)^\top \\ \left(-2\frac{bmy(y+\alpha\xi-\xi)}{(x+y+\alpha\xi)^3}, bm\frac{(x+\alpha\xi)(y+\alpha\xi-\xi)+(x+\xi)y}{(x+y+\alpha\xi)^3}\right)^\top & \left(bm\frac{(x+\alpha\xi)(y+\alpha\xi-\xi)+(x+\xi)y}{(x+y+\alpha\xi)^3}, -2bm\frac{(x+\xi)(x+\alpha\xi)}{(x+y+\alpha\xi)^3}\right)^\top \end{bmatrix}$$

$$D\mathbf{f}_\xi(\mathbf{x},\xi) = \begin{bmatrix} c\alpha y\frac{(-x+y+\alpha\xi)}{(x+y+\alpha\xi)^3} & c\alpha x\frac{(x-y+\alpha\xi)}{(x+y+\alpha\xi)^3} \\ ybm\frac{-x(1-\alpha)-y(1+\alpha)+\alpha\xi(1-\alpha)}{(x+y+\alpha\xi)^3} & bm\frac{(x+y+\alpha\xi)(x(1-\alpha)+2y)-2(xy(1-\alpha)+y^2)}{(x+y+\alpha\xi)^3} \end{bmatrix}$$

Hence in this case we have

$$D\mathbf{f}(\mathbf{x}_0,\xi_0) = \begin{bmatrix} -1 & -\frac{c}{1+\alpha\xi_0} \\ 0 & 0 \end{bmatrix}, \ \mathbf{f}_\xi(\mathbf{x}_0,\xi_0) = \begin{bmatrix} 0 \\ 0 \end{bmatrix}$$

$$D\mathbf{f}_\xi(\mathbf{x}_0,\xi_0) = \begin{bmatrix} 0 & \frac{c\alpha}{(1+\alpha\xi_0)^2} \\ 0 & bm\frac{1-\alpha}{(1+\alpha\xi_0)^2} \end{bmatrix}$$

and

$$D^2\mathbf{f}(\mathbf{x}_0,\xi_0) = \begin{bmatrix} (-2, -\frac{c\alpha\xi_0}{(1+\alpha\xi_0)^2})^\top & (-\frac{c\alpha\xi_0}{(1+\alpha\xi_0)^2}, \frac{2c}{(1+\alpha\xi_0)^2})^\top \\ \left(0, \frac{bm\xi_0(\alpha-1)}{(1+\alpha\xi_0)^2}\right)^\top & \left(\frac{bm\xi_0(\alpha-1)}{(1+\alpha\xi_0)^2}, -\frac{2bm(1+\xi_0)}{(1+\alpha\xi_0)^2}\right)^\top \end{bmatrix}.$$

Also $\mathbf{v} = \left(-\frac{c(\alpha-b)}{b(\alpha-1)}, 1\right)^\top$, $\mathbf{w} = (0,1)^\top$. Clearly

$$\mathbf{w}^T \mathbf{f}_\xi(\mathbf{x}_0, \xi_0) = 0, \mathbf{w}^T \left[D\mathbf{f}_\xi(\mathbf{x}_0, \xi_0)\mathbf{v}\right] = bm\frac{1-\alpha}{(1+\alpha\xi_0)^2} \neq 0$$

and

$$\mathbf{w}^T \left[D^2\mathbf{f}(\mathbf{x}_0, \xi_0)(\mathbf{v}, \mathbf{v})\right] = -\frac{2mc(b-1)}{(1+\alpha\xi_0)^2} - \frac{2bm(1+\xi_0)}{(1+\alpha\xi_0)^2} \neq 0.$$

□

Theorem A.0.4. *The system (2.1.3) undergoes saddle-node bifurcation at the interior equilibrium point* $(x^*, y^*) = \left(\frac{1}{2}\left(1-c+\frac{c}{b}-\xi\right), (b-1)x^* + (b-\alpha)\xi\right)$ *as the parameter* α *passes through the bifurcation value* $\alpha = \alpha_0$ *where*

$$\alpha_0 = 1 - \frac{b}{4c\xi}(1-c+\frac{c}{b}+\xi)^2.$$

Proof. In this case we have the following,

$$\begin{aligned} D\mathbf{f}(\mathbf{x}^*, \alpha_0) &= \begin{bmatrix} x^*\left[-1+\frac{cy^*}{(x^*+y^*+\alpha_0\xi)^2}\right] & -\frac{cx^*(x^*+\alpha_0\xi)}{(x^*+y^*+\alpha_0\xi)^2} \\ \frac{bmy^*(y^*+\alpha_0\xi-\xi)}{(x^*+y^*+\alpha_0\xi)^2} & -\frac{bm(x^*+\xi)y^*}{(x^*+y^*+\alpha_0\xi)^2} \end{bmatrix} \\ &= \begin{bmatrix} x^*\left[-1+\frac{cy^*}{(x^*+y^*+\alpha_0\xi)^2}\right] & -\frac{cx^*(x^*+\alpha_0\xi)}{(x^*+y^*+\alpha_0\xi)^2} \\ \frac{bmy^*(b-1)(x^*+\xi)}{(x^*+y^*+\alpha_0\xi)^2} & -\frac{bm(x^*+\xi)y^*}{(x^*+y^*+\alpha_0\xi)^2} \end{bmatrix} \\ \mathbf{f}_\alpha(\mathbf{x}^*, \alpha_0) &= \begin{bmatrix} \frac{cx^*y^*\xi}{(x^*+y^*+\alpha_0\xi)^2} \\ -\frac{bm(x^*+\xi)y^*\xi}{(x^*+y^*+\alpha_0\xi)^2} \end{bmatrix}, \ D^2\mathbf{f}(\mathbf{x}^*, \alpha_0) = \end{aligned}$$

$$\begin{bmatrix} \left(-2+2\frac{cy^*(y^*+\alpha_0\xi)}{(x^*+y^*+\alpha_0\xi)^3}, -\frac{c(x^*+\alpha_0\xi)(y^*+\alpha_0\xi)+cx^*y^*}{(x^*+y^*+\alpha_0\xi)^3}\right)^\top & \left(-\frac{c(x^*+\alpha_0\xi)(y^*+\alpha_0\xi)+cx^*y^*}{(x^*+y^*+\alpha_0\xi)^3}, 2\frac{cx^*(x^*+\alpha_0\xi)}{(x^*+y^*+\alpha_0\xi)^3}\right)^\top \\ \left(-2\frac{bmy^*(y^*+\alpha_0\xi-\xi)}{(x^*+y^*+\alpha_0\xi)^3}, bm\frac{(x^*+\alpha_0\xi)(y^*+\alpha_0\xi-\xi)+(x^*+\xi)y^*}{(x^*+y^*+\alpha_0\xi)^3}\right)^\top & \left(bm\frac{(x^*+\alpha_0\xi)(y^*+\alpha_0\xi-\xi)+(x^*+\xi)y^*}{(x^*+y^*+\alpha_0\xi)^3}, -2bm\frac{(x^*+\xi)(x^*+\alpha_0\xi)}{(x^*+y^*+\alpha_0\xi)^3}\right)^\top \end{bmatrix}$$

Also $\mathbf{v} = (1,\ b-1)^\top$, $\mathbf{w} = (bm(x^*+\xi)y^*, -cx^*(x^*+\alpha_0\xi))^\top$.

Hence

$$\begin{aligned} \mathbf{w}^T\mathbf{f}_\alpha(\mathbf{x}^*, \alpha_0) &= (bm(x^*+\xi)y^*, -cx^*(x^*+\alpha_0\xi)) \begin{bmatrix} \frac{cx^*y^*\xi}{(x^*+y^*+\alpha_0\xi)^2} \\ -\frac{bm(x^*+\xi)y^*\xi}{(x^*+y^*+\alpha_0\xi)^2} \end{bmatrix} \\ &= \frac{1}{(x^*+y^*+\alpha_0\xi)^2} \times [bmcx^*(x^*+\xi)y^{*2}\xi + bmcx^*(x^*+\xi)(x^*+\alpha_0\xi)y^*\xi] \\ &= \frac{bmcx^*(x^*+\xi)y^*\xi}{(x^*+y^*+\alpha_0\xi)^2} \times [y^* + (x^*+\alpha_0\xi)] \\ &= \frac{bmcx^*(x^*+\xi)y^*\xi}{(x^*+y^*+\alpha_0\xi)} \\ &= mcx^*y^*\xi \neq 0. \end{aligned}$$

$$D^2\mathbf{f}(\mathbf{x}^*,\alpha_0)(\mathbf{v},\mathbf{v}) = \begin{bmatrix} -2+2\frac{cy^*(y^*+\alpha_0\xi)}{(x^*+y^*+\alpha_0\xi)^3} - 2(b-1)c\frac{(x^*+\alpha_0\xi)(y^*+\alpha_0\xi)+x^*y^*}{(x^*+y^*+\alpha_0\xi)^3} + 2(b-1)^2\frac{cx^*(x^*+\alpha_0\xi)}{(x^*+y^*+\alpha_0\xi)^3} \\ -2\frac{bmy^*(y^*+\alpha_0\xi-\xi)}{(x^*+y^*+\alpha_0\xi)^3} + 2(b-1)bm\frac{(x^*+\alpha_0\xi)(y^*+\alpha_0\xi-\xi)+(x^*+\xi)y^*}{(x^*+y^*+\alpha_0\xi)^3} - 2(b-1)^2bm\frac{(x^*+\xi)(x^*+\alpha_0\xi)}{(x^*+y^*+\alpha_0\xi)^3} \end{bmatrix}$$

$$= \frac{2}{(x^*+y^*+\alpha_0\xi)^3}\times \begin{bmatrix} -(x^*+y^*+\alpha_0\xi)^3 + cy^*(y^*+\alpha_0\xi) - (b-1)c[(x^*+\alpha_0\xi)(y^*+\alpha_0\xi)+x^*y^*] + (b-1)^2cx^*(x^*+\alpha_0\xi) \\ -bmy^*(y^*+\alpha_0\xi-\xi) + (b-1)bm[(x^*+\alpha_0\xi)(y^*+\alpha_0\xi-\xi)+(x^*+\xi)y^*] - (b-1)^2bm(x^*+\xi)(x^*+\alpha_0\xi) \end{bmatrix}$$

Thus $\mathbf{w}^T\left[D^2\mathbf{f}(\mathbf{x}^*,\alpha_0)(\mathbf{v},\mathbf{v})\right] =$

$$\begin{aligned}
&-2bm(x^*+\xi)y^* + \frac{2}{(x^*+y^*+\alpha_0\xi)^3}\times[bm(x^*+\xi)y^*\{cy^*(y^*+\alpha_0\xi)- \\
&(b-1)c((x^*+\alpha_0\xi)(y^*+\alpha_0\xi)+x^*y^*)+(b-1)^2cx^*(x^*+\alpha_0\xi)\} - cx^*(x^*+\alpha_0\xi) \\
&\{-bmy^*(y^*+\alpha_0\xi-\xi)+(b-1)bm((x^*+\alpha_0\xi)(y^*+\alpha_0\xi-\xi)+(x^*+\xi)y^*)- \\
&(b-1)^2bm(x^*+\xi)(x^*+\alpha_0\xi)\}] \\
=\ &-2bm(x^*+\xi)y^* + \frac{2bmc}{(x^*+y^*+\alpha_0\xi)^3}\times[(x^*+\xi)y^*\{y^*(y^*+\alpha_0\xi)- \\
&(b-1)((x^*+\alpha_0\xi)(y^*+\alpha_0\xi)+x^*y^*)+(b-1)^2x^*(x^*+\alpha_0\xi)\} - x^*(x^*+\alpha_0\xi) \\
&\{-y^*(b-1)(x^*+\xi)+(b-1)((x^*+\alpha_0\xi)(b-1)(x^*+\xi)+(x^*+\xi)y^*)- \\
&(b-1)^2(x^*+\xi)(x^*+\alpha_0\xi)\}] \\
=\ &-2bm(x^*+\xi)y^* + \frac{2bmc(x^*+\xi)}{(x^*+y^*+\alpha_0\xi)^3}\times[y^*\{y^*(y^*+\alpha_0\xi)- \\
&(b-1)((x^*+\alpha_0\xi)(y^*+\alpha_0\xi)+x^*y^*)+(b-1)^2x^*(x^*+\alpha_0\xi)x^*(x^*+\alpha_0\xi) \\
&\{-y^*(b-1)+(b-1)((x^*+\alpha_0\xi)(b-1)+y^*)-(b-1)^2(x^*+\alpha_0\xi)\}] \\
=\ &-2bm(x^*+\xi)y^* + \frac{2bmc(x^*+\xi)y^*}{(x^*+y^*+\alpha_0\xi)^3}\times \\
&[y^*(y^*+\alpha_0\xi)-(b-1)((x^*+\alpha_0\xi)(y^*+\alpha_0\xi)+x^*y^*)+(b-1)^2x^*(x^*+\alpha_0\xi)] \\
=\ &-2bm(x^*+\xi)y^* + \frac{2bmc(x^*+\xi)y^*}{(x^*+y^*+\alpha_0\xi)^3}\times[y^*\{(b-1)x^*+b\xi\}- \\
&(b-1)((x^*+\alpha_0\xi)(y^*+\alpha_0\xi)+x^*y^*)+(b-1)\{(y^*+\alpha_0\xi)-b\xi\}(x^*+\alpha_0\xi)] \\
=\ &-2bm(x^*+\xi)y^* + \frac{2bmc(x^*+\xi)y^*}{(x^*+y^*+\alpha_0\xi)^3}\times[b\xi y^*-b(b-1)(x^*+\alpha_0\xi)\xi] \\
=\ &-2bm(x^*+\xi)y^* + \frac{2b^2mc\xi(x^*+\xi)y^*}{(x^*+y^*+\alpha_0\xi)^3}\times[y^*-(b-1)(x^*+\alpha_0\xi)] \\
=\ &-2bm(x^*+\xi)y^* + \frac{2b^2mc\xi(x^*+\xi)y^*}{(x^*+y^*+\alpha_0\xi)^3}\times[(b-1)x^*+(b-\alpha_0)\xi-(b-1)(x^*+\alpha_0\xi)] \\
=\ &-2bm(x^*+\xi)y^* + \frac{2b^2mc\xi(x^*+\xi)y^*}{(x^*+y^*+\alpha_0\xi)^3}\times[b\xi-\alpha_0\xi-b\alpha_0\xi+\alpha_0\xi] \\
=\ &-2bm(x^*+\xi)y^* + \frac{2b^3mc\xi^2(1-\alpha_0)(x^*+\xi)y^*}{(x^*+y^*+\alpha_0\xi)^3}
\end{aligned}$$

$$
\begin{aligned}
&= -2bm(x^*+\xi)y^* + \frac{2b^2mc\xi^2(1-\alpha_0)y^*}{(x^*+y^*+\alpha_0\xi)^2} \\
&= -2bm(x^*+\xi)y^* + \frac{2b^2mc\xi^2y^*}{(x^*+y^*+\alpha_0\xi)^2} \times \frac{b}{4c\xi}(1-c+\frac{c}{b}+\xi)^2 \\
&= -2bm(x^*+\xi)y^* + \frac{2m\xi y^*}{(x^*+\xi)^2} \times b(x^*+\xi)^2 \\
&= -2bm(x^*+\xi)y^* + 2bm\xi y^* \\
&= -2bmx^*y^* \neq 0.
\end{aligned}
$$

□

Appendix B

Turing Bifurcation

The system (4.1.2) can be rewritten as follows

$$\mathbf{U}_t = D\nabla^2\mathbf{U} + F(\mathbf{U}), \mathbf{U_n}(\mathbf{S},t) = 0,\ \mathbf{S} \in \partial\Omega,\ t > 0, \tag{B.0.1}$$

where $\mathbf{U} = (x,y)^\top, D = \text{diag}(d_1,d_2)$ and $F(\mathbf{U}) = \left[x\,(1-x) - \frac{cxy}{x+y+\alpha\xi},\quad m\left(\frac{b[x+\xi]}{x+y+\alpha\xi} - 1\right)y\right]^\top$.

Definition [36]: An uniform stationary solution $\mathbf{U}^*$ of the system (B.0.1) is said to undergo a Turing bifurcation at $\mu = \mu_0$ if $\mathbf{U}^*$ changes its stability at μ_0 and in some neighborhood of μ_0 there exists a one-parameter family of non-constant stationary solution of the system (B.0.1).

Keeping ξ fixed, taking $\alpha \in \mathbb{R}_+$ as a bifurcation parameter and $\mathbf{U}^* = (x_2,y_2)^\top$ as an uniform stationary solution of the system (B.0.1), we now prove following theorem with the help of Theorem 13.5 [58] and Section 5 [36].

Theorem B.0.5. *Let $\mathbf{c}_{p1}$ and $\mathbf{c}_{p2}$ be the eigenvectors of the matrix $B_p = J_2 - \lambda_p D$ corresponding to the eigenvalues σ_{p1} and σ_{p2} respectively. Assume that*

(i) $d_2 > d_1 > 0,\ tr\ J_2 < 0\ \ and\ \ \det J_2 > 0,$

(ii) $\mathbf{c}_{p2} \nparallel \left.\frac{\partial J_2}{\partial\alpha}\right|_{\alpha=\alpha_0} \mathbf{c}_{p1},$

(iii) $\xi > 0.$

Then there exists a $p \in \mathbb{N}$ s.t. $H(\lambda_p)\Big|_{\alpha=\alpha_0} = 0$ i.e. at $\alpha = \alpha_0$, uniform stationary solution $\mathbf{U}^*$ of the system (B.0.1) undergoes a Turing bifurcation.

Proof. The introduction of transformation $\mathbf{X} = \mathbf{U} - \mathbf{U}^*$ reduces the system (B.0.1) to the following form,

$$\mathbf{X}_t = D\nabla^2\mathbf{X} + J_2\mathbf{X} + G(\mathbf{X}),\ \mathbf{X_n}(\mathbf{S},t) = 0,\ \mathbf{S} \in \partial\Omega,\ t > 0,$$

where J_2 is the Jacobian matrix of F at $\mathbf{U}^*$ and $G(\mathbf{X}) = F(\mathbf{X}+\mathbf{U}^*) - J_2\mathbf{X}$. For any non-uniform stationary solution $\mathbf{U}$ of the system (B.0.1), $\mathbf{X} = \mathbf{U} - \mathbf{U}^*$ satisfies the following equation

$$D\nabla^2\mathbf{X} + J_2\mathbf{X} + G(\mathbf{X}) = 0,\ \mathbf{X_n}(\mathbf{S},t) = 0,\ \mathbf{S} \in \partial\Omega,\ t > 0.$$

Let $f : \mathbb{R} \times \mathcal{B}_1 \longrightarrow \mathcal{B}_2$ be defined as,

$$f(\alpha, \mathbf{X}) = D\nabla^2\mathbf{X} + J_2\mathbf{X} + G(\mathbf{X})$$

where $\mathcal{B}_1$ and $\mathcal{B}_2$ are Banach spaces and also let $L_0 = D_2 f(\alpha_0, 0)$ and $L_1 = D_1 D_2 f(\alpha_0, 0)$. Then $f(\alpha, 0) = 0\ \forall\ \alpha > 0$ and

$$D_2 f(\alpha_0,0)\upsilon = (D\nabla^2 + J_2)\upsilon = (J_2 - \lambda_j D)\upsilon \text{ and } D_1 D_2 f(\alpha_0,0)\upsilon = \frac{\partial J_2}{\partial \alpha}\Big|_{\alpha=\alpha_0}\upsilon.$$

The spectrum of L_0 is given by the eigenvalues of σ_{jk} of the matrices $B_j = J_2 - \lambda_j D$ evaluated at $\alpha = \alpha_0$, where $j = 0, 1, 2, \ldots$ and $k = 1, 2$. In order to have $\det B_j = 0$ for some fixed j (say p), let σ_{p1} is the simple zero eigenvalue of the matrix B_p and the corresponding eigenvector is $\mathbf{c}_{p1}$. Also the eigenfunction of L_0 corresponding to eigenvalue σ_{p1}, is the non-uniform stationary solution of linearized system (4.3.1), which is given by $\mathbf{c}_{p1}\psi_p(\mathbf{S})$. The set of orthogonal functions $\psi_n(\mathbf{S}),\ n = 0, 1, 2 \ldots p \ldots$ can be obtained by following eigenvalue problem

$$\nabla^2\psi_n = -\lambda\psi_n,\ \mathbf{S} \in \Omega, \psi_{\mathbf{n}} = 0, \mathbf{S} \in \partial\Omega,$$

Thus we have the null space and range space of the operator L_0 as,

$$\begin{aligned}
N(L_0) &= \text{span}\{\text{eigenfunction of } L_0 \text{ corresponding to simple zero eigenvalue}\} \\
&= \text{span}\{\mathbf{c}_{p1}\psi_p(\mathbf{S})\} \\
R(L_0) &= (\mathbf{U} \in C(\Omega,\mathbb{R}) \times C(\Omega,\mathbb{R}) : \int_\Omega \langle \mathbf{U}, \mathbf{c}_{p2}\psi_p(\mathbf{S})\rangle d\mathbf{S} = 0) \cup \text{span}\{\mathbf{c}_{p2}\psi_p(\mathbf{S})\} \\
&= (\mathbf{U} \in C(\Omega,\mathbb{R}) \times C(\Omega,\mathbb{R}) : \text{The fourier expansion of } \mathbf{U} \text{ does not contain the} \\
&\quad \text{term } \psi_p(\mathbf{S})) \cup \text{span}\{\mathbf{c}_{p2}\psi_p(\mathbf{S})\}
\end{aligned}$$

Clearly here, $\dim[N(L_0)] = 1$ and $\text{codim}[R(L_0)] = 1$. Also

$$L_1\mathbf{c}_{p1}\psi_p(\mathbf{S}) = \frac{\partial J_2}{\partial \alpha}\Big|_{\alpha=\alpha_0}\mathbf{c}_{p1}\psi_p(\mathbf{S}).$$

If $\mathbf{c}_{p2} \nparallel \frac{\partial J_2}{\partial \alpha}\mathbf{c}_{p1}$, then we have, $L_1\mathbf{c}_{p1}\psi_p(\mathbf{S}) \notin R(L_0)$. Taking $Z = R(L_0)$, we see that all the hypothesis of the Theorem 13.5 [58] are satisfied. Hence, we conclude that there is a $\delta > 0$ and a C^1-curve $(\alpha, \phi) : (-\delta, \delta) \longrightarrow \mathbb{R} \times Z$ s.t.$\alpha(0) = \alpha_0, \phi(0) = 0$ and $f(\alpha(s), \mathbf{X}(\mathbf{S}, s)) = f(\alpha(s), s(\mathbf{c}_{p1}\psi_p +$

$\phi(s))) = 0$. Now we have a non-uniform stationary solution of (B.0.1) with $\alpha = \alpha(s)$ for $|s| < \delta$ in following form

$$\mathbf{U}(\mathbf{S}, s) = \mathbf{U}^* + s\mathbf{c}_{p1}\psi_p + o(s^2).$$

Thus we conclude that at $\alpha = \alpha_0$, the uniform stationary solution $\mathbf{U}^*$ of (B.0.1) undergoes Turing bifurcation. The critical value α_0 can be determined by solving equation $H_{\lambda_p} = 0$ by keeping rest of the parameters fixed. □

Appendix C

Quadratic Equation for Abscissa of Equilibrium Points of System (5.3.1)

$$\begin{aligned}
(b-1)x+(b-\alpha)\xi-\frac{(1-qE-x)\,(x+\alpha\xi)}{x+qE+c-1} &= 0\\
\Rightarrow ((b-1)x+(b-\alpha)\xi)(x+qE+c-1)-(1-qE-x)(x+\alpha\xi) &= 0\\
\Rightarrow x[(b-1)(x+qE+c-1)]+\xi(b-\alpha)(x+qE+c-1)- & \\
[x+(1-qE)\alpha\xi-x^2-(\alpha\xi+qE)x] &= 0\\
\Rightarrow (b-1)x^2+((b-1)(qE+c-1)+\xi(b-\alpha))x+ & \\
\xi(b-\alpha)(qE+c-1)+x^2-(1-\alpha\xi-qE)x-(1-qE)\alpha\xi &= 0\\
\Rightarrow bx^2+((b-1)(qE+c-1)+\xi(b-\alpha)-(1-\alpha\xi-qE))x+ & \\
\xi(b-\alpha)(qE+c-1)-(1-qE)\alpha\xi &= 0\\
\Rightarrow bx^2+((b-1)(c-1)+b(\xi+qE)-1)x+ & \\
\xi[(b-\alpha)(qE+c-1)-(1-qE)\alpha] &= 0\\
\Rightarrow bx^2+(bc-b-c+b(\xi+qE))x+\xi(b(qE+c-1)-\alpha c) &= 0\\
\Rightarrow x^2+(c-1-\frac{c}{b}+\xi+qE)x+\xi(qE+c-1-\frac{\alpha c}{b}) &= 0.
\end{aligned}$$

Alternative Form of Abscissa of Equilibrium Points of System (5.3.1)

From prey and predator's isocline of the system (5.3.1) we have

$$\begin{aligned}
(1-x_i)-\frac{c((b-1)x_i+(b-\alpha)\xi)}{x_i+(b-1)x_i+(b-\alpha)\xi+\alpha\xi}-qE &= 0\\
\Rightarrow (1-x_i)-\frac{c((b-1)x_i+(b-1)\xi+(1-\alpha)\xi)}{bx_i+b\xi}-qE &= 0
\end{aligned}$$

$$\begin{aligned}
\Rightarrow (1-x_i) - \frac{c((b-1)(x_i+\xi)+(1-\alpha)\xi)}{b(x_i+\xi)} - qE &= 0 \\
\Rightarrow (1-x_i) - \frac{c(b-1)}{b} - \frac{c(1-\alpha)\xi}{b(x_i+\xi)} - qE &= 0 \\
\Rightarrow (1-x_i) - \frac{c(b-1)}{b} + \frac{c(\alpha-1)\xi}{b(x_i+\xi)} - qE &= 0
\end{aligned}$$

which gives

$$x_i = 1 - \frac{c(b-1)}{b} + \frac{c(\alpha-1)\xi}{b(x_i+\xi)} - qE$$

Singular Optimal Equilibrium Solution for the Ratio-Dependent Model

Recall the costate equations for the ratio-dependent model,

$$\begin{aligned}
\frac{d\lambda_1}{dt} &= -\frac{\partial \mathcal{H}}{\partial x} = -e^{-\delta t}pqE - \lambda_1\left(1 - 2x - \frac{cy^2}{(x+y)^2} - qE\right) - \lambda_2\frac{bmy^2}{(x+y)^2}, \\
\frac{d\lambda_2}{dt} &= -\frac{\partial \mathcal{H}}{\partial y} = \lambda_1\frac{cx^2}{(x+y)^2} - m\lambda_2\left(\frac{bx^2}{(x+y)^2} - 1\right).
\end{aligned} \tag{C.0.1}$$

After considering the interior equilibrium point of system (5.2.1) and solving for interior equilibrium point of system (C.0.1), we obtain

$$\begin{aligned}
-e^{-\delta t}pq\bar{E} - \lambda_1\bar{x}\left(-1 + \frac{c\bar{y}}{(\bar{x}+\bar{y})^2}\right) - \lambda_2\frac{bm\bar{y}^2}{(\bar{x}+\bar{y})^2} &= 0 \\
\lambda_1\frac{c\bar{x}^2}{(\bar{x}+\bar{y})^2} - m\lambda_2\left(\frac{b\bar{x}^2}{(\bar{x}+\bar{y})^2} - 1\right) &= 0
\end{aligned}$$

$$\begin{aligned}
\Rightarrow e^{-\delta t}pq\bar{E} - \lambda_1\bar{x}\left(-1 + \frac{c(b-1)x_i}{(b\bar{x})^2}\right) - \lambda_2\frac{bm(b-1)^2\bar{x}^2}{(b\bar{x})^2} &= 0 \\
\lambda_1\frac{c\bar{x}^2}{(b\bar{x})^2} - m\lambda_2\left(\frac{b\bar{x}^2}{(b\bar{x})^2} - 1\right) &= 0
\end{aligned}$$

$$\begin{aligned}
\Rightarrow -e^{-\delta t}pq\bar{E} - \lambda_1\left(-\bar{x} + \frac{c}{b^2}(b-1)\right) - \lambda_2\frac{m}{b}(b-1)^2 &= 0 \\
\lambda_1\frac{c}{b^2} + \lambda_2\frac{m}{b}(b-1) &= 0
\end{aligned}$$

As $\delta \to 0$, we get

$$\begin{aligned}
\lambda_1\left(-\bar{x} + \frac{c}{b^2}(b-1)\right) + \lambda_2\frac{m}{b}(b-1)^2 &= -pq\bar{E} \\
\lambda_1\frac{c}{b^2} + \lambda_2\frac{m}{b}(b-1) &= 0
\end{aligned}$$

$$\begin{aligned}\bar{\lambda_1} &= \frac{pq\bar{E}}{\bar{x}}\\ \bar{\lambda_2} &= -\frac{c}{mb(b-1)}\times\frac{pq\bar{E}}{\bar{x}}\end{aligned}$$

We substitute the values $(\bar{x},\bar{y},\bar{\lambda_1},\bar{\lambda_2})$ into $\frac{\partial H}{\partial E}=(pqx-c_1)-\lambda_1 qx=0$ (with $\delta\to 0$), to obtain the singular optimal equilibrium solution. Hence, along the singular optimal equilibrium, we have,

$$\begin{aligned}(pqx-c_1)-\lambda_1 qx &= 0\\ \Rightarrow (pqx-c_1)-\frac{pqE}{x}qx &= 0\\ \Rightarrow (pqx-c_1)-pq^2E &= 0\\ \Rightarrow (pqx-c_1)+pq(x-(1-c+\frac{c}{b})) &= 0\\ \Rightarrow 2pqx-c_1-pq(1-c+\frac{c}{b}) &= 0\end{aligned}$$

Hence

$$\widetilde{x}=\frac{1}{2}\left[\frac{c_1}{pq}+(1-c+\frac{c}{b})\right].$$

Legendre's Condition for the Ratio-Dependent Model

Recall that the Hamiltonian for the ratio-dependent model is given by,

$$\mathcal{H}=e^{-\delta t}\left[pqx-c_1\right]E+\lambda_1\left[x\left(1-x\right)-\frac{cxy}{x+y}-qEx\right]+\lambda_2\left[m\left(\frac{bx}{x+y}-1\right)y\right].$$

As $\delta\to 0$, we have the following

$$\begin{aligned}\mathcal{H}_E &= pqx-c_1-\lambda_1 qx\\ D\mathcal{H}_E &= pq\dot{x}-\dot{\lambda_1}qx-\lambda_1 q\dot{x}\\ D^2\mathcal{H}_E &= (p-\lambda_1)q\ddot{x}-\ddot{\lambda_1}qx-2\dot{\lambda_1}q\dot{x}\\ [D^2\mathcal{H}_E]_E &= [(p-\lambda_1)q\ddot{x}]_E-[\ddot{\lambda_1}qx]_E-2[\dot{\lambda_1}q\dot{x}]_E\end{aligned}$$

Now

$$\begin{aligned}(p-\lambda_1)q\ddot{x} &= (p-\lambda_1)q\left[\dot{x}-2x\dot{x}-\frac{c(x+y)(\dot{x}y+x\dot{y})-cxy(\dot{x}+\dot{y})}{(x+y)^2}-qE\dot{x}\right]\\ &= (p-\lambda_1)q\left[\dot{x}(1-2x)-\frac{c(\dot{x}y^2+x^2\dot{y})}{(x+y)^2}-qE\dot{x}\right]\\ \Rightarrow [(p-\lambda_1)q\ddot{x}]_E &= (p-\lambda_1)q\left[(-qx)(1-2x)-\frac{c(-qx)y^2}{(x+y)^2}-qE(-qx)\right]\\ &= -(p-\lambda_1)q^2x\left[1-2x-\frac{cy^2}{(x+y)^2}-qE\right]\end{aligned}$$

$$
\begin{aligned}
\ddot{\lambda_1} qx &= \left[-\dot{\lambda_1}\left(1-2x-\frac{cy^2}{(x+y)^2}-qE\right)-\dot{\lambda_2}\frac{bmy^2}{(x+y)^2}-\right.\\
&\quad \lambda_1\left(-2\dot{x}-\frac{2c(x+y)y\dot{y}-2cy^2(\dot{x}+\dot{y})}{(x+y)^3}\right)-\\
&\quad \left.\lambda_2\frac{2bm(x+y)y\dot{y}-2bmy^2(\dot{x}+\dot{y})}{(x+y)^3}\right]qx\\
&= -qx\left[\dot{\lambda_1}\left(1-2x-\frac{cy^2}{(x+y)^2}-qE\right)+\dot{\lambda_2}\frac{bmy^2}{(x+y)^2}-2\lambda_1\dot{x}-\right.\\
&\quad \left.2\left(\lambda_1 c-\lambda_2 bm\right)\frac{(x+y)y\dot{y}-y^2(\dot{x}+\dot{y})}{(x+y)^3}\right]\\
&= -qx\left[\dot{\lambda_1}\left(1-2x-\frac{cy^2}{(x+y)^2}-qE\right)+\dot{\lambda_2}\frac{bmy^2}{(x+y)^2}-2\lambda_1\dot{x}-\right.\\
&\quad \left.2\left(\lambda_1 c-\lambda_2 bm\right)\frac{(x\dot{y}-\dot{x}y)y}{(x+y)^3}\right]\\
\Rightarrow [\ddot{\lambda_1} qx]_E &= -qx\left[(-(p-\lambda_1)q)\left(1-2x-\frac{cy^2}{(x+y)^2}-qE\right)-2\lambda_1(-qx)-\right.\\
&\quad \left.2\left(\lambda_1 c+\lambda_2 bm\right)\frac{(-qx)y^2}{(x+y)^3}\right]\\
&= -q^2x\left[-(p-\lambda_1)\left(1-2x-\frac{cy^2}{(x+y)^2}-qE\right)+2\lambda_1 x-2\left(\lambda_1 c-\right.\right.\\
&\quad \left.\left.\lambda_2 bm\right)\frac{xy^2}{(x+y)^3}\right].\\
[\dot{\lambda_1} q\dot{x}]_E &= 0.
\end{aligned}
$$

Thus we have

$$
\begin{aligned}
[D^2\mathcal{H}_E]_E &= -(p-\lambda_1)q^2x\left[1-2x-\frac{cy^2}{(x+y)^2}-qE\right]+\\
&\quad q^2x\left[-(p-\lambda_1)\left(1-2x-\frac{cy^2}{(x+y)^2}-qE\right)+2\lambda_1 x-2\left(\lambda_1 c-\lambda_2 bm\right)\frac{xy^2}{(x+y)^3}\right]\\
&= 2q^2x\left[-(p-\lambda_1)\left(1-2x-\frac{cy^2}{(x+y)^2}-qE\right)+\lambda_1 x-\left(\lambda_1 c-\lambda_2 bm\right)\frac{xy^2}{(x+y)^3}\right]
\end{aligned}
$$

At the singular equilibrium point, we have,

$$
\begin{aligned}
[D^2\mathcal{H}_E]_E &= 2q^2\widetilde{x}\left[-(p-\widetilde{\lambda_1})\left(1-2\widetilde{x}-\frac{c(b-1)^2}{b^2}-q\widetilde{E}\right)+\widetilde{\lambda_1}\widetilde{x}-\left(\widetilde{\lambda_1}c-\widetilde{\lambda_2}bm\right)\frac{(b-1)^2}{b^3}\right]\\
&= 2q^2\widetilde{x}\left[(2p-\widetilde{\lambda_1})\widetilde{x}+(p-\widetilde{\lambda_1})\left(-1+\frac{c(b-1)^2}{b^2}+q\widetilde{E}\right)-\left(\widetilde{\lambda_1}c-\widetilde{\lambda_2}bm\right)\frac{(b-1)^2}{b^3}\right]\\
&= -2q^2\tilde{x}\left[(\widetilde{\lambda_1}-2p)\widetilde{x}+(\widetilde{\lambda_1}-p)\left(-1+\frac{c}{b^2}(b-1)^2+q\widetilde{E}\right)+\frac{\left(\widetilde{\lambda_1}c-\widetilde{\lambda_2}bm\right)}{b^3}(b-1)^2\right].
\end{aligned}
$$

Singular Optimal Equilibrium Solution for the Modified Ratio-Dependent Model

Recall the costate equations for the modified ratio-dependent model,

$$\begin{aligned}\frac{d\lambda_1}{dt} &= -e^{-\delta t}pqE - \lambda_1\left(1-2x-\frac{cy(y+\alpha\xi)}{(x+y+\alpha\xi)^2}-qE\right)-\lambda_2\frac{bmy(y+\alpha\xi-\xi)}{(x+y+\alpha\xi)^2},\\ \frac{d\lambda_2}{dt} &= \lambda_1\frac{cx(x+\alpha\xi)}{(x+y+\alpha\xi)^2}-m\lambda_2\left(\frac{b\,(x+\xi)\,(x+\alpha\xi)}{(x+y+\alpha\xi)^2}-1\right).\end{aligned} \tag{C.0.2}$$

After considering the interior equilibrium point of the system (5.3.1) and solving for interior equilibrium point of system (C.0.2), we obtain

$$\begin{aligned}-e^{-\delta t}pqE-\lambda_1 x\left(-1+\frac{cy}{(x+y+\alpha\xi)^2}\right)-\lambda_2\frac{bmy(y+\alpha\xi-\xi)}{(x+y+\alpha\xi)^2} &= 0\\ \lambda_1\frac{cx(x+\alpha\xi)}{(x+y+\alpha\xi)^2}+\lambda_2\frac{bm(x+\xi)y}{(x+y+\alpha\xi)^2} &= 0\end{aligned}$$

As $\delta\to 0$, above system of equations can be written as

$$\begin{aligned}A_1\lambda_1+A_2\lambda_2 &= -pqE\\ B_1\lambda_1+B_2\lambda_2 &= 0\end{aligned} \tag{C.0.3}$$

where $A_1 = x_2\left(-1+\frac{cy_2}{(x_2+y_2+\alpha\xi)^2}\right), A_2 = \frac{bmy_2(y_2+\alpha\xi-\xi)}{(x_2+y_2+\alpha\xi)^2}, B_1 = \frac{cx_2(x_2+\alpha\xi)}{(x_2+y_2+\alpha\xi)^2}$ and $B_2 = \frac{bm(x_2+\xi)y_2}{(x_2+y_2+\alpha\xi)^2}$. Since $A_1B_2-A_2B_1 = -\det J_{(x_2,y_2)}$, therefore, as long as $\det J_{(x_2,y_2)}\neq 0$ there exist an unique pair $(\lambda_1,\lambda_2) = (-\frac{B_2pqE}{A_1B_2-A_2B_1}, \frac{B_1pqE}{A_1B_2-A_2B_1})$ of solution of the system (C.0.3). Now we have

$$\mathcal{H} = e^{-\delta t}\left[(pqx-c_1)\,E-c_2\xi\right]+\lambda_1\left[x\,(1-x)-\frac{cxy}{x+y+\alpha\xi}-qEx\right]+\lambda_2\left[m\left(\frac{b\,[x+\xi]}{x+y+\alpha\xi}-1\right)y\right].$$

Since $\mathcal{H}$ is linear in control E, so the optimal control is combination of bang-bang and singular control. The condition that maximizes $\mathcal{H}$ for E is given by

$$\frac{\partial\mathcal{H}}{\partial E} = e^{-\delta t}(pqx-c_1)-\lambda_1 qx = 0.$$

Taking $\delta\to 0$, we substitute the interior equilibrium of systems (5.3.1) and (C.0.2) into equation $\frac{\partial\mathcal{H}}{\partial E}=0$, to obtain the singular optimal equilibrium solution (x^*,y^*),

$$\begin{aligned}(pqx-c_1)-\lambda_1 qx &= 0\\ \Rightarrow (pqx-c_1)+\frac{B_2pqE}{A_1B_2-A_2B_1}qx &= 0\\ \Rightarrow (A_1B_2-A_2B_1)(pqx-c_1)+B_2pqEqx &= 0\\ \Rightarrow \frac{b^2mx(x+\xi)y}{(x+y+\alpha\xi)^4}\left[-b(x+\xi)^2+c\xi(1-\alpha)\right](pqx-c_1)+\frac{bm(x+\xi)y}{(x+y+\alpha\xi)^2}pqEqx &= 0\\ \Rightarrow \frac{bx}{(x+y+\alpha\xi)^2}\left[-b(x+\xi)^2+c\xi(1-\alpha)\right](pqx-c_1)+pqEqx &= 0\end{aligned}$$

$$\Rightarrow \frac{bx}{(x+y+\alpha\xi)^2}\left[-b(x+\xi)^2+c\xi(1-\alpha)\right](pqx-c_1)+pq\left[(1-x)-\frac{cy}{x+y+\alpha\xi}\right]x = 0$$

$$\Rightarrow \frac{b}{(x+y+\alpha\xi)^2}\left[-b(x+\xi)^2+c\xi(1-\alpha)\right](pqx-c_1)+pq\left[(1-x)-\frac{cy}{x+y+\alpha\xi}\right] = 0$$

$$\Rightarrow \frac{b}{(x+y+\alpha\xi)}\left[-b(x+\xi)^2+c\xi(1-\alpha)\right](pqx-c_1)+pq\left[(1-x)(x+y+\alpha\xi)-cy\right] = 0$$

$$\Rightarrow \frac{1}{(x+\xi)}\left[-b(x+\xi)^2+c\xi(1-\alpha)\right](pqx-c_1)+pq\left[b(1-x)(x+\xi)-c(b-1)x-c(b-\alpha)\xi\right] = 0$$

$$\Rightarrow \frac{1}{(x+\xi)}\left[-b(x^2+\xi^2+2\xi x)+c\xi(1-\alpha)\right](pqx-c_1)+$$
$$pq\left[b(-x^2+(1-\xi)x+\xi)-c(b-1)x-c(b-\alpha)\xi\right] = 0$$

$$\Rightarrow \frac{1}{(x+\xi)}\left[-bx^2-2b\xi x+c\xi(1-\alpha)-b\xi^2\right](pqx-c_1)+$$
$$pq\left[-bx^2+(b(1-\xi)-c(b-1))x+b\xi-c(b-\alpha)\xi\right] = 0$$

$$\Rightarrow \frac{1}{(x+\xi)}\left[-bx^2-2b\xi x+c\xi(1-\alpha)-b\xi^2\right](pqx-c_1)+$$
$$pq\left[-bx^2+(b(1-c-\xi)+c)x+(b-c(b-\alpha))\xi\right] = 0$$

$$\Rightarrow pqx\left[-bx^2-2b\xi x+c\xi(1-\alpha)-b\xi^2\right]+pqx\left[-bx^2+(b(1-c-\xi)+c)x+(b-c(b-\alpha))\xi\right]-$$
$$c_1\left[-bx^2-2b\xi x+c\xi(1-\alpha)-b\xi^2\right]+pq\xi\left[-bx^2+(b(1-c-\xi)+c)x+(b-c(b-\alpha))\xi\right] = 0$$

$$\Rightarrow pqx\left[-bx^2-2b\xi x+c\xi(1-\alpha)-b\xi^2-bx^2+(b(1-c-\xi)+c)x+(b-c(b-\alpha))\xi\right]-$$
$$c_1\left[-bx^2-2b\xi x+c\xi(1-\alpha)-b\xi^2\right]+pq\xi\left[-bx^2+(b(1-c-\xi)+c)x+(b-c(b-\alpha))\xi\right] = 0$$

$$\Rightarrow pqx\left[-2bx^2+((b(1-c-\xi)+c)-2b\xi)x+c\xi-c\alpha\xi-b\xi^2+b\xi-bc\xi+c\alpha\xi\right]+$$
$$b(c_1-pq\xi)x^2+(2bc_1\xi+pq\xi(b(1-c-\xi)+c))x-c\xi(1-\alpha)c_1+bc_1\xi^2+pq(b-c(b-\alpha))\xi^2 = 0$$

$$\Rightarrow pqx\left[-2bx^2+(b+c-bc-3b\xi)x+(b+c-b\xi-bc)\xi\right]+$$
$$b(c_1-pq\xi)x^2+(2bc_1+pq(b+c-bc-b\xi))\xi x+\xi(-c(1-\alpha)c_1+bc_1\xi+pq(b-c(b-\alpha))\xi) = 0$$

$$\Rightarrow -2bpqx^3+(bc_1+(-4b\xi+b+c-bc)pq)x^2+(pq(b+c-b\xi-bc)\xi+$$
$$(2bc_1+pq(b+c-bc-b\xi))\xi)x+\xi(-c(1-\alpha)c_1+bc_1\xi+pq(b-c(b-\alpha))\xi) = 0$$

Finally, we have following cubic equation to be satisfied at singular optimal equilibrium solution

$$-2bpqx^{*3}+\left[bc_1+(-4b\xi+b+c-bc)pq\right]x^{*2}+2\left[bc_1+pq(b+c-bc-b\xi)\right]\xi x^* +\xi\left[-c(1-\alpha)c_1+bc_1\xi+pq(b-c(b-\alpha))\xi\right]=0. \tag{C.0.4}$$

Legendre's Condition for the Modified Ratio-Dependent Model

For this case we have

$$\begin{aligned}
\mathcal{H}_E &= pqx - c_1 - \lambda_1 qx \\
D\mathcal{H}_E &= pq\dot{x} - \dot{\lambda_1} qx - \lambda_1 q\dot{x} \\
D^2\mathcal{H}_E &= (p-\lambda_1)q\ddot{x} - \ddot{\lambda_1} qx - 2\dot{\lambda_1} q\dot{x} \\
[D^2\mathcal{H}_E]_E &= [(p-\lambda_1)q\ddot{x}]_E - [\ddot{\lambda_1} qx]_E - 2[\dot{\lambda_1} q\dot{x}]_E
\end{aligned}$$

$$\begin{aligned}
(p-\lambda_1)q\ddot{x} &= (p-\lambda_1)q\left[\dot{x} - 2x\dot{x} - \frac{c(x+y+\alpha\xi)(\dot{x}y + x\dot{y}) - cxy(\dot{x}+\dot{y})}{(x+y+\alpha\xi)^2} - qE\dot{x}\right] \\
&= (p-\lambda_1)q\left[\dot{x}(1-2x) - \frac{c[(\dot{x}y^2 + x^2\dot{y}) + \alpha\xi(\dot{x}y + x\dot{y})]}{(x+y+\alpha\xi)^2} - qE\dot{x}\right] \\
\Rightarrow [(p-\lambda_1)q\ddot{x}]_E &= (p-\lambda_1)q\left[(-qx)(1-2x) - \frac{c[(-qx)y^2 + \alpha\xi(-qx)y]}{(x+y+\alpha\xi)^2} - qE(-qx)\right] \\
&= -(p-\lambda_1)q^2x\left[1 - 2x - \frac{cy(y+\alpha\xi)}{(x+y+\alpha\xi)^2} - qE\right] \\
\ddot{\lambda_1} qx &= \left[-\dot{\lambda_1}\left(1 - 2x - \frac{cy(y+\alpha\xi)}{(x+y+\alpha\xi)^2} - qE\right) - \dot{\lambda_2}\frac{bmy(y+\alpha\xi-\xi)}{(x+y+\alpha\xi)^2} - \right. \\
&\quad \lambda_1\left(-2\dot{x} - \frac{c(x+y+\alpha\xi)(2y\dot{y}+\alpha\xi) - 2cy(y+\alpha\xi)(\dot{x}+\dot{y})}{(x+y+\alpha\xi)^3}\right) - \\
&\quad \left.\lambda_2\frac{bm(x+y+\alpha\xi)(2y\dot{y}+\alpha\xi-\xi) - 2bmy(y+\alpha\xi-\xi)(\dot{x}+\dot{y})}{(x+y+\alpha\xi)^3}\right] qx \\
&= -qx\left[\dot{\lambda_1}\left(1 - 2x - \frac{cy(y+\alpha\xi)}{(x+y+\alpha\xi)^2} - qE\right) + \dot{\lambda_2}\frac{bmy(y+\alpha\xi-\xi)}{(x+y+\alpha\xi)^2} + \right. \\
&\quad \lambda_1\left(-2\dot{x} - \frac{c(x+y+\alpha\xi)(2y\dot{y}+\alpha\xi) - 2cy(y+\alpha\xi)(\dot{x}+\dot{y})}{(x+y+\alpha\xi)^3}\right) + \\
&\quad \left.\lambda_2\frac{bm(x+y+\alpha\xi)(2y\dot{y}+\alpha\xi-\xi) - 2bmy(y+\alpha\xi-\xi)(\dot{x}+\dot{y})}{(x+y+\alpha\xi)^3}\right] \\
\Rightarrow [\ddot{\lambda_1} qx]_E &= -qx\left[(-(p-\lambda_1)q)\left(1 - 2x - \frac{cy(y+\alpha\xi)}{(x+y+\alpha\xi)^2} - qE\right) - \right. \\
&\quad \left.2\lambda_1(-qx) + 2\lambda_1 c\frac{(-qx)y(y+\alpha\xi)}{(x+y+\alpha\xi)^3} - 2\lambda_2 bm\frac{(-qx)y(y+\alpha\xi-\xi)}{(x+y+\alpha\xi)^3}\right] \\
&= -q^2x\left[-(p-\lambda_1)\left(1 - 2x - \frac{cy(y+\alpha\xi)}{(x+y+\alpha\xi)^2} - qE\right) + 2\lambda_1\left(x - \frac{cxy(y+\alpha\xi)}{(x+y+\alpha\xi)^3}\right) + \right. \\
&\quad \left.2\lambda_2 bm\frac{xy(y+\alpha\xi-\xi)}{(x+y+\alpha\xi)^3}\right] \\
[\dot{\lambda_1} q\dot{x}]_E &= 0
\end{aligned}$$

Thus

$$\begin{aligned}[D^2\mathcal{H}_E]_E &= -(p-\lambda_1)q^2x\left[1-2x-\frac{cy(y+\alpha\xi)}{(x+y+\alpha\xi)^2}-qE\right]+\\ &\quad q^2x\left[-(p-\lambda_1)\left(1-2x-\frac{cy(y+\alpha\xi)}{(x+y+\alpha\xi)^2}-qE\right)+2\lambda_1\left(x-\frac{cxy(y+\alpha\xi)}{(x+y+\alpha\xi)^3}\right)+\right.\\ &\quad \left.2\lambda_2 bm\frac{xy(y+\alpha\xi-\xi)}{(x+y+\alpha\xi)^3}\right]\end{aligned}$$

Along singular optimal equilibrium point, we have,

$$\begin{aligned}[D^2\mathcal{H}_E]_E &= -2q^2x^2\left[(\lambda_1-p)\left(1-\frac{cy}{(x+y+\alpha\xi)^2}\right)+\lambda_1\left(1-\frac{cy}{(x+y+\alpha\xi)^2}+\frac{cxy}{(x+y+\alpha\xi)^3}\right)+\right.\\ &\quad \left.\lambda_2 bm\frac{y(y+\alpha\xi-\xi)}{(x+y+\alpha\xi)^3}\right]\\ &= -2q^2x^2\left[(2\lambda_1-p)\left(1-\frac{cy}{(x+y+\alpha\xi)^2}\right)+(\lambda_1 cx+\lambda_2 bm(y+\alpha\xi-\xi))\frac{y}{(x+y+\alpha\xi)^3}\right].\end{aligned}$$

Relation between $\widetilde{x}$ and x^*

Rewriting the cubic equation (C.0.4) as

$$\begin{aligned}-2bpqx^{*3}+\left[bc_1+pq(b+c-bc-4b\xi)\right]x^{*2}+2\left[bc_1+pq(b+c-bc-b\xi)\right]\xi x^*&\\ +\xi^2\left[bc_1+pq(b+c-bc)\right]+\xi[c(\alpha-1)c_1+cpq(\alpha-1)\xi] &= 0\\ \Rightarrow -2bpq\left[x^*-\frac{1}{2}\left(\frac{c_1}{pq}+(1-c+\frac{c}{b})\right)\right](x^*+\xi)^2+c\xi(\alpha-1)(c_1+pq\xi) &= 0\\ \Rightarrow -2bpq(x^*-\widetilde{x})(x^*+\xi)^2+c\xi(\alpha-1)(c_1+pq\xi) &= 0.\end{aligned}$$

Bibliography

[1] M. Kot, Elements of mathematical ecology, *Cambridge University Press*, 2001.

[2] M. Bandyopadhyay & J. Chattopadhyay, Ratio-dependent predator-prey model: effect of environmental fluctuation and stability, *Nonlinearity*, vol. 18, no. 2, pp. 913-936, 2005.

[3] C.S. Holling, The components of predation as revealed by a study of small-mammal predation of the European pine sawfly, *The Canadian Entomologist*, vol. 91, no. 5, pp. 293-320, 1959.

[4] C.S. Holling, The functional response of predators to prey density and its role in mimicry and population regulation, *Memoirs of the Entomological Society of Canada*, vol. 97, suppl. S45, pp. 5-60, 1965.

[5] C.S. Holling, The functional response of invertebrate predators to prey density, *Memoirs of the Entomological Society of Canada*, vol. 98, suppl. S48 , pp. 5-86, 1966.

[6] R. Arditi & L.R. Ginzburg, Coupling in predator-prey dynamics: ratio-dependence, *Journal of Theoretical Biology*, vol. 139, no. 3, pp. 311-326, 1989.

[7] Y. Kuang & E. Beretta, Global qualitative analysis of a ratio-dependent predator-prey system, *Journal of Mathematical Biology*, vol. 36, no. 4, pp. 389-406, 1998.

[8] D. Xiao & S. Ruan, Global dynamics of a ratio-dependent predator-prey system, *Journal of Mathematical Biology*, vol. 43, no. 3, pp. 268-290, 2001.

[9] C. Jost, O. Arino & R. Arditi, About deterministic extinction in ratio-dependent predator-prey models, *Bulletin of Mathematical Biology*, vol. 61, no. 1, pp. 19-32, 1999.

[10] P.C.J. van Rijn, Y.M. van Houten & M.W. Sabelis, How plants benefit from providing food to predators even when it is also edible to herbivores, *Ecology*, vol. 83, no. 10, pp. 2664-2679, 2002.

[11] P.D.N. Srinivasu, B.S.R.V. Prasad & M. Venkatesulu, Biological control through provision of additional food to predators : A theoretical study, *Theoretical Population Biology*, vol. 72, no. 1, pp. 111-120, 2007.

[12] R.D. Holt, Predation, apparent competition, and the structure of prey communities, *Theoretical Population Biology*, vol. 12, no. 2, pp. 197-229, 1977.

[13] J.D. Harwood, & J.J. Obrycki, The role of alternative prey in sustaining predator populations, *Proceedings of the Second International Symposium on Biological Control of Arthropods*, pp. 453-462, 2005.

[14] R.D. Holt, Spatial heterogeneity, indirect interactions, and the coexistence of prey species, *The American Naturalist*, vol. 124, no. 3, pp. 377-406, 1984.

[15] R.D. Holt & J.H. Lawton, The ecological consequences of shared natural enemies, *Annual Review of Ecology and Systematics*, vol. 25, pp. 495-520, 1994.

[16] M. W. Sabelis & P.C.J. van Rijn, When does alternative food promote biological pest control? *Proceedings of the Second International Symposium on Biological Control of Arthropods*, pp. 428-437, 2005.

[17] M. van Baalen, V. Krivan, P.C.J. van Rijn & M.W. Sabelis, Alternative food, switching predators, and the persistence of predator-prey systems. *The American Naturalist*, vol. 157, no. 5, pp. 512-524, 2001.

[18] P.D.N. Srinivasu & B.S.R.V. Prasad, Time optimal control of an additional food provided predator-prey system with applications to pest management and biological conservation, *Journal of Mathematical Biology*, vol. 60, no. 4, pp. 591-613, 2010.

[19] P.D.N. Srinivasu & B.S.R.V. Prasad, Role of quantity of additional food to predators as a control in predator-prey systems with relevance to pest management and biological conservation, *Bulletin of Mathematical Biology*, vol. 73, no. 10, pp. 2249-2276, 2011.

[20] Y. Du & J. Shi, Some recent results on diffusive predator-prey models in spatially heterogeneous environment, *Nonlinear Dynamics and Evolution Equations, Fields Institute Communications*, vol. 48, pp. 95-135, 2006.

[21] C.B. Huffaker, Experimental studies on predation: Despersion factors and predator-prey oscilasions, *Hilgardia*, vol. 27, no. 14, pp. 343-383, 1958.

[22] A. M. Turing, The chemical basis of morphogenesis, *Philosophical Transactions of the Royal Society of London. Series B: Biological Sciences*, vol. 237, no. 641, pp. 37-72, 1952.

[23] L. A. Segel & J. L. Jackson, Dissipative structure: An explanation and an ecological example, *Journal of Theoretical Biology*, vol. 37, no. 3, pp. 545-559, 1972.

[24] M. Banerjee, Spatial pattern formation in ratio-dependent model: higher-order stability analysis, *Mathematical Medicine and Biology*, vol. 28, no. 2, pp. 111-128, 2011.

[25] M. Banerjee & S. Petrovskii, Self-organised spatial patterns and chaos in a ratio-dependent predator-prey system, *Theoretical Ecology*, vol. 4, no. 1, pp. 37-53, 2011.

[26] H. Malchow, Motional instabilities in prey-predator systems, *Journal of Theoretical Biology*, vol. 204, no. 4, pp. 639-647, 2000.

[27] A. B. Medvinsky, S. V. Petrovskii, I. A. Tikhonova, H. Malchow & B-L. Li, Spatiotemporal complexity of plankton and fish dynamics, *SIAM Review*, vol. 44, no. 3, pp. 311-370, 2002.

[28] S. Petrovskii, B-L. Li & H. Malchow, Transition to spatiotemporal chaos can resolve the paradox of enrichment, *Ecological Complexity*, vol. 1, no. 1, pp. 37-47, 2004.

[29] X. Guan, W. Wang & Y. Cai, Spatiotemporal dynamics of a Leslie-Gower predator-prey model incorporating a prey refuge, *Nonlinear Analysis: Real World Applications*, vol. 12, no. 4, pp. 2385-2395, 2011.

[30] G-Q. Sun, G. Zhang, Z. Jin & L. Li, Predator cannibalism can give rise to regular spatial pattern in a predator-prey system, *Nonlinear Dynamics*, vol. 58, no. 1-2, pp. 75-84, 2009.

[31] W. Wang, L. Zhang, H. Wang & Z. Li, Pattern formation of a predator-prey system with Ivlev-type functional response, *Ecological Modelling*, vol. 221, no. 2, pp. 131-140, 2010.

[32] M. Haque, Existence of complex patterns in the Beddington-DeAngelis predator-prey model, *Mathematical Biosciences*, vol. 239, no. 2, pp. 179-190, 2012.

[33] M. Baurmann, T. Gross & U. Feudel, Instabilities in spatially extended predator-prey systems: Spatio-temporal patterns in the neighborhood of Turing-Hopf bifurcations, *Journal of Theoretical Biology*, vol. 245, no. 2, pp. 220-229, 2007.

[34] L. Braverman & E. Braverman, Stability analysis and bifurcations in a diffusive predator-prey system, *Discrete and Continuous Dynamical Systems Supplements*, vol. 2009, pp. 92-100, 2009.

[35] W. Wang, Y. Cai, Y. Zhu & Z. Guo, Allee-effect-induced instability in a reaction-diffusion predator-prey model, *Abstract and Applied Analysis*, vol. 2013, 10 pages, 2013.

[36] M. Lizana & J. J. Marlin V., Pattern formation in a reaction diffusion ratio-dependent predator-prey model, *Notas de Matematica*, no. 239, pp. 1-16, 2005.

[37] M. Banerjee, Self-replication of spatial patterns in a ratio-dependent predator-prey model, *Mathematical and Computer Modelling*, vol. 51, no. 1-2, pp. 44-52, 2010.

[38] S. Aly, I. Kim & D. Sheen, Turing instability for a ratio-dependent predator-prey model with diffusion, *Applied Mathematics and Computation*, vol. 217, no. 17, pp. 7265-7281, 2011.

[39] C. W. Clark, Mathematical bioeconomics: The optimal management of renewable resources, *John Wiley & Sons*, 1990.

[40] B.S. Goh, Management and analysis of biological populations, *Elsevier*, 1980.

[41] P.D.N. Srinivasu, Bioeconomics of a renewable resource in presence of a predator, *Nonlinear Analysis: Real World Applications*, vol. 2, no. 4, pp. 497-506, 2001.

[42] J. Hoekstra & J.C.J.M. van den Bergh, Harvesting and conservation in a predator-prey system, *Journal of Economic Dynamics & Control*, vol. 29, no. 6, pp. 1097-1120, 2005.

[43] D. Xiao & L.S. Jennings, Bifurcations of a ratio-dependent predator-prey system with constant rate harvesting, *SIAM Journal on Applied Mathematics*, vol. 65, no. 3, pp. 737-753, 2005.

[44] P. Lenzini & J. Rebaza, Nonconstant predator harvesting on ratio-dependent predator-prey models, *Applied Mathematical Sciences*, vol. 4, no. 16, pp. 791-803, 2010.

[45] T.K. Kar & B. Ghosh, Sustainability and optimal control of an exploited prey-predator system through provision of alternative food to predator, *BioSystems*, vol. 109, no. 2, pp. 220-232, 2012.

[46] Y. Lv, R. Yuan & Y. Pei, A prey-predator model with harvesting for fishery resource with reserve area, *Applied Mathematical Modelling*, vol. 37, no. 5, pp. 3048-3062, 2013.

[47] N.C. Apreutesei, An optimal control problem for a prey-predator system with a general functional response, *Applied Mathematics Letters*, vol. 22, no. 7, pp. 1062-1065, 2009.

[48] N. Apreutesei, G. Dimitriu & R. Stefanescu, Time optimal control problem for predator-prey systems, *Buletinul Institutului Politehnic din Iasi. Sectia I. Matematica. Mecanica Teoretica. Fizica*, vol. 57, no. 61(2), pp. 19-28, 2011.

[49] L. Perko, Differential equations and dynamical systems, *Springer-Verlag*, 2001.

[50] M. Haque, Ratio-dependent predator-prey models of interacting populations, *Bulletin of Mathematical Biology*, vol. 71, no. 2, pp. 430-452, 2009.

[51] N.F. Britton, Essential mathematical biology, *Springer*, 2003.

[52] D.S. Jones, M.J. Plank & B.D. Sleeman, Differential equations and mathematical biology, *Chapman & Hall/CRC*, 2009.

[53] J.D. Murray, Mathematical biology II: Spatial models and biomedical applications, *Springer*, 2003.

[54] A. C. Chiang, Elements of dynamic optimization, *McGraw-Hill*, 1999.

[55] K. Chaudhuri, Dynamic optimization of combined harvesting of a two-species fishery, *Ecological Modelling*, vol. 41, no. 1-2, pp. 17-25, 1988.

[56] T. Faria, Stability and bifurcation for a delayed predator-prey model and the effect of diffusion, *Journal of Mathematical Analysis and Applications*, vol. 254, no. 2, pp. 433-463 2001.

[57] P. Feng, Analysis of a delayed predator-prey model with ratio-dependent functional response and quadratic harvesting, *Journal of Applied Mathematics and Computing*, vol. 44, no. 1-2, pp. 251-262, 2014.

[58] J. Smoller, Shock waves and reaction-diffusion equations, *Springer-Verlag*, 1983.

List of accepted or communicated papers

Based on the work in this thesis, the following research articles have been accepted or communicated.

1. Dinesh Kumar & Siddhartha P. Chakrabarty, "A predator-prey model with additional food supply to predators: Dynamics and applications", *Communicated*.

2. Dinesh Kumar & Siddhartha P. Chakrabarty, "Additional food induced Turing patterns for a diffusive predator-prey model", *Communicated*.

3. Dinesh Kumar & Siddhartha P. Chakrabarty, "A comparative study of bioeconomic ratio-dependent predator-prey model with and without additional food to predators", accepted in *Nonlinear Dynamics* (DOI: 10.1007/s11071-014-1848-5), 2014.

4. Dinesh Kumar & Siddhartha P. Chakrabarty, "Optimal control of pest by supply of additional food to predators in a predator-prey system", accepted in *Journal of Advanced Research in Dynamical and Control Systems*.